

# Reply to Anthony Doré

Dear Prof. Doré,

thank you very much for your input on the manuscript, it is highly appreciated. Here is our reply to your comments. We hope the changes we implemented improve the shortcomings of the manuscript highlighted by your comments and suggestions. Please do not hesitate to contact us shall this not be the case for some comments.

## 1. Comments from Prof. Doré

Comment 1: This very interesting paper should certainly be published in *Solid Earth*, not because it provides a definitive solution to the Barents Sea tectonic mosaic, but because it provides a bold and well-argued alternative to the current basement models. In essence, the model would glue the pieces of the Barents Sea (and specifically Svalbard) together in the Neoproterozoic, thus eliminating the idea of later Caledonian assembly from different terranes. It would also put paid to the concept of "Barentsia", the putative microcontinent including Svalbard, formed between two supposed sutures representing arms of the Caledonian orogen.

Comment 2: So how convincing is the interpretation of the Timanian grain extending across from Russia to Svalbard? The idea has to some extent been "out there" for a while, based on the distinct cross-cutting trend of the Tiddlybanken Basin, and the offshore extension of the Trollfjord-Komagelv fault (not strictly Timanian, and actually contested by the lead author elsewhere). But my first reaction on seeing the seismic lines in Fig. 3 was scepticism that such detailed interpretations of deep basement structure could be made from such difficult data. Having to look at the seismic lines with my neck at a right-angle didn't help..... Yes I can see what might be thrust stacks, but I can see lots of other patterns too. That's what happens when you look at noisy data. However, it's good that this is an open review. Others can also take a look and tell me whether I'm being fair or not. Also in the interests of being fair, the authors have looked at a lot more seismic than I have, and for longer - plus the local panels shown in Figure 4 are more convincing.

Comment 3: A significant weakness in the paper's argument, acknowledged by the authors, is the non-observation of these Timanian structures on Svalbard despite the existence of a few apparently Timanian metamorphic dates. You would really think such a pervasive and dominant tectonic

regime, actually not very deeply buried on the seismic lines, would be expressed onshore. The reasons given for the absence are depth of burial and obscuring by later superimposed tectonic events. The latter argument, in particular, is pretty thin based on what the seismic leads us to expect.

Comment 4: Despite these reservations, i think this one can get by with minor revision only. It is very well-written (thanks!) and the illustrations are mainly of good quality. I suggest the following improvement:

1) The multi-panel figures (particularly 3 and 4) are confusing, particularly in online formal. Why not simply call all the different panels different figures? It would make things so much easier.

Comment 5: 2) In any case, the seismic sections are wrongly labelled on Fig. 1. Unless I've got it badly wrong, they should read 3a, 3b etc., (not "2"). The first three sections need readable direction indicators (N-S etc.).

Comment 6: 3) The paper badly needs its own plate tectonic reconstruction (not just the one that is being challenged, Fig. 2). What is your alternative? How was the Barents basement assembled?

Comment 7: Pushing the Iapetus suture even farther west is OK, but where specifically?

Comment 8: And what is the implication for Caledonian assembly, and supposed Laurentian affinity of parts of Svalbard?

Comment 9: How does this idea fit with Caledonian thrust sheets extending as far east as (south of) the Varanger Peninsula? A few simple sketches would suffice to show what you are thinking.

Comment 10: Although these are comparatively minor changes, i look forward to seeing what others say. I'm happy to take a quick look at any revisions. I'm still not sure whether I agree with the idea, but I strongly believe it should be out there and part of the debate.

## **2. Author's reply**

Comment 1: agreed.

Comment 2: agreed, though the data the authors investigated for the present study did not include much noise. The authors of the present manuscript emphasize that high-resolution versions of the figures are available on DataverseNO to evaluate the work presented (<https://dataverse.no/dataset.xhtml?persistentId=doi:10.18710/CE8RQH>).

Comment 3: Seismic sections in Figure 3a–c show Timanian portions of the thrust systems (i.e., not related to Caledonian and post-Caledonian brittle overprints, e.g., listric brittle faults and offsets

of the seafloor) are buried under at least 2.0–2.5 seconds (TWT; i.e., several kilometers thick) successions of Phanerozoic sediments in the Barents Sea and Storfjorden. In its shallowest segment in Nordmannsfonna where it is folded into an anticline, the Kongsfjorden–Cowanodden fault zone is still buried under at least 1.0 second (TWT) of sediments (Figure 3d–e), which still corresponds to a depth of at least 2.5–4.5 kilometers based on seismic velocities for Pennsylvanian to Cretaceous sediments from Gernigon et al. (2018). The authors of the present manuscript do not argue that Timanian fault systems are buried everywhere in the Svalbard Archipelago, especially because they were uplifted and exhumed in western Spitsbergen due to strong Caledonian contraction (and subsequent Eureka contraction). Based on the arguments presented by previous workers for the Vimsodden–Kosibapasset Shear Zone in southern Spitsbergen (e.g., Bjørnerud, 1990; Bjørnerud et al. 1991; Majka et al., 2008, 2012; Mazur et al., 2009), it is highly probable that this major fault zone formed during the Timanian Orogeny as a top-SSW thrust, thus generating the observed regional unconformity between Neoproterozoic and latest Neoproterozoic metasedimentary rocks in the area. In addition, recent dating by Faehnrich et al. (2020) along the Vimsodden–Kosibapasset Shear Zone and other related minor fault zones in southern Spitsbergen further illustrate the point of the authors of the present manuscript about the overprinted character of Timanian thrusts in Spitsbergen. The Vimsodden–Kosibapasset Shear Zone yielded exclusively Caledonian ages (their sample 16-62A), whereas related parallel minor shear zones were only mildly reactivated–overprinted by later Caledonian contraction and preserved partly their Timanian signal (their samples 16-25A and 16-73A). This is discussed in the present manuscript lines 878–887.

Comment 4: the authors of the present manuscript understand the reviewer’s perspective here, but changing the labels of Figure 3a–e may not be ideal. At the moment, when reading the manuscript, the reader will only need to remember number “3” to know that the referred “Figure 3” (a–e) refers to seismic data (and will therefore most likely not have to interrupt his/her reading to double check). However, if these labels were to be changed into Figures 3 to 7, the reader will have to remember 5 numbers and may have to disrupt her/his reading more often.

Placing the seismic lines together also aids comparison. Setting Figure 3a–e as separate figures will likely mean that they appear on different pages in the paper, meaning that readers will have to keep flipping back and forth to compare observations from different lines. As such, the authors of the present manuscript would therefore prefer to keep Figure 3a–e together. Nonetheless, the authors

of the present manuscript are open to changing the labels and therefore await further instructions from both referees and from the editor.

Comment 5: agreed. However, the labels of the seismic sections are as large as they can be and, should it be necessary, they are possible to read better from the high-resolution of the figures on DataverseNO ([doi.org/10.18710/CE8RQH](https://doi.org/10.18710/CE8RQH)).

Comment 6: agreed.

Comment 7: agreed. Based on the present manuscript's findings, the only natural location for the Iapetus suture is in western Spitsbergen where blueschist and eclogite of Caledonian age are recorded (Horsfield, 1972; Dallmeyer et al., 1990a; Ohta et al., 1995). This is discussed lines 1048–1053 in the present manuscript.

Comment 8: agreed. The present findings have implications both for Caledonian assembly and for the affinity of northeastern Spitsbergen with Greenland. The present manuscript does briefly discuss the tectonic implications of the presented findings in the final sub-section of the discussion. However, in order to keep the manuscript focused and to a reasonable length, these issues will be discussed in a future short manuscript, which will also integrate further datasets (e.g., paleontology) to infer a geodynamic evolution. Points of emphasis will include the use of paleontology to infer terrane separation in plate tectonics reconstructions (e.g., thousands of kilometers separation of northeastern Svalbard from Baltica based on differences in Ordovician trilobites; Fortey and Cocks, 2003).

Comment 9: agreed, although the authors of the present manuscript think that this is beyond the scope of the present study, which focuses on advancing the idea that Timanian thrust systems are present across Svalbard and the Barents Sea. Several papers are currently under development that consider the geodynamics implications of the presented findings more broadly, including one in which implications for Caledonian tectonics are considered. For examples, the idea of deep Timanian thrust systems crosscutting the whole Barents Sea and Svalbard fit well with the presence of Caledonian thrust sheets as far as southwest of the Varanger Peninsula since these represent the shallow portion of the crust. If Timanian thrusts are present at depth > 2–3 kilometers in Svalbard and the northwestern Barents Sea, it is therefore conceivable that such thrust systems are present at depth in northern Norway too. However, the commonly accepted Timanian front being the Trollfjorden–Komagelva Fault Zone on the Varanger Peninsula, it is therefore not required to discuss the impact of the present manuscript's findings on Caledonian nappes south of the

Trollfjorden–Komagelva Fault Zone and of this fault’s western continuation. A key element in the upcoming years will be to further constrain the nature and location of its extent offshore onto the Finnmark Platform. The lead author has attempted to address this issue during his Ph.D. (Koehl et al., 2018, 2019). It is the lead author’s belief that the models presented in both Ph.D. manuscripts are (partly to completely) wrong and need updating, especially in the light of the geometry and attitude of Timanian thrust systems in Svalbard and the Barents Sea.

Comment 10: agreed.

### **3. Changes implemented**

Comment 1: none required by the reviewer.

Comment 2: none required by the reviewer.

Comment 3: none.

Comment 4: awaiting further instructions from the editor and reviewers.

Comment 5: changed the labels of the seismic sections in Figure 1 to “3a–e”.

Comment 6: added the proposed plate tectonics alternative as Figure 8.

Comment 7: none.

Comment 8: none.

Comment 9: see reply to comment 6.

Comment 10: none required by the reviewer.

### **4. Additional changes implemented**

-Lines 80–81: added “, and imply that the Norwegian Barents Sea and Svalbard basement may contain Timanian structures overprinted during later (e.g., Caledonian) deformation events” for clarity.

-Lines 94–100: split the sentence into two and partly rewrote it to make it easier to read.

-Line 103: added “by future research” for clarity.

-Lines 1004–1005: split the sentence into two and added “. If correct, a Timanian origin for these structures would” to make it more readable.

-Lines 1055 and 1064: added reference to the new Figure 8 as a consequence to Prof. Doré comment 6.

-Lines 1079–1080: added “We interpret these thrust systems as being related to the Neoproterozoic Timanian Orogeny.” for clarity.

# Reply to Jeremy Rimando

Dear Dr. Rimando,

thank you very much for your input on the manuscript, it is highly appreciated. Here is our reply to your comments. We hope the changes we implemented improve the shortcomings of the manuscript highlighted by your comments and suggestions. Please do not hesitate to contact us shall this not be the case for some comments.

## 1. Comments from Dr. Rimando

Comment 1: I found this paper very thought-provoking. They propose an alternative mechanism and timing for the accretion of basement terranes in Svalbard and the Barents Sea. They propose that these basement terranes were accreted by top-to-the SSW thrusts faults during the Neoproterozoic ‘Timanian Orogeny,’ rather than by displacement along N–S-striking strike-slip faults during the Paleozoic Caledonian Orogeny. This paper really demonstrates the authors’ breadth of knowledge of the previous work on the structures which they suggest belong to “continuous (undisrupted), hundreds–thousands of kilometers long, Timanian thrust systems.”

Comment 2: However, I think that the paper will require a bit more work to convince readers of the presence of a laterally continuous system of Timanian thrust faults throughout Spitsbergen, Storfjorden, and the Norwegian Barents Sea. As it is, I am not convinced that the authors’ interpretations of a few seismic profiles, including correlation of these interpreted structures with lineaments on gravity, magnetic, and slope direction maps, comprise compelling evidence for the lateral continuity of these WNW-ESE-striking and NNE-dipping Timanian thrusts. Ideally, they should have inspected multiple perpendicular seismic profiles from west to east and correlated these. It might help to include additional representative seismic profiles at different longitudes (and incorporate these in the supplementary file at the very least) to bolster their argument for a continuous thrust system.

Comment 3: The lineaments in the gravity and magnetic anomaly maps that the authors claim to be the continuation of the thrust faults could be anything. Even if these were faults, these might display different fault styles, kinematics, and/or timing of deformation. Granted that observing other kinematics on these WNW-ESE-striking faults does not rule out the possibility that these are

the prolongation of the Timanian thrusts (i.e., overprinting may have happened), interpreting more seismic profiles and including a discussion similar to the section 'Devonian–Carboniferous normal overprint–reactivation' should help clarify this.

Comment 4: In short, I do not think the spatial coverage of the data and the amount of analysis conducted is sufficient to suggest the presence of such a large, continuous thrust system. The authors could either do additional analyses or at least describe their level of confidence in their mapping of different portions of the fault system, and be clear about which traces are speculative and which traces are certain.

Comment 5: In some instances, it's difficult to follow their line of reasoning for describing a lateral continuous Timanian thrust fault system. They claim that the structures they observed in the northwestern Norwegian Barents Sea are comparable to structures observed onshore and offshore in other areas, but it is unclear how some of their descriptions support such claims. For instance, the Vimsodden–Kosibapasset Shear Zone (VKSZ) is dominantly strike-slip. It is not clear how this is proof that the VKSZ displays similar configuration and kinematics and, consequently, represents the westward continuation of the Kinnhøgda–Daudbjørnpynten fault zone.

Comment 6: They describe associated map view folds and they explain the VKSZ's strike-slip kinematics, albeit much later in the text, through strong overprinting by the Caledonian Orogeny. What is the scale and timing of the folds that are observed in map view along the VKSZ? Is there proof that these are Timanian and not folding related to the Caledonian ductile shear zone? While later paragraphs seem to clarify the nature of this folding, the manner in which the VKSZ example is presented as proof does not seem convincing. Instead, it creates confusion. I only cite one example, but I suggest that the authors review how they presented their other arguments for an extensive Timanian thrust system.

Comment 7: As noted by Tony Doré (Reviewer 1), I am also not convinced with why these major thrust systems in Svalbard went unnoticed before. They argue that strong overprinting of the VKSZ by Caledonian Orogeny explains why such thrust systems were not identified before, but in an earlier paragraph they describe folds in map view (which are presumably large and obvious) as proof of the onshore continuation of this thrust system. I would expect to see more exposures of the Timanian thrusts onshore, despite 'deep burial' since, as they themselves claim, these areas onshore would have been intensely deformed, and most likely experienced high uplift and exhumation due to their proximity to the Caledonian collision zones.



Comment 8: On its own, this paper doesn't really provide definitive evidence of the presence of hundreds-thousands of kilometers long Timanian thrust systems and I think this issue should be addressed before they even consider exploring the impact of the existence of Timanian thrust systems on the tectonic evolution of the region.

Comment 9: Besides, considering that they discuss the impact of these thrust systems on the tectonic evolution of the region, the authors should include schematic diagrams, or better yet, time-lapse images of their proposed plate reconstruction model.

Comment 10: Overall, the paper is well written. A few stylistic changes, including tweaks to figures and consistency in using in-text citation of figures and figure labels, will significantly improve the readability of this paper. Below are a few minor technical comments to consider:

1) Please make sure that all features/places (e.g., Baltica, Caledonides, Norway, Laurentia, Pearya, Sassendalen, Hornsund) you described are included in your maps. In all of the sections, figures (and panel letters) should be cited consistently in the text right after the feature being described to make it easier for readers who are not familiar with the area to locate the features you are referring to. Please also make sure that the labels on the maps are big enough and easy to read. Some of the text might need to be outlined in another color to provide a contrast to the background and some may have to be brought to the topmost layer items on your figure to prevent them from being blocked by other lines/shapes.

Comment 11: 2) I suggest indicating the ages of these 'Timanian fingerprints' on the map to emphasize the contemporaneity of structures and citing the corresponding references on the figure captions as well.

Comment 12: 3) Indicate the abbreviations of geologic features and places in the text, similar to how you did in the figures (e.g., BAFZ for the Baidaratsky fault zone), so that it is easier to locate them on the maps.

Comment 13: 4) Please include a north arrow, a scale bar, and northing and easting labels around the map frame. It's difficult to visualize some descriptions of fault lengths in the text since you did not put any scale bars on your map in fig 1.

Comment 14: 5) The authors plot the other seismic profiles that belong to the DISKOS database on a map, which is good, but these should be labeled and cited in the text alongside citations of previous studies that inspected these particular seismic lines. If there are other previous studies that look into seismic profiles that are not part of the DISKOS database, these should be included as

well. The locations of previous studies which were discussed to provide evidence of the lateral extent of these Timanian thrusts should also be plotted.

Comment 15: 6) Rippington et al. (2010), and the lead author himself in Koehl (2018), cast doubt on the existence of an 'Ellesmerian Orogeny' due to the lack of compelling evidence from cross-cutting relationships and age constraints, but 'Ellesmerian Orogeny' is mentioned several times in the text.

Comment 16: 7) Is 'top-SSW', 'top-E', or 'top-S' standard notation? Why not use 'top-to-SSW'/'top-to-the-SSW', 'top-to-east'/'top-to-the-east', or 'top-to-south'/'top-to-the-south' instead?

Comment 17: 8) I think it is necessary to outline the approximate extent of the Precambrian basement terranes on a map.

Comment 18: 9) In the section geologic setting, can you describe the orientation of the structures (e.g., N-S-striking BFZ and LFZ) as well as the direction of the maximum horizontal stress (and changes thereof) associated with each major tectonic event, to provide context for the kinematics of the structures you describe?

Comment 19: 10) Is there a specific reason for using 'interpret basement-seated structures' instead of 'basement-structures'? It seems like a combination of 'basement-structures' and 'deep-seated.'

Comment 20: 11) Double check the labelling of figures, especially of the seismic profiles on the map (figure 1).

Comment 21: 12) In figure 2, what do you mean by main tectonic stress? Do you mean direction of maximum horizontal stress?

Comment 22: 13) I don't think yellow is the best color to outline reflectors in the pink and purple units in your seismic profile interpretations.

Comment 23: 14) Indicate the location of the potential field data in figure 5 on the map (figure 1) using a box.

Comment 24: 15) 2D seismic profiles only give you the vertical component of displacement, and don't really give a complete picture of the kinematics of faulting. I wonder if the faults you describe as thrust could be oblique or dominantly strike-slip?

Comment 25: 16) The authors cite the paper Koehl et al (in review) a lot. Please refer to the guidelines of EGU (Copernicus Publications) on citations of unpublished work.

Comment 26: 17) Check completeness/accuracy of descriptions of different figure panels and features on figures. Figure 5b shows a slope direction map, but the caption says it's a gravity map.

Comment 27: 18) The authors write in the passive voice too much. I think it's fine to write in the active voice to avoid making sentences too wordy and difficult to understand.

Comment 28: 19) Please make sure if saying "The complete seismic study is also available from the corresponding author upon request" complies with Copernicus Publications' commitment to the 'Coalition on Publishing Data in the Earth and Space Sciences' (COPDESS) and the 'Enabling FAIR (findability, accessibility, interoperability, and reusability) Data Commitment Statement in the Earth, Space, and Environmental Sciences.'

Comment 29: It was a pleasure reviewing your interesting work! I believe the paper is worthy of being published in Solid Earth after addressing the issues I raised. I look forward to hearing your thoughts and I'd be happy to a look at a revised version of this manuscript.

## **2. Author's reply**

Comment 1: agreed.

Comment 2: agreed. However, if Dr. Rimando is referring to the lack of seismic data in the Russian Barents Sea, it is not possible to obtain data on Russian territory outside of Russia and one must physically go to Russia to interpret such data. Thus, for mapping of the Baidaratsky fault zone, the authors of the present manuscript rely on previous seismic interpretation and onshore–offshore by Prof. Lopatin and Prof. Korago (Lopatin et al., 2001; Korago et al., 2004), which are summaries of mapping campaigns in the Russian Barents Sea and onshore northwestern Russia. Regarding the Norwegian sector of the Barents Sea, the authors of the present manuscript did look at many more N-S and E-W profiles but had not secured permission to show these prior to submitting the manuscript. Figure 1 attached the present response to Dr. Rimando's comments shows the whole seismic database used for the present study. The authors of the present manuscript have now secured permission to show the whole dataset and, in addition to those presented in Figure 3a–e or in the supplementary data, the authors of the present manuscript direct the reader to the DISKOS database.

Comment 3: agreed. The lineaments in the gravity and magnetic anomaly map could indeed be anything and the present manuscript does not have the ambition of providing a definitive answer to this. However, the present manuscript presents evidences suggesting that they may represent

Timanian faults and/or folds. Timanian faults–folds onshore Russia with the exact same WNW–ESE strike/trend as those mapped on seismic data in the Norwegian Barents Sea and Svalbard correlate with the eastern continuations of the gravimetric and magnetic anomalies Timanian thrusts (and folds) that coincide with Timanian thrusts in the Norwegian Barents Sea and Svalbard. This interpretation is also backed up by previous studies in Russia (Lopatin et al., 2001; Korago et al., 2004), which have successfully mapped the largest of these Timanian faults all the way to the border with the Norwegian Barents Sea, where they coincide with the eastern continuation of the Kongsfjorden–Cowanodden fault zone (Baidaratsky fault zone) and Trollfjorden–Komagelva Fault Zone (Central Timan Fault; see Figures 1 and 5). The fact that these anomalies display relatively homogeneous character from the Norwegian Barents Sea to the Russian Barents Sea and onshore northwestern Russia further suggest that the geometries and kinematics (and, quite possibly, the timing of formation) of the faults (and folds) are consistent throughout these areas, thus further supporting the model proposed. The only exception would be towards the Uralides farther east in Russia, and in central–western Spitsbergen where these faults would have been strongly overprinted (e.g., Vimsodden–Kosibapasset Shear Zone reactivated as a sinistral strike-slip fault in Caledonian times and rotated into a subvertical fault – Faehnrich et al., 2020; Kongsfjorden–Cowanodden fault zone folded into north- to NNE-plunging Caledonian folds and overprinted by Devonian–Carboniferous brittle normal faults, which were themselves inverted in Cenozoic times in Svalbard and Storfjorden, i.e., close to the active Cenozoic margin of western Spitsbergen, but not farther east). These exceptions are discussed in the present manuscript in section “Phanerozoic reactivation and overprinting of Timanian thrust systems” (starting line 810).

Comment 4: agreed. The authors of the present manuscripts used more seismic data than is available as figures in the manuscript (see response to comment 2) and therefore do believe that spatial coverage of the data is sufficient to support their argumentation (see attached Figure 1 showing the complete seismic database). The authors of the present manuscript also note that they tried to use language throughout the manuscript that acknowledges that their interpretations are tentative. As both reviewers agree, the aim of this work is not to promote a definitive idea but to offer interpretations and a conceptual model that needs to be further tested. However, the authors of the present manuscript concede that the more speculative portions of the mapped faults should be highlighted in Figure 1.

Comment 5: agreed. The Vimsodden–Kosibapasset Shear Zone does display indications for sinistral strike-slip movements. However, these were recently dated to be Caledonian in age (Faehnrich et al., 2020; their sample 16-62A), thus attesting of the reactivation–overprinting history of Timanian faults during subsequent events. Nonetheless, it is clear that amphibolite facies metamorphism along the Vimsodden–Kosibapasset Shear Zone was coeval with the formation of a regional latest Neoproterozoic unconformity north of the shear zone in southwestern Spitsbergen (Bjørnerud, 1990; Bjørnerud et al., 1991; Majka et al., 2008, 2012; Mazur et al., 2009), i.e., similar to the configuration and deformation intensity along Timanian thrust systems in the Barents Sea and Svalbard. Considering the obliquity of the (most likely) Timanian Vimsodden–Kosibapasset Shear Zone to subsequent E–W Caledonian contraction, the WNW–ESE-striking shear zone would have been ideally oriented to be reactivated as a sinistral strike-slip fault in Caledonian times (e.g., Figure 7b in the present manuscript).

Comment 6: map-view folding along all Timanian thrust systems in Svalbard and the Barents Sea are inferred to be Caledonian in age, not Timanian. The Timanian Orogeny is believed to have been a relatively simple event in the Barents Sea and Svalbard’s crust, involving top-SSW thrusting along a series of dominantly NNE-dipping thrust systems. Later on, these thrust systems which were oriented highly oblique to subsequent E–W Caledonian contraction) were reactivated as sinistral strike-slip faults (e.g., Vimsodden–Kosibapasset Shear Zone; Mazur et al., 2009; Faehnrich et al., 2020) and folded into N–S-trending (north-plunging; due to the north-northeastwards dip of the thrusts) folds. These map-view N–S-trending, NNE-plunging folds (see illustration of the geometry of the folds in Figure 3d in E–W cross section and Figure 3e in N–S along-strike section) are not directly related to sinistral strikes-slip reactivation of Timanian faults but represent more gentle deformation of the thrust systems away from the Caledonian margin in western Spitsbergen. Figure 7b illustrates how WNW–ESE-striking Timanian faults were reactivated as sinistral strike-slip faults and/or folded into N–S-trending, NNE-plunging folds during the Caledonian Orogeny. However, the authors of the present manuscript concede that the figure does not illustrate the variation in the intensity of Caledonian reactivation–overprinting along Timanian faults. Timanian faults were intensely deformed along the Caledonian margin in western Spitsbergen and reactivated as sinistral strike-slip faults and folded (e.g., Vimsodden–Kosibapasset Shear Zone), whereas they were only folded in the Barents Sea and eastern Spitsbergen away from the Caledonian margin (Figure 3b). The authors of the present manuscript

are open to redesign/update Figure 7 to include such along-strike variations in reactivation–overprinting intensity should it be judged necessary by both referees and the editor. These along-strike variations also apply to post-Caledonian deformation as shown by the contrast between Figure 3a and Figure 3c where the Kongsfjorden–Cowanodden fault zone was overprinted by Devonian–Carboniferous listric normal faults that were later inverted due to Eurekan contraction in Storfjorden (Figure 3a) and Svalbard (Koehl, 2021 and supplement S2c) but were not inverted farther east, away from the West Spitsbergen Fold-and-Thrust Belt margin (Figure 3c).

Comment 7: disagreed. Timanian thrusts systems onshore Svalbard are either deeply buried and/or intensely overprinted along the western Spitsbergen margin, which was the locus of both Caledonian and Eurekan (and possibly Ellesmerian) contraction. Other arguments as to why they went unnoticed in northwestern Spitsbergen (where some Timanian ages were recorded for eclogite facies metamorphism) are (1) the remoteness of the area and the large amounts of funding required to access potential outcrops and further date them, and (2) the strongly eroded character of outcrops in glaciated areas like Svalbard. Seismic sections in Figure 3a–c clearly show that the Timanian portions of the thrust systems (i.e., not related to Caledonian and post-Caledonian brittle overprints, e.g., listric brittle faults and offsets of the seafloor) are buried under at least 2.0–2.5 seconds (TWT; i.e., several kilometers thick) successions of Phanerozoic sediments in the Barents Sea and Storfjorden. In its shallowest segment in Nordmannsfonna where it is folded into an anticline, the Kongsfjorden–Cowanodden fault zone is still buried under at least 1.0 second (TWT) of sediments (Figure 3d–e), which still corresponds to a depth of at least 2.5–4.5 kilometers based on seismic velocities for Pennsylvanian to Cretaceous sediments from Gernigon et al. (2018). Nevertheless, the authors of the present manuscript do not argue that Timanian fault systems are buried everywhere in the Svalbard Archipelago, especially because they were uplifted and exhumed in western Spitsbergen due to strong Caledonian contraction (and subsequent Eurekan contraction). Based on the arguments presented by previous workers for the Vimsodden–Kosibapasset Shear Zone in southern Spitsbergen (e.g., Bjørnerud, 1990; Bjørnerud et al. 1991; Majka et al., 2008, 2012; Mazur et al., 2009), it is highly probable that this major fault zone formed during the Timanian Orogeny as a top-SSW thrust, thus generating the observed regional unconformity between Neoproterozoic and latest Neoproterozoic metasedimentary rocks in the area. In addition, recent dating by Faehnrich et al. (2020) along the Vimsodden–Kosibapasset Shear Zone and other related minor fault zones in southern Spitsbergen further illustrate the authors’ point about the

overprinted character of Timanian thrusts in western Spitsbergen. The Vimsodden–Kosibapasset Shear Zone yielded exclusively Caledonian ages (their sample 16-62A), whereas related parallel minor shear zones were only mildly reactivated–overprinted by later Caledonian contraction and preserved partly their Timanian signal (their samples 16-25A and 16-73A). This is discussed in the present manuscript lines 878–887.

To the comment as to why these major thrust systems went unnoticed on seismic data despite the data have been acquired in the 90s, the issue is simple. Only very few researchers (if any at all) in the world would have known what to make out of the seismic expression of these faults. The seismic expression of (mylonitic) shear zones on seismic data was first investigated by avant-garde work by Fountain et al. (1984), Hurich et al. (1985), and a few others. But even back then, the shear zone geometries correlated to seismic signals were relatively simple and consisted of linear single mylonitic detachment surfaces. It is only recently that this research front was pushed further by innovative new works like Phillips et al. (2016) and Fazlikhani et al. (2017; to cite only a few) and that kilometers thick shear zones were eventually correlated from onshore field geometries to offshore seismic geometries. This field is being further developed here, especially considering the amount of details (down to 100 meters scale) possible to observe within Timanian thrusts systems in Storfjorden (e.g., SSW-verging asymmetric folds versus mylonitic brittle–ductile shears and detachments; see high-resolution version of Figure 3a and associated zooms in Figure 4d and e). It should also be noted that seismic data around Svalbard have mostly been investigated with emphasis on shallow Paleozoic–Cenozoic sedimentary successions in the perspective of hydrocarbon exploration and carbon storage. Deep basement structures were therefore not a priority but are now being increasingly studied (e.g., Klitzke et al., 2019).

Comment 8: partly agreed. It is true that the present manuscript does not constitute a definitive answer to the structure of basement units in the Barents Sea and Svalbard. Much further work is needed to further investigate the thrust systems described herein and to better constrain their geometry in 3D. However, it is important that this model becomes part of ongoing discussions about the geology of the Barents Sea and Svalbard. These thrust systems cannot be ignored anymore and should be top-priority targets in the next few years, e.g., to constrain plate tectonics models in the late Neoproterozoic to Cenozoic, or to explore for hydrocarbons or minerals, or for carbon storage, or even studying the hazard risk they present (e.g., Mitchell et al., 1990; Pirli et al., 2013). Regarding the 3D geometry of Timanian thrust systems, no 3D seismic data exist in the

northern Barents Sea since it is not open for hydrocarbon exploration. However, high-resolution 3D seismic data on the Loppa High do further illustrate the model argued for in the present manuscript. These data being private and located in the southern Barents Sea, they will be described and discussed in a future manuscript.

Comment 9: agreed. This is a great point and the authors of the present manuscript agree that the present findings will lead to a new plate tectonics model for the Norwegian Arctic in the 650–0 Ma period. However, considering the recent discovery of the Timanian thrusts systems described in the present manuscript, it is without saying that a new plate tectonics model is beyond the scope of the paper. However, a new model is currently being worked out using GPlates and will follow up on the present manuscript's findings and its implications for plate tectonics reconstructions. Nevertheless, the authors of the present manuscript agree that a local and simple plate tectonics model should be included to the manuscript as suggested by Prof. Doré. Following Prof. Doré's recommendation, the authors of the present manuscript propose to include such a model as Figure 8.

Comment 10: agreed.

Comment 11: disagreed. This would overcrowd a figure already crowded with information. In addition, the age of Timanian fingerprints in other Arctic areas is not the point of the manuscript.

Comment 12: agreed.

Comment 13: agreed.

Comment 14: labelling each seismic section in Figure 1 would overcrowd the figure with trivial information. Instead, it is possible to obtain the name of each seismic section from the main author or from the Norwegian Petroleum Directorate. The authors of the present manuscript also feel that mentioning which specific studies did inspect which specific seismic lines in the Barents Sea would lead to a significant amount of irrelevant text. It is safe to assume that each previous study referenced in the present manuscript does include an overview of the database it used to support its own conclusions. If Dr. Rimando has any particular suggestion of previous works not acknowledged in the present study, the authors of the present manuscript welcome any addition, provided that it adds to the manuscript and allows further discussion. To the knowledge of the authors of the present manuscript, all seismic lines in the northern Norwegian Barents Sea are part of the DISKOS database. Again, if Dr. Rimando is aware of any data or contribution not



acknowledged or discussed but should have, the authors of the present manuscript would welcome its addition to the manuscript.

The authors of the present manuscript feel that adding the “locations of previous studies which were discussed to provide evidence of the lateral extent of these Timanian thrusts” by, e.g., adding a frame for each study’s extent in Figure 1, is irrelevant and would overcrowd an already crowded figure. If the reader is interested in the extent of a previous study or in the database used in a previous study, she/he should refer to the associated publication and/or contact the relevant author(s) if needed.

Comment 15: agreed. The Ellesmerian Orogeny, though believed not to have occurred by the lead author, is still commonly thought to be part of the geological history of Svalbard. In the present manuscript, it is only mentioned in the introduction and geological setting sections, and in the discussion where it is refuted as a possible cause of the accretion of Svalbard’s basement terranes. However, it does not constitute the focus of the present manuscript and is therefore not discussed further. This issue will nevertheless be addressed in two manuscripts in preparation.

Comment 16: “top-SSW” is standard, as much as “top-to-the-SSW” is. The former requires fewer words and space and is not less explanatory. The authors of the present manuscript will of course update the manuscript if both reviewers and the editor judge it easier to read and comprehend for the reader.

Comment 17: agreed.

Comment 18: agreed. The strike and trend of geological structures will be added where appropriate but are already stated by dip direction, which are more informative because inform about the trend/strike and dip of the associated geological structure (e.g., “...-dipping”). However, the stress directions and changes of stress direction are mostly speculative and still a matter of debate in most cases. In addition, local variations exist (e.g., Brøggerhalvøya segment of the West Spitsbergen Fold-and-Thrust Belt which trends WNW–ESE, i.e., oblique to the rest of the fold-and-thrust belt). Stress directions will therefore not be added.

Comment 19: agreed. Yes indeed, it is a combination of “basement structure” and “deep-seated”. If this is not correct, it may be rephrased of course.

Comment 20: agreed. The labels of seismic sections in Figure 1 are erroneous.

Comment 21: agreed. The label in Figure 2 was rephrased to “Max. horizontal stress”.

Comment 22: agreed. However, these reflections need to be displayed in the same scheme (color/pattern) as their counter-parts in other units.

Comment 23: agreed.

Comment 24: agreed. The faults the present study deals with are actually oblique-slip. However, it is neither possible nor useful for the present manuscript to establish/discuss this issue. As mentioned by Dr. Rimando, it is important to establish the continuity of Timanian structures first. The oblique-slip character of the fault systems discussed in the present manuscript will be discussed in two other manuscripts. Two major lines of evidence suggest oblique-slip kinematics: (1) recent (2008–2019) deep (c. 15–16 kilometers) earthquakes in Storfjorden erroneously ascribed to a putative NE–SW-striking fault in Storfjorden suggest recent–ongoing sinistral-reverse oblique-slip movements along the KCFZ, BFZ, and KDFZ, and (2) major N–S-trending, Caledonian and Devonian basement ridges (e.g., Atomfjella Antiform; Witt-Nilsson et al., 1998) are offset left-laterally by c. 10–25 kilometers and in a reverse (top-SSW) fashion by c. 5–5.5 kilometers across the KCFZ.

Comment 25: agreed. However, this pre-print is already accessible at the following link: [https://www.researchgate.net/publication/349124816\\_Devonian-Carboniferous\\_collapse\\_and\\_segmentation\\_of\\_the\\_Billefjorden\\_Trough\\_and\\_Eurekan\\_inversion-overprint\\_and\\_strain\\_partitioning\\_and\\_decoupling\\_along\\_inherited\\_WNW-ESE-striking\\_faults?\\_sg=qtceO8VLbOUVZh5i5AT30gZbnAY8wO5q4mbX\\_u98eKImEuLQS8aOqk0mc6guKuoXeagQlv1F3v9ZoAwHOfdtHSpw5RoUCAQcOUcC6Usc.EPUrQi5OpABDFpUHLXMyvgdMKcNL97-WXB5QVOsPluieVegj9fNgWuQ8QAIKNQrv-0jIEvVkbheFo1nTMDjVcg](https://www.researchgate.net/publication/349124816_Devonian-Carboniferous_collapse_and_segmentation_of_the_Billefjorden_Trough_and_Eurekan_inversion-overprint_and_strain_partitioning_and_decoupling_along_inherited_WNW-ESE-striking_faults?_sg=qtceO8VLbOUVZh5i5AT30gZbnAY8wO5q4mbX_u98eKImEuLQS8aOqk0mc6guKuoXeagQlv1F3v9ZoAwHOfdtHSpw5RoUCAQcOUcC6Usc.EPUrQi5OpABDFpUHLXMyvgdMKcNL97-WXB5QVOsPluieVegj9fNgWuQ8QAIKNQrv-0jIEvVkbheFo1nTMDjVcg). The EGU guidelines state that “Works "submitted to", "in preparation", "in review", or only available as preprint should also be included in the reference list”.

Comment 26: agreed. Figure 5b is a slope map of gravimetric data. This should be specified.

Comment 27: agreed.

Comment 28: agreed. The authors of the present manuscript are not allowed to transfer data from the DISKOS database directly to another party. Although the data are publicly accessible, the concerned party should submit inquiries to the Norwegian Petroleum Directorate.

Comment 29: agreed.

### **3. Changes implemented**

Comment 1: none required by the reviewer.

Comment 2: modified Fig. 1b in the present manuscript to include the complete seismic database as in the attached Figure 1.

Comment 3: none.

Comment 4: “Speculative” portions of the faults (i.e., portions of the faults that are not demonstrated and argued for in the present study, but that are known from other ongoing manuscripts and studies) were added as dotted yellow lines in Figure 1b and c. Also see response to comment 2.

Comment 5: none.

Comment 6: awaiting further instructions from the editor and the two reviewers.

Comment 7: none.

Comment 8: none.

Comment 9: included a new Figure 8.

Comment 10: added “Hs” to Figure 1c and “Hs: Hornsund; ” line 1535, “Norway” to Figure 1b, and “Pearya” in Figure 1a.

Comment 11: none.

Comment 12: added abbreviations of all major fault zones to the text lines 71, 86, 87, 88, 90, 135, 136, and 308–310.

Comment 13: added scale bars and north arrow (or “North Pole”) labels to Figure 1a–c.

Comment 14: none but may include reference to other studies if Dr. Rimando has any specific study in mind that should be cited in the present manuscript.

Comment 15: none required by the reviewer.

Comment 16: may update the text if judged necessary by the reviewers and editor.

Comment 17: added “NE terrane”, “SW terrane” and “NW terrane” labels in Figure 2.

Comment 18: added “NNE-dipping” lines 86, 89, 91, 119, 121, 123, and 152, “gently north-plunging” lines 88, and 142–143, “N–S-trending” lines 142, 144, and 145–146, and “N–S-striking” lines 135, and 193, and “E–W-trending” line 172.

Comment 19: may be adjusted into “deep-seated” or “basement structure” if incorrect use of English language. Awaiting further instructions from the editor and reviewers.

Comment 20: changed the labels of seismic sections in Figure 1.

Comment 21: rephrased label to “maximum horizontal stress”.

Comment 22: none.

Comment 23: added a white dashed frame in Figure 1b showing the location of potential field data in Figure 5, and “(see location as a dashed white frame in Figure 1b)” line 1572.

Comment 24: none required by the reviewer.

Comment 25: none required by the reviewer.

Comment 26: added “for gravimetric data” lines 542–543 and “of gravimetric data” line 573.

Comment 27: changed from passive to active form lines 18, 21–22, 57, 92–97, 131, 139–142, 145, 216–219, 225–229, 232–233, 422–428, 530–534, 650–653, and 797–801.

Comment 28: removed “The complete seismic study is also available from the corresponding author upon request.” lines 1113–1114.

Comment 29: none required by the reviewer.

#### **4. Additional changes implemented**

-Lines 80–81: added “, and imply that the Norwegian Barents Sea and Svalbard basement may contain Timanian structures overprinted during later (e.g., Caledonian) deformation events” for clarity.

-Lines 94–100: split the sentence into two and partly rewrote it to make it easier to read.

-Line 103: added “by future research” for clarity.

-Lines 1004–1005: split the sentence into two and added “. If correct, a Timanian origin for these structures would” to make it more readable.

-Lines 1055 and 1064: added reference to the new Figure 8 as a consequence to Prof. Doré comment 6.

-Lines 1079–1080: added “We interpret these thrust systems as being related to the Neoproterozoic Timanian Orogeny.” for clarity.

**Attached figures**

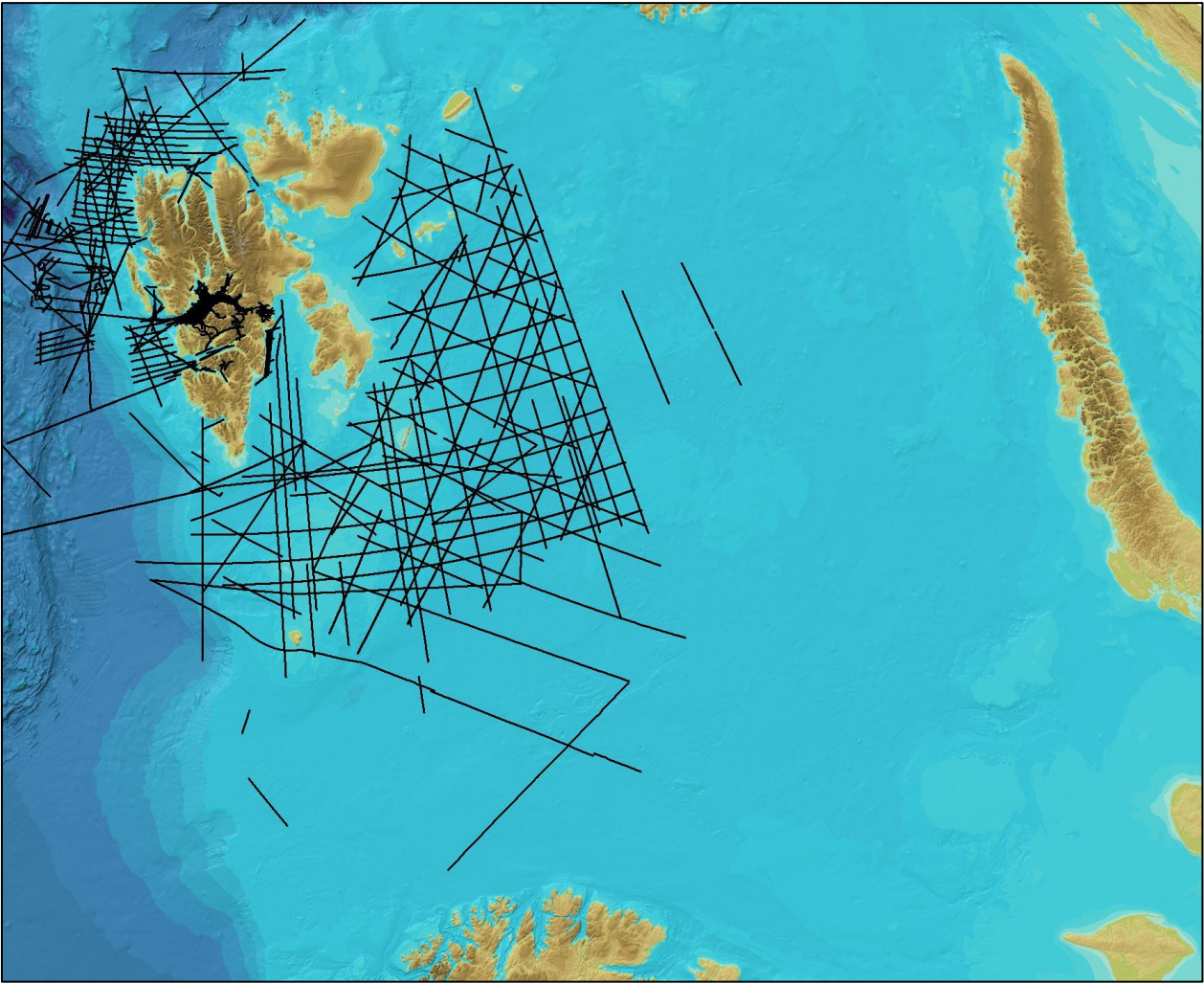


**Figure 1: Seismic database in Svalbard and the Barents Sea.**

# 1 Impact of Timanian thrust systems on the late 2 Neoproterozoic–Phanerozoic tectonic evolution of the 3 Barents Sea and Svalbard

4  
5 Jean-Baptiste P. Koehl<sup>1,2,3,4</sup>, Craig Magee<sup>5</sup>, Ingrid M. Anell<sup>6</sup>

6 <sup>1</sup>Centre for Earth Evolution and Dynamics (CEED), University of Oslo, PO Box 1028 Blindern, N-0315 Oslo,  
7 Norway.

8 <sup>2</sup>Department of Geosciences, UiT The Arctic University of Norway in Tromsø, N-9037 Tromsø, Norway.

9 <sup>3</sup>Research Centre for Arctic Petroleum Exploration (ARCEX), UiT The Arctic University of Norway in Tromsø, N-  
10 9037 Tromsø, Norway.

11 <sup>4</sup>CAGE – Centre for Arctic Gas Hydrate, Environment and Climate, UiT The Arctic University of Norway in  
12 Tromsø, N-9037 Tromsø, Norway.

13 <sup>5</sup>School of Earth Science and Environment, University of Leeds, Leeds, LS2 9JT, United Kingdom.

14 <sup>6</sup>Department of Geosciences, University of Oslo, P.O. Box 1047 Blindern, N-0316 Oslo, Norway.

15 **Correspondence:** Jean-Baptiste P. Koehl ([jean-baptiste.koehl@uit.no](mailto:jean-baptiste.koehl@uit.no))

16

## 17 **Abstract**

18 The Svalbard Archipelago ~~is composed~~consists of three basement terranes that record a  
19 complex Neoproterozoic–Phanerozoic tectonic history, including four contractional events  
20 (Grenvillian, Caledonian, Ellesmerian, and Eurekan) and two episodes of collapse- to rift-related  
21 extension (Devonian–Carboniferous and late Cenozoic). ~~These Previous studies suggest these~~ three  
22 terranes ~~are thought to have~~likely accreted during the early–mid Paleozoic Caledonian and  
23 Ellesmerian orogenies. Yet recent geochronological analyses show that the northwestern and  
24 southwestern terranes of Svalbard both record an episode of amphibolite (–eclogite) facies  
25 metamorphism in the latest Neoproterozoic, which may relate to the 650–550 Ma Timanian  
26 Orogeny identified in northwestern Russia, northern Norway and the Russian Barents Sea.  
27 However, discrete Timanian structures have yet to be identified in Svalbard and the Norwegian  
28 Barents Sea. Through analysis of seismic reflection, and regional gravimetric and magnetic data,  
29 this study demonstrates the presence of continuous, several kilometers thick, NNE-dipping, deeply  
30 buried thrust systems that extend thousands of kilometers from northwestern Russia to northeastern  
31 Norway, the northern Norwegian Barents Sea, and the Svalbard Archipelago. The consistency in

32 orientation and geometry, and apparent linkage between these thrust systems and those recognized  
33 as part of the Timanian Orogeny in northwestern Russia and Novaya Zemlya suggests that the  
34 mapped structures are likely Timanian. If correct, these findings would ~~indicate~~imply that  
35 Svalbard's three basement terranes and the Barents Sea were accreted onto northern Norway during  
36 the Timanian Orogeny and should, hence, be attached to Baltica and northwestern Russia in future  
37 Neoproterozoic–early Paleozoic plate tectonics reconstructions. In the Phanerozoic, the study  
38 suggests that the interpreted Timanian thrust systems represented major preexisting zones of  
39 weakness that were reactivated, folded, and overprinted by (i.e., controlled the formation of new)  
40 brittle faults during later tectonic events. These faults are still active at present and can be linked  
41 to folding and offset of the seafloor.

42

### 43 **Introduction**

44 Recognizing and linking tectonic events across different terranes is critical to plate  
45 reconstructions. In the latest Neoproterozoic (at ca. 650–550 Ma), portions of northwestern Russia  
46 (e.g., Timan Range and Novaya Zemlya) and the Russian Barents Sea were accreted to northern  
47 Baltica by top-SSW thrusting during the Timanian Orogeny (Olovyanishnikov et al., 2000;  
48 Kostyuchenko et al., 2006). Discrete Timanian structures with characteristic WNW–ESE strikes  
49 are sub-orthogonal to the N–S-trending Caledonian grain formed during the closure of the Iapetus  
50 Ocean (Gee et al., 1994; Witt-Nilsson et al., 1998; Johansson et al., 2004; 2005). Thus far,  
51 Timanian structures have only been identified in onshore–nearshore areas of northwestern Russia  
52 and northeastern Norway and offshore in the Russian Barents Sea and southeasternmost Norwegian  
53 Barents Sea (Barrère et al., 2009, 2011; Marelló et al., 2010; Gernigon et al., 2018; Hassaan et al.,  
54 2020a, 2020b). Therefore, the nature of basement rocks in the northern and southwestern  
55 Norwegian Barents Sea remains debatable. Some studies suggest a NE–SW-trending Caledonian  
56 suture within the Barents Sea (Gudlaugsson et al., 1998; Gee and Teben'kov, 2004; Breivik et al.,  
57 2005; Gee et al., 2008; Knudsen et al., 2019), whereas others argue for a swing into a N–S trend  
58 and merging of Norway and Svalbard's Caledonides, which ~~are expected to~~probably continue into  
59 northern Greenland (Ziegler, 1988; Gernigon and Brönnér, 2012; Gernigon et al., 2014).  
60 Regardless, these models solely relate basement structures in the northern and southwestern  
61 Norwegian Barents Sea to the Caledonian Orogeny, implying that Laurentia and Svalbard were not  
62 involved in the Timanian Orogeny and were separated from Baltica by the Iapetus Ocean in the

63 latest Neoproterozoic (Torsvik and Trench, 1991; Cawood et al., 2001; Cocks and Torsvik, 2005;  
64 Torsvik et al., 2010; Merdith et al., 2021).

65 Nonetheless, geochronological data yielding Timanian ages suggest that deformation and  
66 metamorphism contemporaneous of the Timanian Orogeny affected parts of the Svalbard  
67 Archipelago and Laurentia and, possibly, all Arctic regions (Estrada et al., 2018; Figure 1  
68 4a): (1) eclogite facies metamorphism (620–540 Ma; Peucat et al., 1989; Dallmeyer et al., 1990b)  
69 and eclogite facies xenoliths of mafic–intermediate granulite in Quaternary volcanic rocks are  
70 found in northern Spitsbergen (648–556 Ma; Griffin et al., 2012); (2) amphibolite facies  
71 metamorphism (643 ± 9 Ma; Majka et al., 2008, 2012, 2014; Mazur et al., 2009) and WNW–ESE-  
72 striking shear zones like the Vimsodden–Kosibapasset Shear Zone (VKSZ; Figure 1b–c) occur in  
73 southwestern Spitsbergen (600–537 Ma; Manecki et al., 1998; Faehnrich et al., 2020); and (3)  
74 xenoliths of the subduction-related Midtkap igneous suite in northern Greenland yield Timanian  
75 ages (628–570 Ma; Rosa et al., 2016; Estrada et al., 2018). In addition, several recent studies also  
76 show the presence of NW–SE- to E–W-trending basement grain in the Norwegian Barents Sea,  
77 which could possibly represent Timanian fabrics and structures (Figure 1  
78 4b; Barrère et al., 2009, 2011; Marelllo et al., 2010; Klitzke et al., 2019). Following these developments, a few paleo-  
79 plate reconstructions now place Svalbard together with Baltica in the latest Neoproterozoic–  
80 Paleozoic (e.g., Vernikovsky et al., 2011), and imply that the Norwegian Barents Sea and Svalbard  
81 basement may contain Timanian structures overprinted during later (e.g., Caledonian) deformation  
82 events.

83 To test the origin of basement grain in the northern Norwegian Barents Sea and Svalbard,  
84 the present study focuses on several kilometers deep structures identified on 2D seismic reflection  
85 data and correlated using regional gravimetric and magnetic data. These newly identified structures  
86 trend WNW–ESE, i.e., parallel to the Timanian structural grain in northwestern Russia and  
87 northern Norway (Figure 1  
88 4a–c). The structures are described and interpreted based on their  
89 geometry and potential kinematic indicators, and are compared to well-known examples of  
90 Caledonian and Timanian fabrics and structures elsewhere, e.g., onshore Norway (e.g., NNE-  
91 dipping Trollfjorden–Komagelva Fault Zone – TKFZ; Siedlecka and Siedlecki, 1967; Siedlecka,  
92 1975), in Svalbard (e.g., gently north-plunging Atomfjella Antiform – AA; Witt-Nilsson et al.,  
93 1998), in northwestern Russia (NNE-dipping Central Timan Fault – CTF; Siedlecka and Roberts,  
1995; Olovyanishnikov et al., 2000; Kostyuchenko et al., 2006), and in the southern Norwegian

Formatted: Font: 12 pt, Not Bold

Formatted: Font: 12 pt, Not Bold, Not Italic

Formatted: Font: 12 pt, Not Bold

Formatted: Font: 12 pt, Not Bold, Not Italic

Formatted: Font: 12 pt, Not Bold

Formatted: Font: 12 pt, Not Bold, Not Italic

Formatted: Font: 12 pt, Not Bold

Formatted: Font: 12 pt, Not Bold, Not Italic



94 Barents Sea (Barrère et al., 2011; Gernigon et al., 2014) and the Russian Barents Sea (NNE-dipping  
95 Baidaratsky fault zone – BaFZ; Lopatin et al., 2001; Korago et al., 2004; Figure 1b–c). The present  
96 contribution proposes Aa scenario involving several episodes of deformation starting in the  
97 ~~(~~Timanian Orogeny, and involving reactivation and overprinting of Timanian structures during the  
98 Caledonian Orogeny, Devonian–Carboniferous extension, Triassic extension, Eurekan tectonism,  
99 and present-day tectonism), ~~is proposed and~~ Having established that Timanian structure may be  
100 present across the Barents Sea and Svalbard, we briefly discuss the potential implications for the  
101 tectonic evolution of the Barents Sea and the Svalbard Archipelago and associated basins (e.g., Ora  
102 and Olga basins; Anell et al., 2016) ~~are discussed~~.

Formatted: Font: 12 pt, Not Bold

Formatted: Font: 12 pt, Not Bold, Not Italic

103 Should our interpretation of discrete Timanian structures throughout the Norwegian  
104 Barents Sea and Svalbard be validated by future research, it would support accretion of these  
105 terranes to Baltica in the late Neoproterozoic and place the Caledonian suture farther west than is  
106 commonly suggested (e.g., Breivik et al., 2005; Gernigon et al., 2014), thus leading to a major  
107 revision of plate tectonics models. In addition, constraining the extent and reactivation history of  
108 such faults may shed some light on their influence on younger tectonic events, such as Caledonian,  
109 Ellesmerian and Eurekan contraction, Devonian–Carboniferous collapse–rifting, and late Cenozoic  
110 breakup and ongoing extension.

111

## 112 **Geological setting**

### 113 *Timanian Orogeny*

114 The Timanian Orogeny corresponds to a ca. 650–550 Ma episode of NNE–SSW  
115 contractional deformation that affected northwestern Russia and northeastern Norway. During this  
116 tectonic episode, crustal-scale, WNW–ESE-striking, NNE-dipping thrusts systems with south-  
117 southwestwards transport direction (top-SSW; Siedlecka and Siedlecki, 1967; Siedlecka, 1975;  
118 Figure 1~~Figure 1b~~), accreted portions of the Russian Barents Sea and northwestern Russia onto  
119 northeastern Baltica, including Novaya Zemlya, Severnaya Zemlya, the Kanin Peninsula, the  
120 Timan Range, and the Kola Peninsula (Siedlecka and Roberts, 1995; Olovyaniishnikov et al.,  
121 2000; Roberts and Siedlecka, 2002; Gee and Pease, 2004; Kostyuchenko et al., 2006; Lorenz et al.,  
122 2008; Marelllo et al., 2013) and the Varanger Peninsula in northeastern Norway (Siedlecka and  
123 Siedlecki, 1967; Siedlecka, 1975; Roberts and Olovyaniishnikov, 2004; Herrevold et al., 2009;  
124 Drachev, 2016; Figure 1~~Figure 1a~~). Major Timanian thrusts include the NNE-dipping Baidaratsky

Formatted: Font: 12 pt, Not Bold

Formatted: Font: 12 pt, Not Bold, Not Italic

Formatted: Font: 12 pt, Not Bold

Formatted: Font: 12 pt, Not Bold, Not Italic

125 fault zone in the Russian Barents Sea and Novaya Zemlya (~~Figure 1~~Figure 1a–b; Eldholm and  
126 Ewing, 1971, their figure 4 profile C–D; Lopatin et al., 2001; Korago et al., 2004; Drachev, 2016),  
127 the NNE-dipping Central Timan Fault on the Kanin Peninsula and the Timan Range (Siedlecka  
128 and Roberts, 1995; Olovyanishnikov et al., 2000; Kostyuchenko et al., 2006), and the NNE-dipping  
129 Trollfjorden–Komagelva Fault Zone in northern Norway (Siedlecka and Siedlecki, 1967;  
130 Siedlecka, 1975; Herrevold et al., 2009).

Formatted: Font: 12 pt, Not Bold

Formatted: Font: 12 pt, Not Bold, Not Italic

### 132 *Accretion of Svalbard basement terranes in the early Paleozoic*

133 The Svalbard Archipelago consists of three Precambrian basement terranes (Figure 2),  
134 some of which show affinities with Greenland (northwestern and northeastern terranes), whereas  
135 others are possibly derived from Pearya (southwestern terrane; Harland and Wright, 1979; Ohta et  
136 al., 1989; Gee and Teben'kov, 2004; Labrousse et al., 2004; Piepjohn et al., 2013; Fortey and  
137 Bruton, 2013). These terranes ~~are inferred to have possibly~~ accreted during the mid-Paleozoic  
138 Caledonian (collision of Greenland with Svalbard and Norway at ca. 460–410 Ma; Horsfield, 1972;  
139 Dallmeyer et al., 1990a; Johansson et al., 2004, 2005; Faehrich et al., 2020) and Late Devonian  
140 Ellesmerian orogenies (Piepjohn, 2000; Majka and Kosminska, 2017). In these models, accretion  
141 was facilitated via hundreds of kilometers of displacement along (arcuate) N–S-striking strike-slip  
142 faults, such as the Billefjorden Fault Zone (BFZ – Harland, 1969; Harland et al., 1992; Labrousse  
143 et al., 2008) and the Lomfjorden Fault Zone (LFZ – Piepjohn et al., 2019; Figure 2~~Figure 2~~),  
144 although other studies suggest more limited strike-slip displacement (Lamar et al., 1986; Manby  
145 and Lyberis, 1992; Manby et al., 1994; Lamar and Douglass, 1995). Some previous workers  
146 assumed that ~~t~~hese large (strike-slip?) faults ~~are assumed to have~~ extended thousands of  
147 kilometers southwards and ~~to~~ represented the continuation of Caledonian faults in Scotland (Norton  
148 et al., 1987; Dewey and Strachan, 2003). Caledonian contraction resulted in the formation of large  
149 fold and thrust complexes, such as the N–S-trending, gently north-plunging Atomfjella Antiform  
150 in northeastern Spitsbergen (Gee et al., 1994; Witt-Nilsson et al., 1998) and the N–S-trending  
151 Rijpdalen Anticline in Nordaustlandet (Johansson et al., 2004; 2005; Dumais and Brönnner, 2020),  
152 whereas Ellesmerian tectonism ~~is thought to may~~ have formed narrow N–S-trending fold and thrust  
153 belts, like the Dickson Land and Germaniahelvøya fold-thrust zones (McCann, 2000; Piepjohn,  
154 2000; Dallmann and Piepjohn, 2020).

Formatted: Font: 12 pt, Not Bold

Formatted: Font: 12 pt, Not Bold, Not Italic

155 In northern Norway, Timanian thrusts were reactivated–overprinted in subsequent tectonic  
156 events (e.g., Caledonian Orogeny and late–post-Caledonian collapse–rifting) as dominantly strike-  
157 to oblique-slip faults (Siedlecka and Siedlecki, 1971; Roberts et al., 1991; Herrevold et al., 2009;  
158 Rice, 2014). A notable example is the folding and reactivation of Timanian fabrics and structures  
159 (e.g., [NNE-dipping](#) Trollfjorden–Komagelva Fault Zone) during the Caledonian Orogeny  
160 (Siedlecka and Siedlecki, 1971; Herrevold et al., 2009) and intrusion of Mississippian dolerite  
161 dykes along steeply dipping WNW–ESE-striking brittle faults that overprint the Trollfjorden–  
162 Komagelva Fault Zone onshore–nearshore northern Norway (Roberts et al., 1991; Lippard and  
163 Prestvik, 1997; Nasuti et al., 2015; Koehl et al., 2019).

164

#### 165 *Late Paleozoic post-Caledonian collapse and rifting*

166 In the latest Silurian–Devonian, extensional collapse of the Caledonides led to the  
167 deposition of several kilometers thick sedimentary basins such as the Devonian Graben in northern  
168 Spitsbergen (Gee and Moody-Stuart, 1966; Friend et al., 1966; Friend and Moody-Stuart, 1972;  
169 Murascov and Mokin, 1979; Manby and Lyberis, 1992; Manby et al., 1994; Friend et al., 1997;  
170 McCann, 2000; Dallmann and Piepjohn, 2020). In places, N–S-trending basement ridges  
171 potentially exhumed as metamorphic core complexes along bowed, reactivated detachments, such  
172 as the Keisarhjelmen Detachment in northwestern Spitsbergen (Braathen et al., 2018).

173 In the latest Devonian–Mississippian, coal-rich sedimentary strata of the Billefjorden  
174 Group were deposited within normal fault-bounded basins throughout Spitsbergen (Cutbill and  
175 Challinor, 1965; Harland et al., 1974; Cutbill et al., 1976; Aakvik, 1981; Koehl and Muñoz-Barrera,  
176 2018; Koehl, 2020a) and the Norwegian Barents Sea (Koehl et al., 2018a; Tonstad, 2018). As rift-  
177 related normal faulting evolved, Pennsylvanian sedimentation was localized into a few, several  
178 kilometers deep, N–S-trending basins like the Billefjorden Trough (Cutbill and Challinor, 1965;  
179 Braathen et al., 2011; Koehl et al., 2021 in review) and the [E–W-trending](#) Ora Basin (Anell et al.,  
180 2016). In the Permian, rift-related faulting stopped and platform carbonates were deposited  
181 throughout Svalbard (Cutbill and Challinor, 1965) and the Barents Sea (Larssen et al., 2005).

182 Overall, the several kilometers thick, late Paleozoic sedimentary succession deposited  
183 during late–post-Caledonian extension buried Proterozoic basement rocks. As a result, these rocks  
184 are sparsely exposed and, thus, difficult to study.

185

186 ***Mesozoic sedimentation and magmatism***

187 In the Mesozoic, Svalbard and the Barents Sea remained tectonically quiet and were only  
188 affected by minor Triassic normal faulting (e.g., Anell et al., 2013; Osmundsen et al., 2014; Ogata  
189 et al., 2018; Smyrak-Sikora et al., 2020). In the Early Cretaceous, Svalbard was affected by a  
190 regional episode of magmatism recorded by the intrusion of numerous dykes and sills of the  
191 Diabasodden Suite (Senger et al., 2013).

192  
193 ***Early Cenozoic Eurekan tectonism***

194 The opening of the Labrador Sea and Baffin Bay between Greenland and Arctic Canada in  
195 the early Cenozoic (Chalmers and Pulvercraft, 2001; Oakey and Chalmers, 2012) led to the  
196 collision of northern Greenland with Svalbard and the formation of a fold-and-thrust belt with top-  
197 east thrusts and east-verging folds in western Spitsbergen (Dallmann et al., 1993). In eastern  
198 Spitsbergen, this deformation event is characterized by dominantly thin-skinned deformation  
199 structures, including décollements, some of which showing westwards transport directions  
200 (Andresen et al., 1992; Haremo and Andresen, 1992). Notably, the N–S-striking Agardhbukta  
201 Fault, a major splay/segment of the **N–S-striking** Lomfjorden Fault Zone, accommodated reverse  
202 and, possibly, strike-slip movements during this event (Piepjohn et al., 2019).

203  
204 ***Late Cenozoic opening of the Fram Strait***

205 After the end of extension in the Labrador Sea and Baffin Bay, the Fram Strait started to  
206 open in the earliest Oligocene (Engen et al., 2008). Tectonic extension and break-up in the Fram  
207 Strait resulted in the formation of two major, NW–SE-striking transform faults (Lowell, 1972;  
208 Thiede et al., 1990; **Figure 1Figure 1b**).

209  
210 **Methods and datasets**

211 Seismic surveys from the DISKOS database (see **Figure 1Figure 1b–c** and supplement S1  
212 for location) were used to interpret basement-seated structures and related, younger, brittle  
213 overprints (**Figure 3Figure 3a–f** and **Figure 4Figure 4a–h** and supplement S2). Other features of  
214 interest include potential dykes, which commonly appear as high positive reflections on seismic  
215 data. The geology interpreted from onshore seismic data was directly correlated to geological maps  
216 of the Norwegian Polar Institute (e.g., Dallmann, 2015). Where possible, interpretation of offshore

Formatted: Font: 12 pt, Not Bold

Formatted: Font: 12 pt, Not Bold, Not Italic

Formatted: Font: 12 pt, Not Bold

Formatted: Font: 12 pt, Not Bold, Not Italic

Formatted: Font: 12 pt, Not Bold

Formatted: Font: 12 pt, Not Bold, Not Italic

Formatted: Font: 12 pt, Not Bold

Formatted: Font: 12 pt, Not Bold, Not Italic

217 seismic data was tied to onshore geological maps and to exploration wells Raddedalen-1 and  
218 Plurdalen-1 on Edgeøya (Bro and Shvarts, 1983; Harland and Kelly, 1997) and to the Hopen-2 well  
219 on Hopen (Anell et al., 2014; ~~Figure 1~~Figure 1c and supplement S3). The Raddedalen-1 well  
220 penetrated 2823 meters of Upper Permian to Mississippian or Ordovician strata, the Plurdalen well  
221 2351 meters of Middle Triassic to (pre-?) Devonian strata, and the Hopen-2 well 2840 meters of  
222 Middle–Upper Triassic to Pennsylvanian strata (Bro and Shvarts, 1983; Harland and Kelly, 1997;  
223 Anell et al., 2014; Senger et al., 2019). Note that the present contribution favors interpretation of  
224 lower Paleozoic (Ordovician–Silurian) rocks in the Raddedalen-1 well by Bro and Shvarts (1983)  
225 ~~is preferred~~ to that of upper Paleozoic (Upper Devonian–Mississippian) by Cambridge Svalbard  
226 Exploration (see contrasting interpretations in Harland and Kelly, 1997). This is based on the more  
227 detailed lithological, palynological and paleontological analyses by the former, and on the strong  
228 contrast of the lithologies described in the well with Devonian–Mississippian successions on  
229 Svalbard (Cutbill and Challinor, 1965; Cutbill et al., 1976; Friend et al., 1997; Dallmann and  
230 Piepjohn, 2020).

231 The present contribution Only includes a few examples of seismic sections ~~are included~~  
232 ~~in the present contribution~~. However, more interpreted and uninterpreted seismic data are available  
233 as supplements (supplements S1–2) and from the Norwegian Petroleum Directorate (DISKOS  
234 database). None of the seismic sections were depth-converted, and ~~the thicknesses are~~ therefore  
235 appear discussed in seconds (Two-Way Time; TWT). However, local time conversion was  
236 performed to tie seismic wells onshore Edgeøya to seismic section in Storfjorden and depth  
237 conversion was performed locally to evaluate fault displacement. Velocities of Gernigon et al.  
238 (2018) were used in these conversions. ~~Details related to these conversions are shown in~~  
239 Ssupplement S3 includes further details related to these conversions.

240 The correlation of kilometer-thick structures discussed in the present contribution was also  
241 tested using gravimetric and magnetic data in cross section (~~Figure 3~~Figure 3a–f) and regional  
242 magnetic and gravimetric data in the northern Norwegian Barents Sea and Svalbard (Figure  
243 5~~Figure 5~~ and supplement S4) from the Federal Institute for Geosciences and Natural Resources in  
244 Germany in map view (Klitzke et al., 2019). Regional gravimetric and magnetic data are also used  
245 to interpret deep basement fabrics and structures, e.g., regional folds (gravimetric highs commonly  
246 associated with major anticlines of thickened dense basement (i.e., Precambrian) rocks and  
247 gravimetric lows with synclines with less dense sedimentary basins) and large faults that commonly

Formatted: Font: 12 pt, Not Bold

Formatted: Font: 12 pt, Not Bold, Not Italic

Formatted: Font: 12 pt, Not Bold

Formatted: Font: 12 pt, Not Bold, Not Italic

Formatted: Font: 12 pt, Not Bold

Formatted: Font: 12 pt, Not Bold, Not Italic

248 correlate with elongated gravimetric and/or magnetic anomalies (e.g., Koehl et al., 2019), and to  
249 discuss the relationship of the described structures with known structural trends in onshore  
250 basement rocks in Russia, Norway and Svalbard.

251

## 252 **Results and interpretations**

253 First, the interpretation of seismic data are described by area, including (1) Storfjorden  
254 (between Edgeøya and Spitsbergen) and the northeastern part of the Norwegian Barents Sea (east  
255 of Edgeøya), (2) Nordmannsfonna to Sassenfjorden onshore–nearshore the eastern–central part of  
256 Spitsbergen, and (3) the northwestern part of the Norwegian Barents Sea between Bjørnøya and  
257 Spitsbergen (Figure 1b–c). Description in each area starts with deep Precambrian basement  
258 rocks and shallow sedimentary rock units, and ends with deep brittle–ductile structures and with  
259 shallow brittle faults. Then, potential field data and regional gravimetric and magnetic anomalies  
260 in the Barents Sea and Svalbard are described, and compared and correlated to seismic data and to  
261 major Timanian and Caledonian fabrics and structures onshore northwestern Russia, Svalbard and  
262 Norway. Please see high resolution versions of all the figures and supplements on DataverseNO  
263 ([doi.org/10.18710/CE8RQH](https://doi.org/10.18710/CE8RQH)).

264

### 265 *Structures in the northwestern–northeastern Norwegian Barents Sea, Storfjorden and central–* 266 *eastern Spitsbergen*

#### 267 *Storfjorden and northeastern Norwegian Barents Sea*

#### 268 Folded Precambrian–lower Paleozoic basement rocks

269 Seismic facies at depths of 2–6 seconds (TWT) typically comprise successions of laterally  
270 discontinuous (< three kilometers long), sub-horizontal, moderately curving–undulating,  
271 moderate–high-amplitude seismic reflections that alternate with packages of highly-disrupted  
272 and/or curved low-amplitude seismic reflections (see yellow lines within pink and purple units in  
273 Figure 3a and Figure 4a). The curving geometries of the moderate–high amplitude  
274 reflections display a typical kilometer- to hundreds of meter-scale wavelength and are commonly  
275 asymmetric, seemingly leaning/verging towards the south/SSW (see yellow lines in Figure 4  
276 4b). Based on ties with well bores on Edgeøya (Raddedalen-1 well; Bro and Shvarts, 1983; Harland  
277 and Kelly, 1997), these asymmetric, undulate features most likely correspond to SSW-verging  
278 folds in Precambrian–lower Paleozoic basement rocks. In places, apparent reverse offsets of these

Formatted: Font: 12 pt, Not Bold

Formatted: Font: 12 pt, Not Bold, Not Italic

Formatted: Font: 12 pt, Not Bold

Formatted: Font: 12 pt, Not Bold, Not Italic

Formatted: Font: 12 pt, Not Bold

Formatted: Font: 12 pt, Not Bold, Not Italic

Formatted: Font: 12 pt, Not Bold

Formatted: Font: 12 pt, Not Bold, Not Italic

279 undulate reflections align along moderately–gently north- to NNE-dipping surfaces (see red lines  
280 in Figure 4 ~~Figure 4~~a and c), which are therefore interpreted as minor, top-south/SSW, brittle  
281 thrusts.

Formatted: Font: 12 pt, Not Bold

Formatted: Font: 12 pt, Not Bold, Not Italic

### 282 Upper Paleozoic–Mesozoic sedimentary successions

283 In Storfjorden and the northwestern Norwegian Barents Sea, shallow (0–3 seconds TWT)  
284 seismic reflections above folded and thrust Precambrian–lower Paleozoic basement rocks show  
285 significantly more continuous patterns (>> five kilometers), gently curving–undulating geometries  
286 and only local disruptions by shallow, dominantly NNE-dipping, high-angle listric disruptions (see  
287 yellow lines within orange unit in Figure 3 ~~Figure 3~~a and c). In the northeastern Barents Sea, these  
288 reflections are largely flat-lying (see yellow lines within orange unit in Figure 3 ~~Figure 3~~b and d).

Formatted: Font: 12 pt, Not Bold

Formatted: Font: 12 pt, Not Bold, Not Italic

289 Based on field mapping campaigns and well-bores in adjacent onshore areas of Spitsbergen,  
290 Edgeøya, Hopen and Bjørnøya (see location in Figure 1 ~~Figure 1~~b), these continuous reflections are  
291 interpreted as mildly folded upper Paleozoic–Mesozoic (–Cenozoic?) sedimentary strata  
292 (Dallmann and Krasil’scikov, 1996; Harland and Kelly, 1997; Worsley et al., 2001; Dallmann,  
293 2015). The Permian–Triassic boundary was correlated throughout the northern Norwegian Barents  
294 Sea and Storfjorden by using the tie of Anell et al. (2014) to the Hopen-2 well.

Formatted: Font: 12 pt, Not Bold

Formatted: Font: 12 pt, Not Bold, Not Italic

Formatted: Font: 12 pt, Not Bold

Formatted: Font: 12 pt, Not Bold, Not Italic

Formatted: Font: 12 pt, Not Bold

Formatted: Font: 12 pt, Not Bold, Not Italic

### 295 Deep thrust systems

296 The packages of sub-horizontal, moderately curving–undulating (folded Precambrian–  
297 lower Paleozoic basement) reflections alternate laterally from north to south with 20–60 kilometers  
298 wide, up to four seconds thick (TWT), upwards-thickening, wedge-shaped packages (areas with  
299 high concentrations of black lines in Figure 3 ~~Figure 3~~a and d). These wide upwards-thickening  
300 packages consist of two types of reflections. First, they include planar, continuous, gently–  
301 moderately north- to NNE-dipping, sub-parallel, high-amplitude reflections that commonly merge  
302 together downwards and that can be traced and correlated on several seismic sections in Storfjorden  
303 (black lines in Figure 3 ~~Figure 3~~a). Upwards, these reflections terminate against high-amplitude  
304 convex-upwards reflections interpreted as intra- Precambrian–lower Paleozoic basement  
305 reflections (fuchsia lines in Figure 3 ~~Figure 3~~a and c) or continue as moderately NNE-dipping  
306 disruption surfaces that offset these intra-basement reflections top-SSW (e.g., offset intra-  
307 Precambrian unconformities in Figure 3 ~~Figure 3~~a and c and Figure 4 ~~Figure 4~~d).

Formatted: Font: 12 pt, Not Bold

Formatted: Font: 12 pt, Not Bold, Not Italic

Formatted: Font: 12 pt, Not Bold

Formatted: Font: 12 pt, Not Bold, Not Italic

Formatted: Font: 12 pt, Not Bold

Formatted: Font: 12 pt, Not Bold, Not Italic

Formatted: Font: 12 pt, Not Bold

Formatted: Font: 12 pt, Not Bold, Not Italic

Formatted: Font: 12 pt, Not Bold

Formatted: Font: 12 pt, Not Bold, Not Italic

308 Second, sub-parallel, high-amplitude reflections bound wedge-shaped, upwards-thickening  
309 packages of asymmetric, curved, south- to SSW-leaning, moderately north- to NNE-dipping,

310 moderate-amplitude reflections showing narrow (< one kilometer wide) upwards-convex  
311 geometries (Figure 4d). These asymmetric reflections also commonly appear as gently  
312 north- to NNE-dipping packages of Z-shaped reflections bounded by sub-parallel, planar, high-  
313 amplitude reflections (see yellow lines in Figure 4e). Asymmetric, south- to SSW-leaning,  
314 convex-upwards reflections are interpreted as south- to SSW-verging fold anticlines reflecting  
315 relatively low amounts of plastic deformation of layered rocks.

316 The alternation of packages of layered rocks folded into SSW-verging folds (yellow lines  
317 in Figure 3a-c) with packages of planar, NNE-dipping, sub-parallel, high-amplitude  
318 reflections (black lines in Figure 3a-c) suggest that the latter reflection packages represent  
319 zones where initial layering was destroyed and/or possibly reoriented, i.e., areas that  
320 accommodated larger amounts of deformation and tectonic displacement. Thus, planar, gently-  
321 moderately north- to NNE-dipping, high-amplitude reflections (black lines in Figure 3a-  
322 c) are interpreted as low-angle brittle-ductile thrust systems. We name these thrust systems (from  
323 north to south) the Steiløya-Krylen (SKFZ), Kongsfjorden-Cowanodden (KCFZ),  
324 Bellsundbanken (BeFZ), and Kinnhøgda-Daubjørnpynten fault zones (KDFZ; Figure 3a  
325 and supplement S2a-b; see Figure 1c for location of the thrusts).

326 The relatively high-amplitude character of planar, NNE-dipping reflections within the  
327 thrusts suggest that these tectonic structures consist of sub-parallel layers of rocks and minerals  
328 with significantly different physical properties. A probable explanation for such laterally  
329 continuous and consistently high-amplitude reflections is partial recrystallization of rocks layers-  
330 mineral bands into rocks and minerals with significantly higher density along intra-thrust planes  
331 that accommodated large amounts of displacement (e.g., mylonitization; Fountain et al., 1984;  
332 Hurich et al., 1985). In places, packages of aggregates of Z-shaped reflections bounded upwards  
333 and downwards by individual low-angle thrust surfaces are interpreted as forward-dipping duplex  
334 structures (e.g., Boyer and Elliott, 1982) reflecting relatively strong plastic deformation between  
335 low-angle, brittle-ductile (mylonitic?) thrusts (see yellow lines in Figure 4e).

336 The Kongsfjorden-Cowanodden, Bellsundbanken, and Kinnhøgda-Daubjørnpynten fault  
337 zones can be traced east-southeast of Edgeøya as a similar series of 20-60 kilometers wide, up to  
338 four seconds thick (TWT), upwards-thickening packages (e.g., black lines in Figure 3d  
339 and supplements S2a). However, their imaging along NNW-SSE-trending seismic sections is  
340 much more chaotic and it is more difficult to identify smaller structures (like south-verging folds

Formatted: Font: 12 pt, Not Bold

Formatted: Font: 12 pt, Not Bold, Not Italic

Formatted: Font: 12 pt, Not Bold

Formatted: Font: 12 pt, Not Bold, Not Italic

Formatted: Font: 12 pt, Not Bold

Formatted: Font: 12 pt, Not Bold, Not Italic

Formatted: Font: 12 pt, Not Bold

Formatted: Font: 12 pt, Not Bold, Not Italic

Formatted: Font: 12 pt, Not Bold

Formatted: Font: 12 pt, Not Bold, Not Italic

Formatted: Font: 12 pt, Not Bold

Formatted: Font: 12 pt, Not Bold, Not Italic

Formatted: Font: 12 pt, Not Bold

Formatted: Font: 12 pt, Not Bold, Not Italic

Formatted: Font: 12 pt, Not Bold

Formatted: Font: 12 pt, Not Bold, Not Italic

Formatted: Font: 12 pt, Not Bold

Formatted: Font: 12 pt, Not Bold, Not Italic



341 and minor thrusts) within each thrust system (e.g., supplement S2a). This suggests that these three  
342 thrust systems strike oblique to NNW–SSE-trending seismic sections (supplement S2a), whereas  
343 they are most likely sub-orthogonal to N–S- to NNE–SSW-trending seismic sections in Storfjorden  
344 (Figure 3a). The only orientation that reconciles these seismic facies variations (i.e., well-  
345 imaged on NNE–SSW-trending seismic sections and poorly imaged by NNW–SSE-trending  
346 seismic sections; Figure 3a and supplement S2a) is an overall WNW–ESE strike.

347 South of each 20–60 kilometers wide packages of thrust surfaces and related fold and  
348 duplex structures, seismic reflections representing Precambrian–lower Paleozoic basement rocks  
349 typically appear as gently curved, convex-upwards, relatively continuous reflections showing sub-  
350 horizontal seismic onlaps (see white arrows in Figure 3a–f). This suggests that  
351 Precambrian–lower Paleozoic basement rocks most likely consist (meta-) sedimentary rocks  
352 (analogous to those observed in northeastern Spitsbergen and Nordaustlandet; Harland et al., 1993;  
353 Stouge et al., 2011) that were deposited in foreland and piggy-back basins ahead of each 20–60  
354 kilometers wide packages (Figure 3a–f).

355 Hence, based on the upwards-thickening geometry of the packages of south- to SSW-  
356 verging folds and of forward-dipping duplexes, on the top-SSW reverse offsets of intra-basement  
357 reflections by low-angle brittle–ductile thrust surfaces, on the upwards truncation of these low-  
358 angle thrusts by intra-basement reflections, and on the overlapping geometries of (meta-)  
359 sedimentary basement rocks south of each set of top-SSW thrust surfaces, the 20–60 kilometers  
360 wide, upwards-thickening, wedge-shaped packages are interpreted as crustal-scale, several  
361 kilometers thick, north- to NNE-dipping, top-SSW, brittle–ductile thrust systems (see fault zones  
362 with high concentration of black lines in Figure 3a–f). These thrust systems include low-  
363 angle, brittle–ductile, mylonitic thrust surfaces (black lines in Figure 4d–e) separating  
364 upwards-thickening thrust sheets that consist of gently to strongly folded basement rocks and  
365 forward-dipping duplex structures (yellow lines in Figure 4d–e). These thrust sheets are  
366 interpreted to reflect accretion and stacking from the north or north-northeast. The interpreted thrust  
367 systems are comparable in seismic facies and thickness to kilometer-thick mylonitic shear zones in  
368 the Norwegian North Sea (Phillips et al. 2016) and southwestern Norwegian Barents Sea (Koehl et  
369 al., 2018).

370 N–S-trending folds

Formatted: Font: 12 pt, Not Bold

Formatted: Font: 12 pt, Not Bold, Not Italic

Formatted: Font: 12 pt, Not Bold

Formatted: Font: 12 pt, Not Bold, Not Italic

Formatted: Font: 12 pt, Not Bold

Formatted: Font: 12 pt, Not Bold, Not Italic

Formatted: Font: 12 pt, Not Bold

Formatted: Font: 12 pt, Not Bold, Not Italic

Formatted: Font: 12 pt, Not Bold

Formatted: Font: 12 pt, Not Bold, Not Italic

Formatted: Font: 12 pt, Not Bold

Formatted: Font: 12 pt, Not Bold, Not Italic, Check spelling and grammar

Formatted: Font: 12 pt, Not Bold

Formatted: Font: 12 pt, Not Bold, Not Italic, Check spelling and grammar

371 On E–W seismic cross sections, reflections of the Kongsfjorden–Cowanodden,  
372 Bellsundbanken, and Kinnhøgda–Daudbjørnpynten fault zones define large, 50–100 kilometers  
373 wide, U-shaped, symmetrical depressions (black lines in [Figure 3Figure 3b](#)) on the edge of which  
374 they are truncated at a high angle and overlain by folded lower Paleozoic and mildly folded to flat-  
375 lying upper Paleozoic (meta-) sedimentary rocks (purple and orange units with associated yellow  
376 lines in [Figure 3Figure 3b](#)). In addition, within these U-shaped depressions, the thrust systems show  
377 curving up and down, symmetrical geometries with 5–15 kilometers wavelength (yellow lines  
378 within the pink unit in [Figure 3Figure 3b](#) and [Figure 4Figure 4f](#)). Also notice the kilometer- to  
379 hundreds of meter-scale undulating pattern of 5–15 kilometers wide curved geometries (yellow  
380 lines in [Figure 4Figure 4f](#)). Based on the truncation and abrupt upward disappearance of high-  
381 amplitude seismic reflections characterizing the thrust systems, the high-angle truncation of the  
382 thrusts is interpreted as a major erosional unconformity (dark blue line in [Figure 3Figure 3b](#) and  
383 pink line in [Figure 4Figure 4f](#)), and the large U-shaped depressions as large N–S- to NNE–SSW-  
384 trending, upright regional folds (black lines in [Figure 3Figure 3b](#)). Furthermore, the 5–15  
385 kilometers wide, symmetrical, curved geometries and associated, kilometer- to hundreds of meter-  
386 scale, undulating pattern of seismic reflections within the thrusts are interpreted as similarly (N–S-  
387 to NNE–SSW-) trending, upright, parasitic macro- to meso-scale folds (yellow lines in [Figure](#)  
388 [3Figure 3b](#) and [Figure 4Figure 4f](#)).

### 389 Shallow brittle faults

390 In places, near the top of the 20–60 kilometers wide thrust systems (Kongsfjorden–  
391 Cowanodden, Bellsundbanken, and Kinnhøgda–Daudbjørnpynten fault zones), low-angle brittle–  
392 ductile thrust surfaces merge upwards with high-angle to vertical, listric, north- to NNE-dipping  
393 disruption surfaces at depths of c. 2–3 seconds (TWT; see red lines in [Figure 3Figure 3a](#) and d).  
394 These listric disruption surfaces truncate shallow, laterally continuous reflections that display  
395 gently curved, symmetric geometries in Storfjorden (yellow lines in [Figure 3Figure 3a](#)) and flat-  
396 lying geometries in the northeastern Norwegian Barents Sea (yellow lines in [Figure 3Figure 3d](#)).  
397 Notably, they show minor, down-NNE normal offsets, and related minor southwards thickening  
398 (towards the disruption) of seismic sub-units within Devonian–Carboniferous (–Permian?)  
399 sedimentary strata in the north, both in Storfjorden and the northeastern Barents Sea ([Figure](#)  
400 [3Figure 3a–d](#) and white double arrows in [Figure 4Figure 4g](#)). In addition, they display minor  
401 reverse offsets and associated gentle upright folding of shallow continuous reflections potentially

Formatted: Font: 12 pt, Not Bold

Formatted: Font: 12 pt, Not Bold, Not Italic

Formatted: Font: 12 pt, Not Bold

Formatted: Font: 12 pt, Not Bold, Not Italic

Formatted: Font: 12 pt, Not Bold

Formatted: Font: 12 pt, Not Bold, Not Italic

Formatted: Font: 12 pt, Not Bold

Formatted: Font: 12 pt, Not Bold, Not Italic

Formatted: Font: 12 pt, Not Bold

Formatted: Font: 12 pt, Not Bold, Not Italic

Formatted: Font: 12 pt, Not Bold

Formatted: Font: 12 pt, Not Bold, Not Italic

Formatted: Font: 12 pt, Not Bold

Formatted: Font: 12 pt, Not Bold, Not Italic

Formatted: Font: 12 pt, Not Bold

Formatted: Font: 12 pt, Not Bold, Not Italic

Formatted: Font: 12 pt, Not Bold

Formatted: Font: 12 pt, Not Bold, Not Italic

Formatted: Font: 12 pt, Not Bold

Formatted: Font: 12 pt, Not Bold, Not Italic

Formatted: Font: 12 pt, Not Bold

Formatted: Font: 12 pt, Not Bold, Not Italic

Formatted: Font: 12 pt, Not Bold

Formatted: Font: 12 pt, Not Bold, Not Italic

Formatted: Font: 12 pt, Not Bold

Formatted: Font: 12 pt, Not Bold, Not Italic

Formatted: Font: 12 pt, Not Bold

Formatted: Font: 12 pt, Not Bold, Not Italic

Formatted: Font: 12 pt, Not Bold

Formatted: Font: 12 pt, Not Bold, Not Italic

402 representing upper Mesozoic (–Cenozoic?) sedimentary deposits in Storfjorden (Figure 3a–c and e, and orange lines in Figure 4h). Note that flat-lying Mesozoic (–Cenozoic?)  
403 sedimentary rocks are not offset in the northeastern Norwegian Barents Sea (Figure 3d).

404  
405 Based on the observed normal offsets and southwards-thickening of Devonian–  
406 Carboniferous (–Permian?) sedimentary strata north of these disruption surfaces (e.g., white double  
407 arrows in Figure 4g), these are interpreted as syn-sedimentary Devonian–Carboniferous  
408 normal faults. The minor reverse offsets and associated gentle upright folding of Mesozoic (–  
409 Cenozoic?) sedimentary rocks in Storfjorden (e.g., orange lines in Figure 4h) suggest that  
410 these normal faults were mildly inverted near Svalbard in the Cenozoic. However, it is unclear  
411 whether inversion in Storfjorden initiated in the early Cenozoic or later. Nonetheless, minor reverse  
412 offset and folding of the seafloor clearly indicate ongoing inversion along these faults (Figure  
413 3a and c, and Figure 4h). Furthermore, considering the merging relationship  
414 between these high-angle listric disruption surfaces and underlying shear zones (i.e., merging black  
415 and red lines in Figure 3a and c–d), we propose that the formation of Devonian–  
416 Carboniferous normal faults was controlled by the crustal-scale, north- to NNE-dipping (inherited)  
417 thrust systems (Kongsfjorden–Cowanodden, Bellsundbanken, and Kinnhøgda–Daudbjørnpynten  
418 fault zones).

419  
420 *Nordmannsonna–Sassenfjorden (eastern–central Spitsbergen)*  
421 Deep thrust system and N–S-trending folds

422 Seismic data from Nordmannsonna to Sassenfjorden in eastern Spitsbergen (see Figure  
423 1c for location) show reflection packages including both planar, continuous, moderately-  
424 dipping high-amplitude reflections and upwards-curving, moderate-amplitude reflections (black  
425 and yellow lines in Figure 3e–f). These two sets are similar to reflection packages  
426 interpreted as low-angle, brittle–ductile mylonitic thrusts bounding packages of south- to SSW-  
427 verging folds in Storfjorden and the northeastern Norwegian Barents Sea (black and yellow lines  
428 in Figure 3a and d, and supplement S2a). In addition, they are located at similar depths (>  
429 2 seconds TWT) and seem to align with the Kongsfjorden–Cowanodden fault zone in Storfjorden  
430 along a WNW–ESE-trending axis. Hence, we interpret the deep, continuous, high-amplitude  
431 reflections in eastern Spitsbergen as the western continuation of the top-SSW Kongsfjorden–  
432 Cowanodden fault zone. This thrust can be traced on seismic data as gently NNE-dipping, high-

Formatted: Font: 12 pt, Not Bold

Formatted: Font: 12 pt, Not Bold, Not Italic

Formatted: Font: 12 pt, Not Bold

Formatted: Font: 12 pt, Not Bold, Not Italic

Formatted: Font: 12 pt, Not Bold

Formatted: Font: 12 pt, Not Bold, Not Italic

Formatted: Font: 12 pt, Not Bold

Formatted: Font: 12 pt, Not Bold, Not Italic

Formatted: Font: 12 pt, Not Bold

Formatted: Font: 12 pt, Not Bold, Not Italic

Formatted: Font: 12 pt, Not Bold

Formatted: Font: 12 pt, Not Bold, Not Italic

Formatted: Font: 12 pt, Not Bold

Formatted: Font: 12 pt, Not Bold, Not Italic

Formatted: Font: 12 pt, Not Bold

Formatted: Font: 12 pt, Not Bold, Not Italic

Formatted: Font: 12 pt, Not Bold

Formatted: Font: 12 pt, Not Bold, Not Italic

Formatted: Font: 12 pt, Not Bold

Formatted: Font: 12 pt, Not Bold, Not Italic

Formatted: Font: 12 pt, Not Bold

Formatted: Font: 12 pt, Not Bold, Not Italic

433 amplitude reflections in Sassendalen and Sassenfjorden–Tempelfjorden (supplement S2c–d), and  
434 possibly in Billefjorden (Koehl et al., 2021 in review, their figure 9a–b).

435 In Nordmannsonna, ~~the Kongsfjorden–Cowanodden fault zone (black lines in Figure 3e–~~  
436 ~~f) is truncated upwards by~~ the base-Pennsylvanian unconformity (white line in ~~Figure 3~~Figure 3e–  
437 f; tied to onshore geological maps; Dallmann, 2015) ~~truncates the Kongsfjorden–Cowanodden fault~~  
438 ~~zone (black lines in Figure 3e–f) upwards and the fault~~ shows pronounced variations in dip  
439 direction, ranging from east-dipping in the east to NNE-dipping in the north and WNW-dipping in  
440 the west, which result into a c. 15–20 kilometers wide, north- to NNE-plunging dome-  
441 shaped/convex-upwards geometry (black lines in ~~Figure 3~~Figure 3e–f). This portion of the thrust  
442 system is interpreted to be folded into a major NNE- to north-plunging upright fold, whose 3D  
443 geometry was accurately constrained due to good seismic coverage in this area (~~Figure 1~~Figure  
444 4c).

445 Small-scale structures within the Kongsfjorden–Cowanodden fault zone also show  
446 asymmetric folds and internal seismic units terminating upwards with convex-upwards reflections  
447 (yellow lines in ~~Figure 3~~Figure 3e–f) suggesting top-SSW nappe thrusting in the northern portion  
448 of the thrust system. However, on E–W cross sections, seismic data reveal a set of west-verging  
449 folds in the east and a more chaotic pattern of symmetrical, dominantly upright folds in the west  
450 (yellow lines in ~~Figure 3~~Figure 3e) and below a major, high-angle, east-dipping disruption surface  
451 (thick red line in ~~Figure 3~~Figure 3e) that crosscuts the Kongsfjorden–Cowanodden fault zone.

#### 452 Shallow brittle faults

453 The high-angle, east-dipping disruption surface (thick red line in ~~Figure 3~~Figure 3e) is  
454 associated with minor subvertical to steeply east-dipping disruption surfaces (thin red lines in  
455 ~~Figure 3~~Figure 3e). This feature shows a major reverse, top-west offset (> 0.5 second TWT) of  
456 seismic units and reflections at depth > 0.75 second (TWT; e.g., black lines in ~~Figure 3~~Figure 3e),  
457 and minor reverse offset (< 0.1 second TWT) and upwards-convex curving of adjacent reflections  
458 at depth < 0.75 second (TWT; white line and yellow lines within blue and units in ~~Figure 3~~Figure  
459 3e). Since the major disruption coincides with the location of the Agardhbukta Fault (Piepjohn et  
460 al., 2019; see ~~Figure 1~~Figure 4 for location) and shows a steep inclination near the surface similar  
461 to that of the Agardhbukta Fault, it is interpreted as the subsurface expression of this fault. The  
462 Agardhbukta Fault offsets the Kongsfjorden–Cowanodden fault zone in a reverse fashion (>0.5  
463 second TWT; black lines in ~~Figure 3~~Figure 3e), and terminates upwards within and slightly offsets

Formatted: Font: 12 pt, Not Bold

Formatted: Font: 12 pt, Not Bold, Not Italic

Formatted: Font: 12 pt, Not Bold

Formatted: Font: 12 pt, Not Bold, Not Italic

Formatted: Font: 12 pt, Not Bold

Formatted: Font: 12 pt, Not Bold, Not Italic

Formatted: Font: 12 pt, Not Bold

Formatted: Font: 12 pt, Not Bold, Not Italic

Formatted: Font: 12 pt, Not Bold

Formatted: Font: 12 pt, Not Bold, Not Italic

Formatted: Font: 12 pt, Not Bold

Formatted: Font: 12 pt, Not Bold, Not Italic

Formatted: Font: 12 pt, Not Bold

Formatted: Font: 12 pt, Not Bold, Not Italic

Formatted: Font: 12 pt, Not Bold

Formatted: Font: 12 pt, Not Bold, Not Italic

Formatted: Font: 12 pt, Not Bold

Formatted: Font: 12 pt, Not Bold, Not Italic

Formatted: Font: 12 pt, Not Bold

Formatted: Font: 12 pt, Not Bold, Not Italic

Formatted: Font: 12 pt, Not Bold

Formatted: Font: 12 pt, Not Bold, Not Italic

Formatted: Font: 12 pt, Not Bold

Formatted: Font: 12 pt, Not Bold, Not Italic

Formatted: Font: 12 pt, Not Bold

Formatted: Font: 12 pt, Not Bold, Not Italic

464 upper Paleozoic–Mesozoic sedimentary rocks (blue and black units and associated yellow lines in  
465 Figure 3Figure 3e), which were correlated to onshore outcrops in eastern Spitsbergen (Andresen et  
466 al., 1992; Haremo and Andresen, 1992; Dallmann, 2015). As a result, these rocks are folded into a  
467 N–S-trending, open, upright fold around the fault tip, both of which suggest top-west movements  
468 along the fault (Figure 3Figure 3e).

#### 469 Pre-Pennsylvanian dykes

470 In the hanging wall and on the eastern flank of the folded Kongsfjorden–Cowanodden fault  
471 zone in Nordmannsfonna, high- to low-amplitude, gently east-dipping seismic reflections, which  
472 possibly represent sedimentary strata (light orange unit in Figure 3Figure 3e), are crosscut but not  
473 offset by moderately west-dipping, high-amplitude planar reflections (blue lines in Figure 3Figure  
474 3e). In NNE–SSW-trending cross-sections, these high-amplitude, cross-cutting seismic reflections  
475 appear sub-horizontal (blue lines in Figure 3Figure 3f). These crosscutting, west-dipping  
476 reflections are mildly folded in places and either terminate upwards within the suggested, gently  
477 east-dipping, sedimentary strata (light orange unit in Figure 3Figure 3e) or are truncated by the  
478 base-Pennsylvanian unconformity (white line in Figure 3Figure 3e). Downwards within the  
479 Kongsfjorden–Cowanodden fault zone (black lines in Figure 3Figure 3e), these inclined reflections  
480 can be vaguely traced as a series of discontinuous, subtle features (see blue lines in Figure 3Figure  
481 3e). In the footwall of the Kongsfjorden–Cowanodden fault zone, the inclined reflections become  
482 more prominent again, still do not offset background reflections, and extend to depths of 3–3.5  
483 seconds (TWT; blue lines in Figure 3Figure 3e). The high amplitude of these planar west-dipping  
484 reflections, the absence of offset across them, and their discontinuous geometries across the  
485 Agardhbukta Fault and the Kongsfjorden–Cowanodden fault zone suggest that they may represent  
486 dykes (see Phillips et al., 2018). Because they appear truncated by the Base-Pennsylvanian  
487 unconformity, we suggest such dykes were emplaced prior to development of this unconformity.  
488 The Kongsfjorden–Cowanodden fault zone is folded into a broad, 15–20 kilometers wide anticline,  
489 and offset > 0.5 second (TWT) by the Agardhbukta Fault, whereas the west-dipping dykes (blue  
490 lines in Figure 3Figure 3e) and the gently east-dipping sedimentary strata they intrude (light orange  
491 unit in Figure 3Figure 3e) are only mildly folded and show no offset across the Agardhbukta Fault  
492 (Figure 3Figure 3e). These differences in deformation suggest that the latter were deformed during  
493 a mild episode of late contraction but not by the same early episode of intense contraction that  
494 resulted in macrofolding of the Kongsfjorden–Cowanodden fault zone.

Formatted: Font: 12 pt, Not Bold

Formatted: Font: 12 pt, Not Bold, Not Italic

Formatted: Font: 12 pt, Not Bold

Formatted: Font: 12 pt, Not Bold, Not Italic

Formatted: Font: 12 pt, Not Bold

Formatted: Font: 12 pt, Not Bold, Not Italic

Formatted: Font: 12 pt, Not Bold

Formatted: Font: 12 pt, Not Bold, Not Italic

Formatted: Font: 12 pt, Not Bold

Formatted: Font: 12 pt, Not Bold, Not Italic

Formatted: Font: 12 pt, Not Bold

Formatted: Font: 12 pt, Not Bold, Not Italic

Formatted: Font: 12 pt, Not Bold

Formatted: Font: 12 pt, Not Bold, Not Italic

Formatted: Font: 12 pt, Not Bold

Formatted: Font: 12 pt, Not Bold, Not Italic

Formatted: Font: 12 pt, Not Bold

Formatted: Font: 12 pt, Not Bold, Not Italic

Formatted: Font: 12 pt, Not Bold

Formatted: Font: 12 pt, Not Bold, Not Italic

Formatted: Font: 12 pt, Not Bold

Formatted: Font: 12 pt, Not Bold, Not Italic

Formatted: Font: 12 pt, Not Bold

Formatted: Font: 12 pt, Not Bold, Not Italic

Formatted: Font: 12 pt, Not Bold

Formatted: Font: 12 pt, Not Bold, Not Italic

495 Cretaceous dykes and sills

496 Near or at the surface, thin, kilometer-wide, lenticular packages of gently dipping,  
497 moderate–high-amplitude seismic reflections (black units in [Figure 3Figure 3e–f](#)) correlate with  
498 surface outcrops of Cretaceous sills of the Diabasodden Suite in eastern Spitsbergen (Senger et al.,  
499 2013; Dallmann, 2015). In places, these sills are associated with areas showing high-frequency  
500 disruptions of underlying sub-horizontal seismic reflections (dotted black lines in [Figure 3Figure](#)  
501 [3f](#)) correlated with onshore occurrences of Pennsylvanian–Mesozoic sedimentary strata (Andresen  
502 et al., 1992; Haremo and Andresen, 1992; Dallmann, 2015). We interpret these areas of high-  
503 frequency disruption in otherwise relatively undisturbed and only mildly deformed Pennsylvanian–  
504 Mesozoic sedimentary strata as zones with occurrences of Cretaceous feeder dykes. Alternatively,  
505 disruption may be related to scattering and attenuation of seismic energy caused on the sills.

506

507 *Stappen High (northwestern Norwegian Barents Sea north of Bjørnøya)*

508 On the Stappen High between Bjørnøya and Spitsbergen ([Figure 1Figure 1c](#)), seismic  
509 reflections at depth of 2–6 seconds (TWT) are dominated by moderate- to high-amplitude  
510 reflections with limited (< five kilometers) lateral continuity showing asymmetric, dominantly  
511 SSW-leaning curving geometries with a few hundreds of meters to a few kilometers width (yellow  
512 lines within pink unit in [Figure 3Figure 3c](#)), i.e., analogous to those in folded Precambrian  
513 basement rocks farther north ([Figure 3Figure 3a](#) and [Figure 4Figure 4a](#)). These reflections are  
514 truncated by gently to moderately NNE- (and subsidiary SSW-) dipping disruption surfaces (black  
515 lines within pink and purple units in [Figure 3Figure 3c](#)), some of which connect upwards with  
516 shallow (0–2 seconds TWT), NNE-dipping, high-angle listric disruptions near Bjørnøya in the  
517 south (red lines in [Figure 3Figure 3c](#)). Notably, major seismic reflections near the upwards  
518 termination of deep, moderately–gently NNE-dipping disruption surfaces display characteristic  
519 gently curving-upwards geometries (yellow lines within pink and purple units in [Figure 3Figure](#)  
520 [3c](#)) and overlying seismic onlaps (white half arrows in [Figure 3Figure 3c](#)) similar to those observed  
521 just south of major NNE-dipping thrust systems in Storfjorden and the northeastern Norwegian  
522 Barents Sea ([Figure 3Figure 3a](#) and supplement S2).

523 We interpret deep (2–6 seconds TWT), curving, discontinuous seismic reflections ((yellow  
524 lines within pink and purple units in [Figure 3Figure 3c](#)) as folded Precambrian–lower Paleozoic  
525 basement rocks, and dominantly NNE-dipping disruption surfaces (black lines within pink and

Formatted: Font: 12 pt, Not Bold

Formatted: Font: 12 pt, Not Bold, Not Italic

Formatted: Font: 12 pt, Not Bold

Formatted: Font: 12 pt, Not Bold, Not Italic

Formatted: Font: 12 pt, Not Bold

Formatted: Font: 12 pt, Not Bold, Not Italic

Formatted: Font: 12 pt, Not Bold

Formatted: Font: 12 pt, Not Bold, Not Italic

Formatted: Font: 12 pt, Not Bold

Formatted: Font: 12 pt, Not Bold, Not Italic

Formatted: Font: 12 pt, Not Bold

Formatted: Font: 12 pt, Not Bold, Not Italic

Formatted: Font: 12 pt, Not Bold

Formatted: Font: 12 pt, Not Bold, Not Italic

Formatted: Font: 12 pt, Not Bold, Not Italic

Formatted: Font: 12 pt, Not Bold

Formatted: Font: 12 pt, Not Bold, Not Italic

Formatted: Font: 12 pt, Not Bold

Formatted: Font: 12 pt, Not Bold, Not Italic

Formatted: Font: 12 pt, Not Bold

Formatted: Font: 12 pt, Not Bold, Not Italic

Formatted: Font: 12 pt, Not Bold

Formatted: Font: 12 pt, Not Bold, Not Italic

526 purple units in [Figure 3](#) as brittle–ductile thrust possibly partly mylonitic, though with  
527 less intense deformation than the major NNE-dipping thrust systems observed farther north in  
528 Storfjorden and the northeastern Norwegian Barents Sea, like the Kongsfjorden–Cowanodden fault  
529 zone. These brittle–ductile thrusts can be traced eastwards on seismic data on the Stappen High  
530 and into the Sørkapp Basin ([Figure 1](#)).

531 Based on their geometries and on gentle folding of the seafloor reflection (yellow lines  
532 within green unit in [Figure 3](#)), shallow, NNE-dipping, high-angle listric disruptions are  
533 interpreted as mildly inverted normal faults overprinting deep NNE-dipping thrusts. Based on  
534 previous fieldwork on Bjørnøya (Worsley et al., 2001), on seismic mapping in the area (Lasabuda  
535 et al., 2018), and on well tie to Hopen and Edgeøya, relatively continuous (> five kilometers)  
536 shallow (0–2 seconds TWT), gently curved–undulating seismic reflections overlying folded  
537 Precambrian–lower Paleozoic basement rocks are interpreted as mildly folded upper Paleozoic–  
538 Mesozoic (–Cenozoic?) sedimentary strata (orange and green units in [Figure 3](#)).

#### 540 *Potential field data and regional gravimetric and magnetic anomalies*

##### 541 *NNE-dipping thrusts*

542 In the northern Barents Sea, Storfjorden and central–eastern Spitsbergen, the seismic  
543 occurrences of the Kongsfjorden–Cowanodden, Bellsundbanken and Kinnhøgda–  
544 Daudbjørnpynten fault zones coincide with gradual, step-like, southwards increases in gravimetry  
545 and, in places, with high magnetic anomalies in cross-section ([Figure 3](#) a–b and d–f).  
546 Similar southwards gradual and step-like increases in the Bouguer and magnetic anomalies  
547 correlate with major thrusts north of Bjørnøya ([Figure 3](#) c; see [Figure 1](#) for  
548 location of Bjørnøya). These patterns suggest that the footwall of the thrust systems consists of  
549 relatively denser rock units, which is supported by seismic interpretation showing thickening of  
550 metamorphosed and folded Precambrian basement rock units (pink unit in [Figure 3](#) a and  
551 c–d) in the footwall of the thrusts [further support this claim](#).

552 In map-view gravimetric and magnetic data, the three thrust systems in Storfjorden (black  
553 lines in [Figure 3](#) a) coincide with three high, WNW–ESE-trending, continuous, gently  
554 undulating (and, in place, merging/splaying) gravimetric and discontinuous magnetic anomalies  
555 (dashed yellow lines in [Figure 5](#) a–c) that are separated from each other by areas showing  
556 relatively low gravimetric and magnetic anomalies (e.g., see green to blue areas in [Figure 5](#)).

Formatted: Font: 12 pt, Not Bold

Formatted: Font: 12 pt, Not Bold, Not Italic

Formatted: Font: 12 pt, Not Bold

Formatted: Font: 12 pt, Not Bold, Not Italic

Formatted: Font: 12 pt, Not Bold

Formatted: Font: 12 pt, Not Bold, Not Italic

Formatted: Font: 12 pt, Not Bold

Formatted: Font: 12 pt, Not Bold, Not Italic

Formatted: Font: 12 pt, Not Bold

Formatted: Font: 12 pt, Not Bold, Not Italic

Formatted: Font: 12 pt, Not Bold

Formatted: Font: 12 pt, Not Bold, Not Italic

Formatted: Font: 12 pt, Not Bold

Formatted: Font: 12 pt, Not Bold, Not Italic

Formatted: Font: 12 pt, Not Bold

Formatted: Font: 12 pt, Not Bold, Not Italic

Formatted: Font: 12 pt, Not Bold

Formatted: Font: 12 pt, Not Bold, Not Italic

Formatted: Font: 12 pt, Not Bold

Formatted: Font: 12 pt, Not Bold, Not Italic

Formatted: Font: 12 pt, Not Bold

Formatted: Font: 12 pt, Not Bold, Not Italic

557 5a). Some of these anomalies extend from central Spitsbergen to Storfjorden and the northern  
558 Barents Sea (below the Ora and Olga basins) as curving, E–W- and NW–SE-trending, 50–100  
559 kilometers wide anomalies (dashed yellow lines in [Figure 5Figure 5a–c](#)). Analogously, thrust  
560 systems north of Bjørnøya ([Figure 3Figure 3c](#)) and north of the Ora and Olga basins (supplement  
561 S2b) correlate with comparable WNW–ESE-trending, curving magnetic and gravimetric anomalies  
562 (dashed yellow lines in [Figure 5Figure 5a–c](#)). The WNW–ESE-trending anomalies appear clearer  
563 by using a slope-direction shader [for gravimetric data](#), which accentuates the contrast between each  
564 trend of anomalies (green and red areas in [Figure 5Figure 5b](#)).

565 Most of the recognized, regional WNW–ESE-trending magnetic and gravimetric anomalies  
566 (dashed yellow lines in [Figure 5Figure 5a–c](#)) can be traced into the Russian Barents Sea where they  
567 are linear and are crosscut by major N–S- to NNW–SSE-trending anomalies (dashed black and  
568 white lines in [Figure 5Figure 5a–c](#)). Subtle WNW–ESE-trending magnetic and gravimetric  
569 anomalies further extend onshore northwestern Russia (e.g., Kanin Peninsula and southern Novaya  
570 Zemlya) where they correlate with major Timanian thrusts and folds, some of which are suspected  
571 to extend thousands of kilometers between northwestern Russia and the Varanger Peninsula in  
572 northern Norway (e.g., Trollfjorden–Komagelva Fault Zone and Central Timan Fault; Siedlecka,  
573 1975; Siedlecka and Roberts, 1995; Olovyanishnikov et al., 2000; Kostyuchenko et al., 2006). In  
574 addition, two of the southernmost WNW–ESE-trending gravimetric and magnetic anomalies  
575 coincide with the location of well known, crustal-scale, SSW-verging Timanian thrust faults, the  
576 Trollfjorden–Komagelva Fault Zone and the Central Timan Fault. Thus, based on their overall  
577 WNW–ESE trend, patterns of alternating highs and lows both for gravimetric and magnetic  
578 anomalies (see [Figure 5Figure 5a](#)), location at the boundary of oppositely dipping slopes (see slope-  
579 direction shader map in [Figure 5Figure 5b](#)), and extensive field studies and seismic and well data  
580 in northwestern Russia (e.g., Kanin Peninsula and Timan Range; Siedlecka and Roberts, 1995;  
581 Olovyanishnikov et al., 2000; Kostyuchenko et al., 2006) and northern Norway (e.g., Varanger  
582 Peninsula; Siedlecka, 1975), WNW–ESE-trending anomalies are interpreted as a combination of  
583 basement-seated Timanian macrofolds and top-SSW reverse faults ([Figure 5Figure 5a–c](#)).

#### 584 *N–S-trending folds*

585  
586 Large N–S-trending open folds (e.g., black and yellow lines in [Figure 3Figure 3b](#)) coincide  
587 with N–S- to NNE–SSW-trending, 20–100 kilometers wide, arcuate gravimetric and magnetic

Formatted: Font: 12 pt, Not Bold

Formatted: Font: 12 pt, Not Bold, Not Italic

Formatted: Font: 12 pt, Not Bold

Formatted: Font: 12 pt, Not Bold, Not Italic

Formatted: Font: 12 pt, Not Bold

Formatted: Font: 12 pt, Not Bold, Not Italic

Formatted: Font: 12 pt, Not Bold

Formatted: Font: 12 pt, Not Bold, Not Italic

Formatted: Font: 12 pt, Not Bold

Formatted: Font: 12 pt, Not Bold, Not Italic

Formatted: Font: 12 pt, Not Bold

Formatted: Font: 12 pt, Not Bold, Not Italic

Formatted: Font: 12 pt, Not Bold

Formatted: Font: 12 pt, Not Bold, Not Italic

Formatted: Font: 12 pt, Not Bold

Formatted: Font: 12 pt, Not Bold, Not Italic

Formatted: Font: 12 pt, Not Bold

Formatted: Font: 12 pt, Not Bold, Not Italic

Formatted: Font: 12 pt, Not Bold

Formatted: Font: 12 pt, Not Bold, Not Italic

Formatted: Font: 12 pt, Not Bold

Formatted: Font: 12 pt, Not Bold, Not Italic

Formatted: Font: 12 pt, Not Bold

Formatted: Font: 12 pt, Not Bold, Not Italic

Formatted: Font: 12 pt, Not Bold

Formatted: Font: 12 pt, Not Bold, Not Italic

Formatted: Font: 12 pt, Not Bold

Formatted: Font: 12 pt, Not Bold, Not Italic

Formatted: Font: 12 pt, Not Bold

Formatted: Font: 12 pt, Not Bold, Not Italic

Formatted: Font: 12 pt, Not Bold

Formatted: Font: 12 pt, Not Bold, Not Italic



588 anomalies (dashed white and black lines in [Figure 5Figure 5a-c](#)), which are highly oblique to  
589 WNW–ESE-trending gravimetric and magnetic anomalies and thrust systems (dashed yellow lines  
590 in [Figure 5Figure 5a-c](#)). Notably, major N–S- to NNE–SSW-trending synclines in [Figure 3Figure](#)  
591 [3b](#) (marked as red lines over a white line in [Figure 5Figure 5a](#) and [c](#) and as pink lines over a red  
592 line in [Figure 5Figure 5b](#)) coincides with similarly trending gravimetric and magnetic anomalies  
593 (dashed black lines in [Figure 5Figure 5a](#) and [c](#) and dashed white lines in [Figure 5Figure 5b](#)). On  
594 the slope-direction shader map [of gravimetric data](#), these N–S- to NNE–SSW-trending anomalies  
595 are localized along the boundary between areas with eastwards- (ca. 90–100°; blue areas in [Figure](#)  
596 [5Figure 5b](#)) and westwards-facing slopes (ca. 270–280°; white areas in [Figure 5Figure 5b](#)).

597 Notably where the main thrusts are preserved, major N–S-trending synforms (see 50–60  
598 kilometers wide U-shaped depression formed by the Kinnhøgda–Daudbjørnpynten fault zone, i.e.,  
599 black lines, in [Figure 3Figure 3b](#)) coincide with gravimetric and magnetic highs (white and black  
600 dashed lines in [Figure 5Figure 5a-c](#)), whereas major antiforms where major NNE-dipping thrusts  
601 are partly eroded (e.g., c. 100 kilometers wide areas where the Kinnhøgda–Daudbjørnpynten fault  
602 zone is absent in [Figure 3Figure 3b](#)) coincide with gravimetric and magnetic lows (the lows are  
603 parallel to white and black dashed lines symbolizing magnetic and gravimetric highs in [Figure](#)  
604 [5Figure 5a-c](#)). The correlation of the interpreted NNE-dipping thrust systems with gravimetric  
605 highs suggests that the thrusts consist of relatively denser rocks. This supports the inferred  
606 mylonitic component of the thrusts because mylonites are relatively denser due to the formation of  
607 high-density minerals with increasing deformation (e.g., Arbaret and Burg, 2003; Colombu et al.,  
608 2015).

609 In the northwestern part of the Barents Sea (i.e., area covered by seismic data presented in  
610 [Figure 3Figure 3](#)), N–S- to NNE–SSW-trending gravimetric and magnetic anomalies (white and  
611 black dashed lines in [Figure 5Figure 5a-c](#)) are typically 20–50 kilometers wide and correlate with  
612 similarly trending Caledonian folds and thrusts onshore Nordaustlandet (e.g., Rijpdalen Anticline;  
613 Johansson et al., 2004; 2005; Dumais and Brønner, 2020) and northeastern Spitsbergen (e.g.,  
614 Atomfjella Antiform; Gee et al., 1994; Witt-Nilsson et al., 1998), whose width is comparable to  
615 that of the anomalies. In the south, N–S- to NNE–SSW-trending gravimetric and magnetic  
616 anomalies merge together and swing into a NE–SW trend onshore–nearshore the Kola Peninsula  
617 and northern Norway. These anomalies mimic the attitude of Caledonian thrusts and folds in the  
618 southern Norwegian Barents Sea (Gernigon and Brønner, 2012; Gernigon et al., 2014) and onshore

Formatted: Font: 12 pt, Not Bold

Formatted: Font: 12 pt, Not Bold, Not Italic

Formatted: Font: 12 pt, Not Bold

Formatted: Font: 12 pt, Not Bold, Not Italic

Formatted: Font: 12 pt, Not Bold

Formatted: Font: 12 pt, Not Bold, Not Italic

Formatted: Font: 12 pt, Not Bold

Formatted: Font: 12 pt, Not Bold, Not Italic

Formatted: Font: 12 pt, Not Bold

Formatted: Font: 12 pt, Not Bold, Not Italic

Formatted: Font: 12 pt, Not Bold

Formatted: Font: 12 pt, Not Bold, Not Italic

Formatted: Font: 12 pt, Not Bold

Formatted: Font: 12 pt, Not Bold, Not Italic

Formatted: Font: 12 pt, Not Bold

Formatted: Font: 12 pt, Not Bold, Not Italic

Formatted: Font: 12 pt, Not Bold

Formatted: Font: 12 pt, Not Bold, Not Italic

Formatted: Font: 12 pt, Not Bold

Formatted: Font: 12 pt, Not Bold, Not Italic

Formatted: Font: 12 pt, Not Bold

Formatted: Font: 12 pt, Not Bold, Not Italic

Formatted: Font: 12 pt, Not Bold

Formatted: Font: 12 pt, Not Bold, Not Italic

Formatted: Font: 12 pt, Not Bold

Formatted: Font: 12 pt, Not Bold, Not Italic

Formatted: Font: 12 pt, Not Bold

Formatted: Font: 12 pt, Not Bold, Not Italic

Formatted: Font: 12 pt, Not Bold

Formatted: Font: 12 pt, Not Bold, Not Italic

619 northern Norway (Sturt et al., 1978; Townsend, 1987; Roberts and Williams, 2013). In the east, N-  
620 S- to NNE-SSW-trending anomalies broaden to up to 150 kilometers in the Russian Barents Sea  
621 (Figure 5a-c).

622 In places, the intersections of high, WNW-ESE- and N-S- to NNE-SSW-trending  
623 gravimetric and magnetic anomalies generate relatively higher, oval-shaped anomalies (e.g., dotted  
624 white lines in Figure 5a and c). Notable examples are found in the Ora and Olga basins  
625 and east and south of these basins (see dotted white lines in Figure 5a and c).

## 627 Discussion

628 In the discussion, we consider the lateral extent of the interpreted NNE-dipping thrust  
629 systems, their possible timing of formation, and potential episodes of reactivation and overprinting.  
630 Then we briefly discuss the implications of these thrust systems for plate tectonics reconstructions  
631 in the Arctic.

632  
633 *Extent of NNE-dipping thrust systems*  
634 Four major NNE-dipping systems of mylonitic thrusts and shear zones (Steiløya-Krylen,  
635 Kongsfjorden-Cowanodden, Bellsundbanken, Kinnhøgda-Daubjørnpynten fault zones) were  
636 identified at depths > 1-2 seconds (TWT) in central-eastern Spitsbergen, Storfjorden and the  
637 northeastern Barents Sea, and several systems with less developed ductile fabrics between  
638 Spitsbergen and Bjørnøya on the Stappen High (Figure 3a-f).

639 The Kongsfjorden-Cowanodden fault zone is relatively easy to trace and correlate in  
640 Sassenfjorden, Sassendalen, Nordmannsonna, Storfjorden and the northeastern Barents Sea (east  
641 of Edgeøya) because (i) the seismic data in the these areas have a high resolution and good  
642 coverage, (ii) internal seismic reflections are characterized by high amplitudes (e.g., brittle-ductile  
643 thrusts and mylonitic shear zones), (iii) kinematic indicators within the thrust system consistently  
644 show dominantly top-SSW sense of shear with SSW-verging fold structures (Figure 3a  
645 and d-f, and supplement S2), (iv) the geometry and kinematics indicators along shallow brittle  
646 overprints are regionally consistent (listric, down-NNE, brittle normal faults; Figure 3a  
647 and d-f), and (v) this thrust consistently coincides with increase in gravimetric and magnetic  
648 anomaly in cross-section (Figure 3a and d) and with analogously trending gravimetric and  
649 magnetic anomalies in central-eastern Spitsbergen and the northern Barents Sea (Figure 5a-c).

Formatted: Font: 12 pt, Not Bold

Formatted: Font: 12 pt, Not Bold, Not Italic

Formatted: Font: 12 pt, Not Bold

Formatted: Font: 12 pt, Not Bold, Not Italic

Formatted: Font: 12 pt, Not Bold

Formatted: Font: 12 pt, Not Bold, Not Italic

Formatted: Font: 12 pt, Not Bold

Formatted: Font: 12 pt, Not Bold, Not Italic

Formatted: Font: 12 pt, Not Bold

Formatted: Font: 12 pt, Not Bold, Not Italic

Formatted: Font: 12 pt, Not Bold

Formatted: Font: 12 pt, Not Bold, Not Italic

Formatted: Font: 12 pt, Not Bold

Formatted: Font: 12 pt, Not Bold, Not Italic

Formatted: Font: 12 pt, Not Bold

Formatted: Font: 12 pt, Not Bold, Not Italic

650 ~~5a~~-b). This thrust system was previously identified below the Ora Basin by Klitzke et al. (2019),  
651 though interpreted as potential Timanian grain instead of a discrete structure. The proposed  
652 correlation based on seismic, and cross-section and map-view gravimetric and magnetic data  
653 suggests a lateral extent of c. 550–600 kilometers along strike for the Kongsfjorden–Cowanodden  
654 fault zone. However, the regional magnetic and gravimetric anomalies associated with this thrust  
655 in the Norwegian Barents Sea and Svalbard extend potentially farther east as a series of WNW–  
656 ESE-trending anomalies to the mainland of Russia (~~Figure 5~~Figure 5a–c). Notably, these anomalies  
657 correlate with the southern edge of Novaya Zemlya (~~Figure 5~~Figure 5a–c) and, more specifically,  
658 with WNW–ESE-striking fault segments of the Baidaratsky fault zone (~~Figure 1~~Figure 1a; Lopatin  
659 et al., 2001; Korago et al., 2004), a major thrust fault that bounds a major basement high in the  
660 central Russian Barents Sea, the Ludlov Saddle (Johansen et al., 1992; Drachev et al., 2010). Thus,  
661 it is possible that the Kongsfjorden–Cowanodden fault zone also extends farther east, possibly  
662 merging with the Baidaratsky fault zone, i.e., with a minimum extent of 1700–1800 kilometers  
663 (~~Figure 5~~Figure 5a–c).

664 The overall NNE-dipping and folded (into NNE-plunging folds) geometry of the  
665 Kongsfjorden–Cowanodden fault zone (~~Figure 3~~Figure 3e–f and Klitzke et al., 2019, their figures  
666 3–5) may explain the alternating NW–SE- and E–W-trending geometry of the gravimetric and  
667 magnetic anomalies correlating with this thrust system (~~Figure 5~~Figure 5a–b). E–W- and NW–SE-  
668 trending segments of these anomalies may represent respectively the western and eastern limbs of  
669 open, gently NNE-plunging macro-anticlines in the northern Norwegian Barents Sea. ~~This is~~  
670 ~~supported by~~ the relatively higher, oval-shaped gravimetric and magnetic anomalies at the  
671 intersection of WNW–ESE- and N–S- to NNE–SSW-trending magnetic and gravimetric highs,  
672 which are interpreted as the interaction of two sub-orthogonal fold trends further support this claim  
673 (~~Figure 5~~Figure 5a and c).

674 Interpretation of seismic sections (~~Figure 3~~Figure 3e–f and supplement S2) and regional  
675 magnetic and gravimetric data (~~Figure 5~~Figure 5a–c) in central–eastern Spitsbergen show that  
676 NNE-dipping, top-SSW Kongsfjorden–Cowanodden and Bellsundbanken fault zones likely extend  
677 westwards into central (and possibly northwestern) Spitsbergen (e.g., Sassendalen, Sassenfjorden,  
678 Tempelfjorden, and Billefjorden; see ~~Figure 1~~Figure 1c for locations). This is further supported by  
679 recent field, bathymetric and seismic mapping in central Spitsbergen showing that (inverted)  
680 Devonian–Carboniferous NNE-dipping brittle normal faults in Billefjorden and Sassenfjorden–

Formatted: Font: 12 pt, Not Bold

Formatted: Font: 12 pt, Not Bold, Not Italic

Formatted: Font: 12 pt, Not Bold

Formatted: Font: 12 pt, Not Bold, Not Italic

Formatted: Font: 12 pt, Not Bold

Formatted: Font: 12 pt, Not Bold, Not Italic

Formatted: Font: 12 pt, Not Bold

Formatted: Font: 12 pt, Not Bold, Not Italic

Formatted: Font: 12 pt, Not Bold

Formatted: Font: 12 pt, Not Bold, Not Italic

Formatted: Font: 12 pt, Not Bold

Formatted: Font: 12 pt, Not Bold, Not Italic

Formatted: Font: 12 pt, Not Bold

Formatted: Font: 12 pt, Not Bold, Not Italic

Formatted: Font: 12 pt, Not Bold

Formatted: Font: 12 pt, Not Bold, Not Italic

Formatted: Font: 12 pt, Not Bold

Formatted: Font: 12 pt, Not Bold, Not Italic

Formatted: Font: 12 pt, Not Bold

Formatted: Font: 12 pt, Not Bold, Not Italic

681 Tempelfjorden merge with kilometer-scale, NNE-dipping, Precambrian basement fabrics and shear  
682 zones at depth (Koehl, 2020a; Koehl et al., 2021 in review). Other examples of WNW–ESE-  
683 trending fabrics include faults within Precambrian basement and Carboniferous sedimentary rocks  
684 in northeastern Spitsbergen (Witt-Nilsson et al., 1998; Koehl and Muñoz-Barrera, 2018), and  
685 within Devonian sedimentary rocks in northern and northwestern Spitsbergen (Friend et al., 1997;  
686 McCann, 2000; Dallmann and Piepjohn, 2020). These suggest a repeated and regional influence of  
687 WNW–ESE-trending thrust systems and associated basement fabrics in Spitsbergen.

688 Analogously to the Kongsfjorden–Cowanodden fault zone, the Bellsundbanken and  
689 Kinnhøgda–Daudbjørnpynten fault zones (Figure 3a) geometries and kinematics on  
690 seismic data, and their coinciding with parallel gravimetric and magnetic anomalies in map view  
691 and with magnetic and gravimetric highs in cross-section suggest that they extend from Storfjorden  
692 to the island of Hopen (Figure 1c, Figure 3a, Figure 5a–c, and supplement  
693 S2). Notably, a 50–100 kilometers wide, NNE–SSW-trending gravimetric and associated magnetic  
694 anomaly interpreted as Caledonian grain in Nordaustlandet (Rijpdalen Anticline; Dumais and  
695 Brønner, 2020) bends across the trace of these two thrust systems (Figure 5a–c). Farther  
696 east, the Bellsundbanken and Kinnhøgda–Daudbjørnpynten fault zones parallel gravimetric and  
697 magnetic, alternating E–W- and NW–SE-trending anomalies that follow the trends and map-view  
698 shapes of the Ora and Olga basins in the northeastern Norwegian Barents Sea (Anell et al., 2016;  
699 see Figure 1b–c for location). This suggests that these two thrust systems extend into the  
700 northeastern Norwegian Barents Sea and, potentially, into the Russian Barents Sea, and affected  
701 the development of Paleozoic sedimentary basins. This is also the case of the Steiløya–Krylen fault  
702 zone (supplement S2b), which coincides with mild, discontinuous, WNW–ESE-trending  
703 gravimetric and magnetic anomalies that extend well into the Russian Barents Sea and, possibly,  
704 across Novaya Zemlya (Figure 5a–c).

705 In southwestern Spitsbergen, field mapping revealed the presence of a major, subvertical,  
706 kilometer-thick, WNW–ESE-striking mylonitic shear zone metamorphosed under amphibolite  
707 facies conditions, the Vimsodden–Kosibapasset Shear Zone (Majka et al., 2008, 2012; Mazur et  
708 al., 2009; see Figure 1c for location). This major sinistral shear zone aligns along a WNW–  
709 ESE-trending axis with the Kinnhøgda–Daudbjørnpynten fault zone in the northwestern  
710 Norwegian Barents Sea (Figure 3a), and shows a folded geometry in map view that is  
711 comparable to that of major NNE-dipping thrust systems in the northern Norwegian Barents Sea

Formatted: Font: 12 pt, Not Bold

Formatted: Font: 12 pt, Not Bold, Not Italic

Formatted: Font: 12 pt, Not Bold

Formatted: Font: 12 pt, Not Bold, Not Italic

Formatted: Font: 12 pt, Not Bold

Formatted: Font: 12 pt, Not Bold, Not Italic

Formatted: Font: 12 pt, Not Bold

Formatted: Font: 12 pt, Not Bold, Not Italic

Formatted: Font: 12 pt, Not Bold

Formatted: Font: 12 pt, Not Bold, Not Italic

Formatted: Font: 12 pt, Not Bold

Formatted: Font: 12 pt, Not Bold, Not Italic

Formatted: Font: 12 pt, Not Bold

Formatted: Font: 12 pt, Not Bold, Not Italic

Formatted: Font: 12 pt, Not Bold

Formatted: Font: 12 pt, Not Bold, Not Italic

Formatted: Font: 12 pt, Not Bold

Formatted: Font: 12 pt, Not Bold, Not Italic

712 (Figure 3a and e-f, Figure 5a-c, and supplement S2; Klitzke et al., 2019). In  
713 addition, the Vimsodden–Kosibapasset Shear Zone juxtaposes relatively old Proterozoic basement  
714 rocks in the north against relatively young rocks in the south, thus suggesting a similar  
715 configuration and kinematics as along the Kinnhøgda–Daubjørnpynnten fault zone in Storfjorden  
716 and the northeastern Norwegian Barents Sea. Moreover, von Gosen and Piepjohn (2001) and Bergh  
717 and Grogan (2003) reported that Devonian–Mississippian sedimentary successions and Cenozoic  
718 fold structures (e.g., Hyrnefjellet Anticline) are offset sinistrally by a few kilometers in Hornsund.  
719 Thus, we propose that the Vimsodden–Kosibapasset Shear Zone extends into Hornsund and  
720 represents the westwards continuation of the Kinnhøgda–Daubjørnpynnten fault zone. This  
721 suggests a minimum extent of 400–450 kilometers for this thrust system (Figure 1b-c and  
722 Figure 5a-c).

#### 724 ***Timing of formation of major NNE-dipping thrust systems and N–S-trending folds***

##### 725 *NNE-dipping thrust systems*

726 The several-kilometer thickness and hundreds–thousands of kilometers along-strike extent  
727 of NNE-dipping thrust systems in central–eastern Spitsbergen, Storfjorden, and the northwestern  
728 and northeastern Norwegian Barents Sea suggest that they formed during a major contractional  
729 tectonic event. The overall WNW–ESE trend and the consistent north-northeastwards dip and top-  
730 SSW sense of shear along the newly evidenced deep thrust systems preclude formation during the  
731 Grenvillian, Caledonian, and Ellesmerian orogenies, and the Eurekan tectonic event. These tectonic  
732 events all involved dominantly E–W-oriented contraction and resulted in the formation of overall  
733 N–S- to NNE–SSW-trending fabrics, structures and deformation belts in Svalbard (i.e., sub-  
734 orthogonal to the newly identified thrust systems) such as the Atomfjella Antiform (Gee et al.,  
735 1994; Witt-Nilsson et al., 1998), the Vestfonna and Rijpdalen anticlines (Johansson et al., 2004;  
736 2005; Dumais and Brønner, 2020), the Dickson Land and Germaniahavøya fold-thrust zones  
737 (McCann, 2000; Piepjohn, 2000; Dallmann and Piepjohn, 2020), and the West Spitsbergen Fold-  
738 and-Thrust Belt and related early Cenozoic structures in eastern Spitsbergen (Andresen et al., 1992;  
739 Haremo and Andresen, 1992; Dallmann et al., 1993), and NE–SW- to NNE–SSW-striking thrusts  
740 and folds in northern Norway (Sturt et al., 1978; Townsend, 1987; Roberts and Williams, 2013)  
741 and the southwestern Barents Sea (Gernigon et al., 2014).

Formatted: Font: 12 pt, Not Bold

Formatted: Font: 12 pt, Not Bold, Not Italic

Formatted: Font: 12 pt, Not Bold

Formatted: Font: 12 pt, Not Bold, Not Italic

Formatted: Font: 12 pt, Not Bold

Formatted: Font: 12 pt, Not Bold, Not Italic

Formatted: Font: 12 pt, Not Bold

Formatted: Font: 12 pt, Not Bold, Not Italic

742 A possible cause for the formation of the observed NNE-dipping thrust systems is the late  
743 Neoproterozoic Timanian Orogeny, which is well known onshore northwestern Russia (e.g., Kanin  
744 Peninsula, Timan Range and central Timan; Siedlecka and Roberts, 1995; Olovyanishnikov et al.,  
745 2000; Kostyuchenko et al., 2006) and northeastern Norway (Varanger Peninsula; Siedlecka and  
746 Siedlecki, 1967; Siedlecka, 1975; Roberts and Olovyanishnikov, 2004), and traces of which were  
747 recently found in southwestern Spitsbergen (Majka et al., 2008, 2012, 2014) and northern  
748 Greenland (Rosa et al., 2016; Estrada et al., 2018). The overall transport direction during this  
749 orogeny was directed towards the south-southwest and most thrust systems show NNE-dipping  
750 geometries (Olovyanishnikov et al., 2000; Kostyuchenko et al., 2006), e.g., the Timanian thrust  
751 front on the Varanger Peninsula in northeastern Norway (Trollfjorden–Komagelva Fault Zone;  
752 Siedlecka and Siedlecki, 1967; Siedlecka, 1975). In addition, the size of Timanian thrust systems  
753 in the Timan Range (e.g., Central Timan Fault) is comparable ( $\geq 3$ –4 seconds TWT; Kostyuchenko  
754 et al., 2006 their figure 17) to that of thrust systems in the northern Norwegian Barents Sea and  
755 Svalbard (Figure 3a and c–d).

756 Thus, based on their overall WNW–ESE strike (Figure 1b–c), their vergence to the  
757 south-southwest (Figure 3a, c–d and f), their coincidence with gravimetric and magnetic  
758 highs (Figure 5a–c), their upward truncation by a major unconformity consistently  
759 throughout the study area (see top-Precambrian unconformity in Figure 3a–d), and the  
760 correlation of these NNE-dipping thrusts (via gravimetric and magnetic anomalies) to similarly  
761 striking and verging structures of comparable size (i.e., several seconds TWT thick) onshore–  
762 nearshore northwestern Russia and northern Norway (Siedlecka, 1975; Siedlecka and Roberts,  
763 1995; Olovyanishnikov et al., 2000; Roberts and Siedlecka, 2002; Gee and Pease, 2004;  
764 Kostyuchenko et al., 2006), NNE-dipping thrusts in the northern Norwegian Barents Sea,  
765 Storfjorden, and central–eastern Spitsbergen are interpreted as the western continuation of  
766 Timanian thrusts.

767 Timanian grain was recently identified in the northeastern Norwegian Barents Sea through  
768 interpretation of new seismic, magnetic and gravimetric datasets shown in Figure 5a–c  
769 (Klitzke et al., 2019). The alignment, coincident location, and matching geometries (e.g., curving  
770 E–W to NW–SE strike/trend and kilometer-wide NNE–SSW-trending anticline) between Timanian  
771 grain and structures mapped by Klitzke et al. (2019) and the major, NNE-dipping, top-SSW thrust  
772 systems described in central–eastern Spitsbergen, Storfjorden and the Norwegian Barents Sea

Formatted: Font: 12 pt, Not Bold

Formatted: Font: 12 pt, Not Bold, Not Italic

Formatted: Font: 12 pt, Not Bold

Formatted: Font: 12 pt, Not Bold, Not Italic

Formatted: Font: 12 pt, Not Bold

Formatted: Font: 12 pt, Not Bold, Not Italic

Formatted: Font: 12 pt, Not Bold

Formatted: Font: 12 pt, Not Bold, Not Italic

Formatted: Font: 12 pt, Not Bold

Formatted: Font: 12 pt, Not Bold, Not Italic

Formatted: Font: 12 pt, Not Bold

Formatted: Font: 12 pt, Not Bold, Not Italic

773 (Figure 3a–f and supplement S2) further support a Timanian origin for the latter. Further  
774 evidence of relic Timanian structural grain as far as the Loppa High and Bjørnøya Basin are  
775 documented by previous magnetic studies and modelling (Marello et al., 2010). Moreover, seismic  
776 mapping suggests that Timanian thrust systems extend well into central Spitsbergen (Figure  
777 3e–f and supplement S2c–d; Koehl, 2020a; Koehl et al., 2021 in review), and regional  
778 gravimetric and magnetic anomaly maps suggest that Timanian thrust systems might extend farther  
779 west to (north-) western Spitsbergen (Figure 5a–c).

780 Probable reasons as to why these major (hundreds–thousands of kilometers long) thrust  
781 systems were not identified before during fieldwork in Svalbard are their burial to high depth (>  
782 1–2 seconds TWT in the study area, i.e., several kilometers below the surface; Figure 3a–  
783 f), and their strong overprinting by younger tectonic events like the Caledonian Orogeny in areas  
784 where they are exposed (e.g., Vimsodden–Kosibapasset Shear Zone in southwestern Spitsbergen;  
785 Faehnrich et al., 2020). Possible areas of interest for future studies include the western and  
786 northwestern parts of Spitsbergen where Caledonian and Eureka E–W contraction contributed to  
787 uplift and exhume deep basement rocks, and where Timanian rocks potentially crop out (e.g.,  
788 Peucat et al., 1989).

#### 790 *N–S-trending folds*

791 N–S-trending upright folds involve the NNE-dipping thrust systems (Figure 3b and  
792 e) and correlate (via gravimetric and magnetic anomalies) with major Caledonian folds in  
793 northeastern Spitsbergen and Nordaustlandet, like the Atomfjella Antiform (Gee et al., 1994; Witt-  
794 Nilsson et al., 1998) and Rijpdalen Anticline (Johansson et al., 2004; 2005; Dumais and Brønner,  
795 2020), with Caledonian grain in the southern Norwegian Barents Sea (Gernigon and Brønner, 2012;  
796 Gernigon et al., 2014), and with major NE–SW-trending Caledonian folds onshore northern  
797 Norway (Sturt et al., 1978; Townsend, 1987; Roberts and Williams, 2013). In addition, the width  
798 of the NE–SW- to N–S-trending gravimetric and magnetic anomalies associated with these folds  
799 increases up to 150 kilometers eastwards, i.e., away from the Caledonian collision zone (Figure  
800 5a–c; Corfu et al., 2014; Gasser, 2014). Thus, N–S-trending folds in the northern  
801 Norwegian Barents Sea are interpreted as Caledonian regional folds in Precambrian–lower  
802 Paleozoic rocks. The relatively broader geometry of Caledonian folds away from the Caledonian  
803 collision zone (e.g., in the Russian Barents Sea) is inferred to be related to gentler fold geometries

Formatted: Font: 12 pt, Not Bold

Formatted: Font: 12 pt, Not Bold, Not Italic

Formatted: Font: 12 pt, Not Bold

Formatted: Font: 12 pt, Not Bold, Not Italic

Formatted: Font: 12 pt, Not Bold

Formatted: Font: 12 pt, Not Bold, Not Italic

Formatted: Font: 12 pt, Not Bold

Formatted: Font: 12 pt, Not Bold, Not Italic

Formatted: Font: 12 pt, Not Bold

Formatted: Font: 12 pt, Not Bold, Not Italic

Formatted: Font: 12 pt, Not Bold

Formatted: Font: 12 pt, Not Bold, Not Italic

804 due to decreasing deformation intensity in this direction. This is further supported by relatively low  
805 grade Caledonian metamorphism in Franz Josef Land (Knudsen et al., 2019; see [Figure 1](#)  
806 [4a–b](#) for location). By contrast, the presence of tighter Caledonian folds near the collision zone in  
807 the northern Norwegian Barents Sea (e.g., [Figure 3](#)  
808 [Figure 3b](#) and e, and Atomfjella Antiform and Rjipdalen Anticline onshore; Gee et al., 1994; Witt-Nilsson et al., 1998; Johansson et al., 2004,  
809 2005; Dumais and Brønner, 2020) is associated with much narrower (20–50 kilometers wide)  
810 gravimetric and magnetic anomalies ([Figure 5](#)  
811 [Figure 5a–c](#)). Note that the Atomfjella Antiform and Rjipdalen Anticline can be directly correlated with 20–50 kilometers wide, N–S-trending high  
812 gravimetric and magnetic anomalies ([Figure 5](#)  
813 [Figure 5a–c](#)). Noteworthy, some of the NNE–SSW-trending folds and anomalies in the northernmost Norwegian Barents Sea may reflect a  
814 combination of Caledonian and superimposed early Cenozoic Eureka folding (e.g., Kairanov et  
815 al., 2018).

816 The interference of WNW–ESE- and N–S- to NNE–SSW-trending gravimetric highs,  
817 which are correlated to Timanian and Caledonian folds respectively, produces oval-shaped  
818 gravimetric and magnetic highs ([Figure 5](#)  
819 [Figure 5a](#)). These relatively higher, oval-shaped gravimetric anomalies are interpreted to correspond to dome-shaped folds resulting from the  
820 interaction of Timanian and Caledonian folds involving refolding of WNW–ESE-trending  
821 Timanian folds during E–W Caledonian contraction. [This interpretation is supported by field](#)  
822 [studies on the Varanger Peninsula in northern Norway and by seismic studies of Timanian thrusts](#)  
823 [off northern Norway where the interaction of Timanian and Caledonian folds produced dome-](#)  
824 [shaped fold structures \(Ramsay, 1962\), e.g., like the Ragnarokk Anticline \(Siedlecka and Siedlecki,](#)  
825 [1971; Koehl, in prep.\) also support this interpretation.](#) Furthermore, Barrère et al. (2011) suggested  
826 that basins and faults in the southern Norwegian Barents Sea are controlled by the interaction of  
827 Caledonian and Timanian structural grain, and Marello et al. (2010) argued that elbow-shaped  
828 magnetic anomalies reflect the interaction of Caledonian and Timanian structural grains in the  
829 Barents Sea, potentially as far west as the Loppa High and the Bjørnøya Basin.

830

### 831 *Phanerozoic reactivation and overprinting of Timanian thrust systems*

#### 832 *Caledonian reactivation and overprint*

833 The geometry of the Kongsfjorden–Cowanodden and Kinnhøgda–Daudbjørnpynten fault  
834 zones in Nordmannsfonna ([Figure 3](#)  
835 [Figure 3e](#)) and the northeastern Norwegian Barents Sea ([Figure](#)

Formatted: Font: 12 pt, Not Bold

Formatted: Font: 12 pt, Not Bold, Not Italic

Formatted: Font: 12 pt, Not Bold

Formatted: Font: 12 pt, Not Bold, Not Italic

Formatted: Font: 12 pt, Not Bold

Formatted: Font: 12 pt, Not Bold, Not Italic

Formatted: Font: 12 pt, Not Bold

Formatted: Font: 12 pt, Not Bold, Not Italic

Formatted: Font: 12 pt, Not Bold

Formatted: Font: 12 pt, Not Bold, Not Italic

Formatted: Font: 12 pt, Not Bold

Formatted: Font: 12 pt, Not Bold, Not Italic

Formatted: Font: 12 pt, Not Bold



835 [3Figure 3b](#); Klitzke et al., 2019), where they are folded into broad NNE-plunging upright anticlines  
836 and synclines suggests that these thrust systems were deformed after they accommodated top-SSW  
837 Timanian thrusting ([Figure 6Figure 6a](#) and [Figure 7Figure 7a](#)). In addition, subsidiary top-west  
838 kinematics (west-verging folds and top-west minor thrusts) suggest that these thrust systems were  
839 partly reactivated–overprinted during an episode of intense E–W contraction ([Figure 6Figure 6b](#)  
840 and [Figure 7Figure 7b](#)). However, west-dipping dykes crosscutting and gently east-dipping  
841 sedimentary strata overlying the eastern part of the folded Kongsfjorden–Cowanodden fault zone  
842 are only mildly folded, and upper Paleozoic sedimentary strata lie flat over folded and partly eroded  
843 Precambrian–lower Paleozoic rocks and the Kinnhøgda–Daudbjørnpynten fault zone, thus  
844 suggesting that these sedimentary strata and dykes were not involved in this episode of E–W  
845 contraction ([Figure 3Figure 3e](#)).

846 A notable episode of E–W contraction in Svalbard is the Caledonian Orogeny in the early–  
847 mid Paleozoic, which resulted in the formation of west-verging thrusts and N–S-trending folds of  
848 comparable size (c. 15–25 kilometers wide) to those affecting the Kongsfjorden–Cowanodden and  
849 Kinnhøgda–Daudbjørnpynten fault zones in Nordmannsfunna and the northern Norwegian Barents  
850 Sea ([Figure 3Figure 3b](#) and [e](#); Klitzke et al., 2019, their figures 3–5), such as the Atomfjella  
851 Antiform in northeastern Spitsbergen (Gee et al., 1994; Witt-Nilsson et al., 1998; Lyberis and  
852 Manby, 1999) and the Rijpdalen Anticline in Nordaustlandet ([Figure 1Figure 1b](#)). Since the NNE-  
853 plunging anticline in Nordmannsfunna does not affect overlying Pennsylvanian–Mesozoic  
854 sedimentary strata ([Figure 3Figure 3e](#)), we propose that they formed during Caledonian contraction  
855 ([Figure 7Figure 7b](#)). This is supported by the involvement of the top-Precambrian unconformity  
856 and underlying NNE-dipping thrusts in N–S- to NNE-SSW-trending folds, and by the truncation  
857 of these folds by the top-Silurian unconformity, which is overlapped by mildly deformed to flat-lying  
858 upper Paleozoic strata ([Figure 3Figure 3b](#) and [Figure 4Figure 4f](#)). Furthermore, structures with  
859 geometries comparable to NNE-plunging folds in the northern Barents Sea and Svalbard were  
860 observed in northern Norway. An example is the Ragnarokk Anticline, a dome-shaped fold  
861 structure along the Timanian front thrust on the Varanger Peninsula, which results from the re-  
862 folding of Timanian thrusts and folds into a NE–SW-trending Caledonian trend (Siedlecka and  
863 Siedlecki, 1971).

864 Further support of a Caledonian origin for upright NNE-plunging folds in eastern  
865 Spitsbergen, Storfjorden and the northern Norwegian Barents Sea is that these folds are relatively

Formatted: Font: 12 pt, Not Bold, Not Italic

Formatted: Font: 12 pt, Not Bold

Formatted: Font: 12 pt, Not Bold, Not Italic

Formatted: Font: 12 pt, Not Bold

Formatted: Font: 12 pt, Not Bold, Not Italic

Formatted: Font: 12 pt, Not Bold

Formatted: Font: 12 pt, Not Bold, Not Italic

Formatted: Font: 12 pt, Not Bold

Formatted: Font: 12 pt, Not Bold, Not Italic

Formatted: Font: 12 pt, Not Bold

Formatted: Font: 12 pt, Not Bold, Not Italic

Formatted: Font: 12 pt, Not Bold

Formatted: Font: 12 pt, Not Bold, Not Italic

Formatted: Font: 12 pt, Not Bold

Formatted: Font: 12 pt, Not Bold, Not Italic

Formatted: Font: 12 pt, Not Bold

Formatted: Font: 12 pt, Not Bold, Not Italic

Formatted: Font: 12 pt, Not Bold

Formatted: Font: 12 pt, Not Bold, Not Italic

Formatted: Font: 12 pt, Not Bold

Formatted: Font: 12 pt, Not Bold, Not Italic

Formatted: Font: 12 pt, Not Bold

Formatted: Font: 12 pt, Not Bold, Not Italic

866 tight in the west, in Nordmannsfonna and the northwestern Barents Sea (Figure 3b and e),  
867 whereas they show gradually gentler and more open geometries in the east, i.e., away from the  
868 Caledonian collision zone (Figure 3b). This is also shown by the gradual eastwards  
869 broadening of regional gravimetric and magnetic anomalies correlated with Caledonian folds  
870 suggesting gentler fold geometries related to decreasing (Caledonian) deformation intensity in this  
871 direction (Figure 5a-c). This contrasts with the homogeneous intensity of deformation  
872 along NNE-dipping thrusts on seismic data and with the homogeneous width of related  
873 gravimetric-magnetic anomalies from west to east in Svalbard and the Barents Sea (Figure 3  
874 3a-f and Figure 5a-c and supplement S2).

875 In Nordmannsfonna, the Caledonian origin of the major 15–20 kilometers wide anticline,  
876 and the truncation of overlying, gently east-dipping, mildly folded sedimentary strata and  
877 crosscutting west-dipping dykes by the base-Pennsylvanian unconformity suggest that these  
878 sedimentary strata and dykes are Devonian (–Mississippian?) in age (Figure 6c-d). This is  
879 supported by the presence of thick Devonian–Mississippian collapse deposits in adjacent areas of  
880 central–northern Spitsbergen (Cutbill et al., 1976; Murascov and Mokin, 1979; Aakvik, 1981;  
881 Gjølberg, 1983; Manby and Lyberis, 1992; Friend et al., 1997), and by Middle Devonian to  
882 Mississippian ages (395–327 Ma) for dykes in central–northern Spitsbergen (Evdokimov et al.,  
883 2006), northern Norway (Lippard and Prestvik, 1997; Guise and Roberts, 2002), and northwestern  
884 Russia (Roberts and Onstott, 1995).

885 The occurrence of a > 0.5 second (TWT) reverse offset of the folded Kongsfjorden–  
886 Cowanodden fault zone and the lack of offset of the Devonian (–Mississippian?) dykes across the  
887 Agardhbukta Fault indicate that the latter fault formed as a top-west thrust during the Caledonian  
888 Orogeny. At depth, the Agardhbukta Fault merges with the eastern flank of the folded  
889 Kongsfjorden–Cowanodden fault zone. This, together with the presence of minor, high-angle, top-  
890 west brittle thrusts within the Kongsfjorden–Cowanodden fault zone (Figure 3e), indicates  
891 that the Agardhbukta Fault reactivated and/or overprinted the eastern portion of the Kongsfjorden–  
892 Cowanodden fault zone in Nordmannsfonna during Caledonian contraction (Figure 6b and  
893 Figure 7b). Depth conversion using seismic velocities from Gernigon et al. (2018) suggest  
894 that the Agardhbukta Fault offset the Kongsfjorden–Cowanodden fault zone by ca. 2.4–2.5  
895 kilometers top-west during Caledonian contraction (Figure 3e and supplement S3g). These  
896 kinematics are consistent with field observation in eastern Spitsbergen by Piepjohn et al. (2019,

Formatted: Font: 12 pt, Not Bold

Formatted: Font: 12 pt, Not Bold, Not Italic

Formatted: Font: 12 pt, Not Bold

Formatted: Font: 12 pt, Not Bold, Not Italic

Formatted: Font: 12 pt, Not Bold

Formatted: Font: 12 pt, Not Bold, Not Italic

Formatted: Font: 12 pt, Not Bold

Formatted: Font: 12 pt, Not Bold, Not Italic

Formatted: Font: 12 pt, Not Bold

Formatted: Font: 12 pt, Not Bold, Not Italic

Formatted: Font: 12 pt, Not Bold

Formatted: Font: 12 pt, Not Bold, Not Italic

Formatted: Font: 12 pt, Not Bold

Formatted: Font: 12 pt, Not Bold, Not Italic

Formatted: Font: 12 pt, Not Bold

Formatted: Font: 12 pt, Not Bold, Not Italic

Formatted: Font: 12 pt, Not Bold

Formatted: Font: 12 pt, Not Bold, Not Italic

Formatted: Font: 12 pt, Not Bold

Formatted: Font: 12 pt, Not Bold, Not Italic

897 their figure 17b). However, Piepjohn et al. (2019) also suggested a significant component of  
898 Mesozoic–Cenozoic, down-east normal movement, which was not identified in Nordmannsfonna.  
899 This suggests either along strike variation in the movement history of the Agardhbukta Fault, either  
900 that the fault mapped on seismic data in Nordmannsfonna does not correspond to the Agardhbukta  
901 Fault of Piepjohn et al. (2019).

902         Considering the presence of crustal-scale, NNE-dipping, hundreds (to thousands?) of  
903 kilometers long (Timanian) thrust systems extending from the Barents Sea (and possibly from  
904 onshore Russia) to central–eastern and southern Spitsbergen and the northwestern Norwegian  
905 Barents Sea (Figure 5a–c) prior to the onset of E–W-oriented Caledonian contraction, it is  
906 probable that such large structures would have (at least partially) been reactivated and/or  
907 overprinted during subsequent tectonic events if suitably oriented. Under E–W contraction, WNW–  
908 ESE-striking, dominantly NNE-dipping Timanian faults would be oriented at c. 30° to the direction  
909 of principal stress and, therefore, be suitable (according to Anderson’s stress model) to  
910 reactivate/be overprinted with sinistral strike-slip movements. Such kinematics were recorded  
911 along the Vimsodden–Kosibapasset Shear Zone in Wedel Jarlsberg Land (Mazur et al., 2009) and  
912 within Hornsund (von Gosen and Piepjohn, 2001).

913         However, recent <sup>40</sup>Ar–<sup>39</sup>Ar geochronological determinations on muscovite within this  
914 structure suggest that this structure formed during the Caledonian Orogeny (Faehnrich et al. 2020).  
915 Nonetheless, the same authors also obtained Timanian ages (600–540 Ma) for (initial) movements  
916 along minor shear zones nearby and parallel to the Vimsodden–Kosibapasset Shear Zone. Since  
917 this large shear zone must have represented a major preexisting zone of weakness when Caledonian  
918 contraction initiated, it is highly probable that it was preferentially chosen to reactivate instead of  
919 minor shear zones. Thus, the Caledonian ages obtained along the Vimsodden–Kosibapasset Shear  
920 Zone most likely reflect complete resetting of the geochronometer along the shear zone due to large  
921 amounts of Caledonian reactivation–overprinting, while minor nearby shear zones preserved traces  
922 of initial Timanian deformation. This is also supported by observations in northern Norway  
923 suggesting that Timanian thrusts (e.g., Trollfjorden–Komagelva Fault Zone) were reactivated as  
924 major strike-slip faults during the Caledonian Orogeny (Roberts, 1972; Herrevold et al., 2009; Rice  
925 2014). This interpretation reconciles the strong differences in dipping angle and depth between the  
926 Kinnhøgda–Daudbjørnpynten fault zone and the Vimsodden–Kosibapasset Shear Zone. The  
927 former was located away from the Caledonian collision zone and essentially retained its initial,

Formatted: Font: 12 pt, Not Bold

Formatted: Font: 12 pt, Not Bold, Not Italic

928 moderately NNE-dipping Timanian geometry and was deeply buried during the Phanerozoic,  
929 whereas the latter was intensely deformed, pushed into a sub-vertical position, and uplifted and  
930 exhumed to the surface because it was located near or within the Caledonian collision zone.

931

### 932 *Devonian–Carboniferous normal overprint–reactivation*

933 In Nordmannsfunna, the wedge shape of Devonian (–Mississippian?) sedimentary strata in  
934 the hanging wall of the Kongsfjorden–Cowanodden fault zone suggest that the eastern portion of  
935 this thrust was reactivated as a gently–moderately dipping extensional detachment (~~Figure 6~~  
936 ~~6c~~) and, thus, that Devonian (–Mississippian?) strata in this area represent analogs to collapse  
937 deposits in northern Spitsbergen. ~~This is supported by the~~ intrusion of west-dipping Devonian (–  
938 Mississippian?) dykes orthogonal to the eastern portion of the thrust system, i.e., orthogonal to  
939 extensional movements along the inverted east-dipping portion of the thrust (~~Figure 3~~  
940 ~~Figure 3e~~ and ~~Figure 6~~  
941 ~~Figure 6d~~) also supports this interpretation. Similar relationships were inferred in  
942 northwestern Spitsbergen, where Devonian collapse sediments were deposited along a N–S-  
943 trending Precambrian basement ridge bounded by a gently dipping, extensional mylonitic  
944 detachment (Braathen et al., 2018).

944 In Sassenfjorden, Storfjorden and the northeastern Norwegian Barents Sea, listric brittle  
945 normal faults showing down-NNE offsets and syn-tectonic thickening within Devonian–  
946 Carboniferous (–Permian?) sedimentary strata merge at depth with the uppermost part of NNE-  
947 dipping Timanian thrust systems like the Kongsfjorden–Cowanodden fault zone (~~Figure 3~~  
948 ~~3a~~ and ~~d~~ and supplement S2c). This indicates that Timanian thrust systems were used as preexisting  
949 zones of weakness during late–post-orogenic collapse of the Caledonides in the Devonian–  
950 Carboniferous (~~Figure 6~~  
951 ~~Figure 6c–e~~ and ~~Figure 7~~  
952 ~~Figure 7c~~).

951 The presence of the Kongsfjorden–Cowanodden fault zone in Storfjorden and below  
952 Edgeøya also explains the strong differences between the Paleozoic sedimentary successions  
953 penetrated by the Plurdalen-1 and Raddendalen-1 exploration wells (Bro and Shvarts, 1983;  
954 Harland and Kelly, 1997). Notably, the Plurdalen-1 well penetrated (at least) ca. 1600 meters thick  
955 Devonian–Mississippian sedimentary rocks in the direct hanging wall of the Kongsfjorden–  
956 Cowanodden fault zone and related listric brittle overprints (~~Figure 3~~  
957 ~~Figure 3a~~), whereas the interpretation of Bro and Shvarts (1983) suggests that the Raddendalen-1 well encountered thin (90–  
958 290 meters thick) Mississippian strata overlying (> 2 kilometers) thick lower Paleozoic

Formatted: Font: 12 pt, Not Bold

Formatted: Font: 12 pt, Not Bold, Not Italic

Formatted: Font: 12 pt, Not Bold

Formatted: Font: 12 pt, Not Bold, Not Italic

Formatted: Font: 12 pt, Not Bold

Formatted: Font: 12 pt, Not Bold, Not Italic

Formatted: Font: 12 pt, Not Bold

Formatted: Font: 12 pt, Not Bold, Not Italic

Formatted: Font: 12 pt, Not Bold

Formatted: Font: 12 pt, Not Bold, Not Italic

Formatted: Font: 12 pt, Not Bold

Formatted: Font: 12 pt, Not Bold, Not Italic

Formatted: Font: 12 pt, Not Bold

Formatted: Font: 12 pt, Not Bold, Not Italic

959 sedimentary rocks ca. 30 kilometers farther northeast, i.e., away from the Kongsfjorden–  
960 Cowanodden fault zone and related overprints. The presence of thick Devonian sedimentary strata  
961 in the direct hanging wall of listric overprints of the Kongsfjorden–Cowanodden fault zone further  
962 supports late–post-Caledonian extensional reactivation–overprinting of NNE-dipping Timanian  
963 thrusts.

964 In central Spitsbergen, recently identified Early Devonian–Mississippian normal faults  
965 formed along and overprinted–reactivated major NNE-dipping ductile (mylonitic) shear zones and  
966 fabrics in Billefjorden (Koehl et al., 2021 in review) and Sassenfjorden–Tempelfjorden (Koehl,  
967 2020a). These show sizes, geometries and kinematics comparable to those of the Kongsfjorden–  
968 Cowanodden fault zone, and are, therefore, interpreted as the western continuation of this thrust  
969 system. The Devonian–Carboniferous extensional reactivation–overprinting of the Kongsfjorden–  
970 Cowanodden fault zone in central Spitsbergen explains the southward provenance of northwards  
971 prograding sedimentary rocks of the uppermost Silurian–Lower Devonian Siktefjellet and Red Bay  
972 groups and Wood Bay Formation and the enigmatic WNW–ESE trend of the southern boundary of  
973 the Devonian Graben in central–northern Spitsbergen (Gee and Moody-Stuart, 1966; Friend et al.,  
974 1966; Friend and Moody-Stuart, 1972; Murascov and Mokin, 1979; Friend et al., 1997; McCann,  
975 2000; Dallmann and Piepjohn, 2020; Koehl et al., 2021 in review).

976

#### 977 *Mild Triassic overprint*

978 The Kongsfjorden–Cowanodden fault zone and associated overprints align with WNW–  
979 ESE- to NW–SE-striking normal faults onshore southern and southwestern Edgeøya in  
980 Kvalpynten, Negerpynten, and Øhmanfjellet (Osmundsen et al., 2014; Ogata et al., 2018). These  
981 faults display both listric and steep planar geometries in cross-section and bound thickened syn-  
982 sedimentary growth strata in lowermost Upper Triassic sedimentary rocks of the Tschermakfjellet  
983 and De Geerdalen formations (Ogata et al., 2018; Smyrak-Sikora et al., 2020). The Norwegian  
984 Barents Sea and Svalbard are believed to have remained tectonically quiet throughout the Triassic  
985 apart from minor deep-rooted normal faulting in the northwestern Norwegian Barents Sea (Anell  
986 et al., 2013) and Uralides-related contraction in the (south-) east (Müller et al., 2019). Hence, we  
987 propose that the progradation and accumulation of thick sedimentary deposits of the Triassic deltaic  
988 systems above the southeastward continuation of the Kongsfjorden–Cowanodden fault zone may  
989 have triggered minor tectonic adjustments resulting in the development of a system of small half-

990 grabens over the thrust system. Alternatively or complementary, the deposition of thick Triassic  
991 deltaic systems may have locally accelerated compaction of sedimentary strata underlying the  
992 Tschermakjellet Formation in south- and southwest-Edgeøya, e.g., of the potential pre-Triassic  
993 syn-tectonic growth strata along the Kongsfjorden–Cowanodden fault zone, and, thus, facilitated  
994 the development of minor half-grabens within the Triassic succession along this thrust system.

995

996 *Eurekan reactivation–overprint*

997 In eastern Spitsbergen, the Agardhbukta Fault segment of the Lomfjorden Fault Zone  
998 truncates the Kongsfjorden–Cowanodden fault zone with a major, > 0.5 second (TWT) top-west  
999 reverse offset (Figure 3e). The Agardhbukta fault also mildly folds Pennsylvanian–  
1000 Mesozoic sedimentary rocks and Cretaceous sills into a gentle upright (fault-propagation) fold with  
1001 no major offset (Figure 6f–g), which is supported by onshore field observations in eastern  
1002 and northeastern Spitsbergen (Piepjohn et al., 2019). Mild folding of Mesozoic sedimentary rocks  
1003 and of Cretaceous intrusions indicates that the Agardhbukta Fault was most likely mildly  
1004 reactivated as a top-west thrust during the early Cenozoic Eurekan tectonic event (Figure 6  
1005 g and Figure 7d).

1006 Seismic data show that high-angle listric Devonian–Carboniferous normal faults were  
1007 mildly reactivated as reverse faults that propagated upwards and gently folded adjacent upper  
1008 Paleozoic–Mesozoic (–Cenozoic?) sedimentary strata in the northwestern Norwegian Barents Sea,  
1009 Storfjorden and central–eastern Spitsbergen (Figure 3a–c and supplement S2), but not in  
1010 the northeastern Norwegian Barents Sea (Figure 3d). Since normal faults were not inverted  
1011 in the east, it is probable that inversion of these faults in central–eastern Spitsbergen, Storfjorden  
1012 and the northwestern Norwegian Barents Sea first occurred during the Eurekan tectonic event in  
1013 the early Cenozoic, when Greenland collided with western Spitsbergen (Figure 7d). This  
1014 is also supported by the gently folded character of Devonian–Mesozoic (–Cenozoic?) sedimentary  
1015 successions in the west (Figure 3a and c), whereas these successions are essentially flat-  
1016 lying (i.e., undeformed) in the east (Figure 3b and d). Nevertheless, folding of the seafloor  
1017 reflection in Storfjorden and the northwestern Norwegian Barents Sea suggests ongoing  
1018 contractional deformation along several of these faults in the northwestern Norwegian Barents Sea  
1019 and Storfjorden (Figure 3a–c).

Formatted: Font: 12 pt, Not Bold

Formatted: Font: 12 pt, Not Bold, Not Italic

Formatted: Font: 12 pt, Not Bold

Formatted: Font: 12 pt, Not Bold, Not Italic

Formatted: Font: 12 pt, Not Bold

Formatted: Font: 12 pt, Not Bold, Not Italic

Formatted: Font: 12 pt, Not Bold

Formatted: Font: 12 pt, Not Bold, Not Italic

Formatted: Font: 12 pt, Not Bold

Formatted: Font: 12 pt, Not Bold, Not Italic

Formatted: Font: 12 pt, Not Bold

Formatted: Font: 12 pt, Not Bold, Not Italic

Formatted: Font: 12 pt, Not Bold

Formatted: Font: 12 pt, Not Bold, Not Italic

Formatted: Font: 12 pt, Not Bold

Formatted: Font: 12 pt, Not Bold, Not Italic

Formatted: Font: 12 pt, Not Bold

Formatted: Font: 12 pt, Not Bold, Not Italic

Formatted: Font: 12 pt, Not Bold

Formatted: Font: 12 pt, Not Bold, Not Italic

1020 Major, top-SSW mylonitic shear zones in Sassenfjorden–Tempelfjorden and Billefjorden  
1021 display early Cenozoic overprints including top-SSW duplexes in uppermost Devonian–  
1022 Mississippian coals of the Billefjorden Group acting as a partial décollement along a major  
1023 basement-seated listric brittle fault (Koehl, 2020a; supplement S2) and NNE-dipping brittle faults  
1024 offsetting the east-dipping Billefjorden Fault Zone by hundreds of meters to several kilometers left-  
1025 laterally (Koehl et al., 2021 in review). Thus, the correlation of the Kongsfjorden–Cowanodden  
1026 fault zone with these top-SSW mylonitic shear zones in Sassenfjorden–Tempelfjorden and  
1027 Billefjorden (see [Figure 1c](#) for location) supports reactivation–overprinting of major NNE-  
1028 dipping Timanian thrust systems as top-SSW, sinistral-reverse, oblique-slip thrusts in the early  
1029 Cenozoic Eureka tectonic event. Such correlation explains the NW–SE trend and the location of  
1030 the northeastern boundary of the Central Tertiary Basin, which terminates just southwest of  
1031 Sassenfjorden and Sassendalen in central Spitsbergen ([Figure 1b–c](#)). It also explains the  
1032 dominance of NW–SE- to WNW–ESE-striking faults within Cenozoic deposits of the Central  
1033 Tertiary Basin (Livshits, 1965a), and the northwestwards provenance (Petersen et al., 2016) and  
1034 northwards thinning of sediments deposited in the basin (Livshits, 1965b), which were probably  
1035 sourced from uplifted areas in the hanging wall of the reactivated–overprinted thrust.

1036 Noteworthy, Livshits (1965a) argued that the Central Tertiary Basin was bounded to the  
1037 north by a major WNW–ESE-striking fault extending from Kongsfjorden to southern Billefjorden–  
1038 Sassenfjorden where the NNE-dipping Kongsfjorden–Cowanodden fault zone was mapped (present  
1039 study; supplement S2). This indicates that the Kongsfjorden–Cowanodden fault zone might extend  
1040 west of Billefjorden and Sassenfjorden, potentially until Kongsfjorden (see [Figure 1c](#) for  
1041 location). Should it be the case, the Kongsfjorden–Cowanodden fault zone would coincide with a  
1042 major terrane boundary in Svalbard, which was speculated to correspond to one or more regional  
1043 WNW–ESE- to N–S-striking faults in earlier works, e.g., Kongsvegen Fault and Lapsdalen Thrust  
1044 (Harland and Horsfield, 1974), Kongsvegen Fault Zone and/or Central–West Fault Zone (Harland  
1045 and Wright, 1979), and Kongsfjorden–Hansbreen Fault Zone (Harland et al., 1993). The presence  
1046 of a major, (inherited Timanian) NNE-dipping, basement-seated fault zone in this area would  
1047 explain the observed strong differences between Precambrian basement rocks in Svalbard’s  
1048 northwestern and southwestern terranes.

1049 In southern Spitsbergen, von Gosen and Piepjohn (2001) and Bergh and Grogan (2003)  
1050 suggested the presence of a WNW–ESE-striking, sinistral-reverse strike-slip fault in Hornsund

Formatted: Font: 12 pt, Not Bold

Formatted: Font: 12 pt, Not Bold, Not Italic

Formatted: Font: 12 pt, Not Bold

Formatted: Font: 12 pt, Not Bold, Not Italic

Formatted: Font: 12 pt, Not Bold

Formatted: Font: 12 pt, Not Bold, Not Italic

1051 based on a one-kilometer left-lateral offset of Devonian–Carboniferous sedimentary successions  
1052 and of the early Cenozoic Hyrnefjellet Anticline across the fjord. This fault is part of the  
1053 Kinnhøgda–Daudbjørnpynten fault zone and was most likely reactivated–overprinted during  
1054 Eureka contraction–transpression in the early Cenozoic.

1055

#### 1056 *Present day tectonism*

1057 Seismic data show that the seafloor reflection is folded and/or offset in a reverse fashion by  
1058 high-angle brittle faults merging at depth with interpreted Timanian thrust systems in Storfjorden  
1059 and just north of Bjørnøya in the northwestern Norwegian Barents (~~Figure 3~~Figure 3a and c, and  
1060 ~~Figure 4~~Figure 4h). This indicates that some of the Timanian thrust systems are still active at  
1061 present and are reactivated/overprinted by reverse faults (~~Figure 7~~Figure 7e). A potential  
1062 explanation for ongoing reactivation–overprinting is transfer of extensional tectonic stress in the  
1063 Fram Strait as ridge–push tectonism through Spitsbergen and Storfjorden.

1064

#### 1065 *Implication for plate tectonics reconstructions of the Barents Sea and Svalbard in the late* 1066 *Neoproterozoic–Paleozoic*

1067 The presence of hundreds to thousands of kilometers long Timanian faults throughout the  
1068 northern Norwegian Barents Sea and central and southwestern (and possibly northwestern?)  
1069 Spitsbergen indicates that the northwestern, northeastern and southwestern basement terranes of  
1070 the Svalbard Archipelago were most likely already accreted together and attached to the Barents  
1071 Sea, northern Norway and northwestern Russia in the late Neoproterozoic (ca. 600 Ma). Svalbard’s  
1072 three terranes were previously thought to have been juxtaposed during the Caledonian and  
1073 Ellesmerian orogenies through hundreds–thousands of kilometers of displacement along presumed  
1074 thousands of kilometers long N–S-striking strike-slip faults like the Billefjorden Fault Zone  
1075 (Harland, 1969; Harland et al. 1992, Labrousse et al., 2008; ~~Figure 2~~Figure 2). The presence of  
1076 laterally continuous (undisrupted), hundreds–thousands of kilometers long, Timanian thrust  
1077 systems from southwestern and central Spitsbergen to the northern Norwegian and Russian Barents  
1078 Sea clearly shows that this is not possible (~~Figure 8~~Figure 8).

1079 The continuous character of these thrust systems from potentially as far as onshore  
1080 northwestern Russia through the Barents Sea and Svalbard precludes any major strike-slip  
1081 displacement along N–S-striking faults such as the Billefjorden Fault Zone and Lomfjorden Fault

Formatted: Font: 12 pt, Not Bold

Formatted: Font: 12 pt, Not Bold, Not Italic

Formatted: Font: 12 pt, Not Bold

Formatted: Font: 12 pt, Not Bold, Not Italic

Formatted: Font: 12 pt, Not Bold

Formatted: Font: 12 pt, Not Bold, Not Italic

Formatted: Font: 12 pt, Not Bold

Formatted: Font: 12 pt, Not Bold, Not Italic

Field Code Changed

Formatted: Font: (Default) Times New Roman

Formatted: Font: Not Bold, Not Italic



1082 Zone (as proposed by Harland et al., 1974, 1992; Labrousse et al., 2008: [Figure 2](#)) and any hard-  
1083 linked connection between these faults in Svalbard and analogous, NE–SW-striking faults in  
1084 Scotland in the Phanerozoic (as proposed by Harland, 1969). Instead, the present work suggests  
1085 that the crust constituting the Barents Sea and the northeastern and southwestern basement terranes  
1086 of Svalbard should be included as part of Baltica in future Arctic plate tectonics reconstructions for  
1087 the late Neoproterozoic–Paleozoic period (i.e., until ca. 600 Ma; [Figure 8](#)). It also suggests that the  
1088 Caledonian suture zone, previously inferred to lie east of Svalbard in the Barents Sea (e.g., Gee  
1089 and Teben’kov, 2004; Breivik et al., 2005; Barrère et al., 2011; Knudsen et al., 2019) may be  
1090 located west of the presently described Timanian thrust systems, i.e., probably west of or in western  
1091 Spitsbergen where Caledonian blueschist and eclogite metamorphism was been recorded in  
1092 Precambrian basement rocks (Horsfield, 1972; Dallmeyer et al., 1990a; Ohta et al., 1995;  
1093 Kosminska et al., 2014).

Formatted: Font: 12 pt, Not Bold

Formatted: Font: 12 pt, Not Bold, Not Italic

Formatted: Font: (Default) Times New Roman

Formatted: Font: Not Bold, Not Italic

1094

## 1095 Conclusions

- 1096 1) Seismic data in the northern Norwegian Barents Sea and Svalbard reveal the existence of  
1097 several systems of hundreds–thousands of kilometers long, several kilometers thick, top-  
1098 SSW ~~Timanian~~ thrusts comprised of brittle–ductile thrusts, mylonitic shear zones and  
1099 associated SSW-verging folds that appear to extend from onshore northwestern Russia to  
1100 the northern Norwegian Barents Sea and to central and southwestern Spitsbergen. A notable  
1101 structure is the Kongsfjorden–Cowanodden fault zone in Svalbard and the Norwegian  
1102 Barents Sea, which likely merges with the Baidaratsky fault zone in the Russian Barents  
1103 Sea and southern Novaya Zemlya. We interpret these thrust systems as being related to the  
1104 Neoproterozoic Timanian Orogeny.
- 1105 2) In the east (away from the Caledonian collision zone), these Timanian thrusts systems were  
1106 folded into NNE-plunging folds, offset, and reactivated as and/or overprinted by top-west,  
1107 oblique-slip sinistral-reverse, brittle–ductile thrusts during subsequent Caledonian (e.g.,  
1108 Agardhbukta Fault segment of the Lomfjorden Fault Zone) and, possibly, during Eurekan  
1109 contraction, and are deeply buried. By contrast, in the west (near or within the Caledonian  
1110 collision zone), Timanian thrusts were intensely deformed, pushed into sub-vertical  
1111 positions, extensively overprinted, and exhumed to the surface.

- 1112 3) In eastern Spitsbergen, a major NNE-dipping Timanian thrust system, the Kongsfjorden–  
1113 Cowanodden fault zone, is crosscut by a swarm of Devonian (–Mississippian?) dykes that  
1114 intruded contemporaneous sedimentary strata deposited during extensional reactivation of  
1115 the eastern portion of the thrust system as a low-angle extensional detachment during late–  
1116 post-Caledonian collapse.
- 1117 4) Timanian thrust systems were overprinted by NNE-dipping, brittle normal faults in the late  
1118 Paleozoic during the collapse of the Caledonides and/or subsequent rifting in the Devonian–  
1119 Carboniferous.
- 1120 5) Timanian thrust systems and associated Caledonian and Devonian–Carboniferous brittle  
1121 overprints (e.g., Agardhbukta Fault) in the northwestern Norwegian Barents Sea and  
1122 Svalbard were mildly reactivated during the early Cenozoic Eurekan tectonic event, which  
1123 resulted in minor folding and minor reverse offsets of Devonian–Mesozoic sedimentary  
1124 strata and intrusions. Timanian thrusts and related overprints in the northeastern Norwegian  
1125 Barents Sea were not reactivated during the Eurekan tectonic event.
- 1126 6) The presence of hundreds–thousands of kilometers long Timanian thrust systems may  
1127 suggests that the Barents Sea and Svalbard’s three basement terranes were already attached  
1128 to northern Norway and northwestern Russia in the late Neoproterozoic (ca. 600 Ma). If  
1129 correct, a Timanian origin for these structures would, precludes any major strike-slip  
1130 movements along major N–S-striking faults like the Billefjorden and Lomfjorden fault  
1131 zones in the Phanerozoic, and suggests-imply that the Caledonian suture zone is located  
1132 west of or in western Spitsbergen.

1133

#### 1134 **Acknowledgements**

1135 The present study was supported by the Research Council of Norway, the Tromsø Research  
1136 Foundation, and six industry partners through the Research Centre for Arctic Petroleum  
1137 Exploration (ARCEX; grant number 228107), the SEAMSTRESS project (grant number 287865),  
1138 and the Centre for Earth Evolution and Dynamics (CEED; grant number 223272). We thank the  
1139 Norwegian Petroleum Directorate and the Federal Institute for Geosciences and Natural Resources  
1140 (BGR) for granting access and allowing publication of seismic, magnetic and gravimetric data in  
1141 Svalbard and the Norwegian Barents Sea. Prof. Steffen Bergh, Dr. Winfried Dallmann, Prof. Jiri  
1142 Konopasek, Assoc. Prof. Mélanie Forien, Dr. Kate Waghorn (UiT The Arctic University of Norway

1143 in Tromsø), Dr. Peter Klitzke (Federal Institute for Geosciences and Natural Resources –  
1144 Germany), Anna Dichiarante (Norway Seismic Array), Rune Matningsdal (Norwegian Petroleum  
1145 Directorate), and Prof. Carmen Gaina (Centre for Earth Evolution and Dynamics, University of  
1146 Oslo) are thanked for fruitful discussion.

1147

#### 1148 **Data availability**

1149 For high-resolution versions of the figures and supplements, the reader is referred to the  
1150 Open Access data repository DataverseNO ([doi.org/10.18710/CE8RQH](https://doi.org/10.18710/CE8RQH)). ~~The complete seismic~~  
1151 ~~study is also available from the corresponding author upon request.~~

1152

#### 1153 **References**

- 1154 Aakvik, R.: Fasies analyse av Undre Karbonske kullførende sedimenter, Billefjorden, Spitsbergen,  
1155 Ph.D. Thesis, University of Bergen, Bergen, Norway, 219 pp., 1981.
- 1156 Andresen, A., Haremo, P., Swensson, E. and Bergh, S. G.: Structural geology around the southern  
1157 termination of the Lomfjorden Fault Complex, Agardhdalen, east Spitsbergen, Norsk Geol.  
1158 Tidsskr., 72, 83–91, 1992.
- 1159 Anell, I., Braathen, A., Olaussen, S. and Osmundsen, P. T.: Evidence of faulting contradicts a  
1160 quiescent northern Barents Shelf during the Triassic, First Break, 31, 67–76, 2013.
- 1161 Anell, I. M., Braathen, A. and Olaussen, S.: Regional constraints of the Sørkapp Basin: A  
1162 Carboniferous relic or a Cretaceous depression, Mar. Petrol. Geol., 54, 123–138, 2014.
- 1163 Anell, I. M., Faleide, J. I. and Braathen, A.: Regional tectono-sedimentary development of the  
1164 highs and basins of the northwestern Barents Shelf, Norsk Geologisk Tidsskrift, 96, 1, 27–  
1165 41, 2016.
- 1166 Arbaret, L. and Burg, J.-P.: Complex flow in lowest crustal, anastomosing mylonites: Strain  
1167 gradients in a Kohistan gabbro, northern Pakistan, J. Geophys. Res., 108, 2467, 2003.
- 1168 Barrère, C., Ebbing, J. and Gernigon, L.: Offshore prolongation of Caledonian structures and  
1169 basement characterization in the western Barents Sea from geophysical modelling,  
1170 Tectonophys., 470, 71–88, 2009.
- 1171 Barrère, C., Ebbing, J. and Gernigon, L.: 3-D density and magnetic crustal characterization of the  
1172 southwestern Barents Shelf: implications for the offshore prolongation of the Norwegian  
1173 Caledonides, Geophys. J. Int., 184, 1147–1166, 2011.

- 1174 Boyer, S. E. and Elliott, D.: Thrust Systems, AAPG Bulletin, 66, 9, 1196–1230, 1982.
- 1175 Braathen, A., Bælum, K., Maher Jr., H. D. and Buckley, S. J.: Growth of extensional faults and  
1176 folds during deposition of an evaporite-dominated half-graben basin; the Carboniferous  
1177 Billefjorden Trough, Svalbard, Norsk Geol. Tidsskr., 91, 137–160, 2011.
- 1178 Braathen, A., Osmundsen, P. T., Maher, H. and Ganerød, M.: The Keisarhjelmen detachment  
1179 records Silurian–Devonian extensional collapse in Northern Svalbard, Terra Nova, 30, 34–  
1180 39, 2018.
- 1181 Breivik, A. J., Mjelde, R., Grogan, P., Shimamura, H., Murai, Y. and Nishimura, Y.: Caledonide  
1182 development offshore–onshore Svalbard based on ocean bottom seismometer, conventional  
1183 seismic, and potential field data, Tectonophys., 401, 79–117, 2005.
- 1184 Bro, E. G. and Shvarts, V. H.: Processing results from drill hole Raddedalen-1, Edge Island,  
1185 Spitzbergen Archipelago, All-Russian Research Institute for Geology and Mineral  
1186 Resources of the World Ocean, St. Petersburg, Pangaea, Report 5750, 1983.
- 1187 Cawood, P. A., McCausland, P. J. A. and Dunning, G. R.: Opening Iapetus: Constraints from the  
1188 Laurentian margin in Newfoundland, GSA Bull., 113, 4, 443–453, 2001.
- 1189 Chalmers, J. A. and Pulvertaft, T. C. R.: Development of the continental margins of the Labrador  
1190 Sea: a review, in: Non-Volcanic Rifting of Continental Margins: A Comparison of  
1191 Evidence from Land and Sea, edited by: Wilson, R. C. L., Taylor, R. B. and Froitzheim,  
1192 N., Geol. Soc. London, Spec. Publi., 187, 77–105, 2001.
- 1193 Cocks, L. R. M. and Torsvik, T. H.: Baltica from the late Precambrian to mid-Palaeozoic times:  
1194 The gain and loss of a terrane’s identity, Earth-Sci. Rev., 72, 39–66, 2005.
- 1195 Colombu, S., Cruciani, G., Fancello, D., Franceschelli, M. and Musumeci, G.: Petrophysical  
1196 properties of a granite-protomylonite-ultramylonite sequence: insight from the Monte  
1197 Grighini shear zone, central Sardinia, Italy, Eur. J. Mineral, 27, 471–486, 2015.
- 1198 Corfu, F., Andersen, T. B. and Gasser, D.: The Scandinavian Caledonides: main features,  
1199 conceptual advances and critical questions, in: New Perspectives on the Caledonides of  
1200 Scandinavia and Related Areas, edited by: Corfu, F., Gasser, D. and Chew, D. M., Geol.  
1201 Soc., London, Spec. Publi., 390, 9–43, 2014.
- 1202 Cutbill, J. L. and Challinor, A.: Revision of the Stratigraphical Scheme for the Carboniferous and  
1203 Permian of Spitsbergen and Bjørnøya, Geol. Mag., 102, 418–439, 1965.

- 1204 Cutbill, J. L., Henderson, W. G. and Wright, N. J. R.: The Billefjorden Group (Early Carboniferous)  
1205 of central Spitsbergen, Norsk Polarinst. Skr., 164, 57–89, 1976.
- 1206 Dallmann, W. K.: Geoscience Atlas of Svalbard, Norsk Polarinstitut, Tromsø, Norway,  
1207 Rapportserie nr. 148, 2015.
- 1208 Dallmann, W. K. and Krasil'scikov, A. A.: Geological map of Svalbard 1:50,000, sheet D20G  
1209 Bjørnøya, Norsk Polarinst. Temakart, 27, 1996.
- 1210 Dallmann, W. K. and Piepjohn, K.: The structure of the Old Red Sandstone and the Svalbardian  
1211 Orogenic Event (Ellesmerian Orogeny) in Svalbard, Norg. Geol. Unders. B., Spec. Publi.,  
1212 15, 106 pp., 2020.
- 1213 Dallmeyer, R. D., Peucat, J. J., Hirajima, T. and Ohta, Y.: Tectonothermal chronology within a  
1214 blueschist–eclogite complex, west-central Spitsbergen, Svalbard: Evidence from  $^{40}\text{Ar}/^{39}\text{Ar}$   
1215 and Rb–Sr mineral ages, Lithos, 24, 291–304, 1990a.
- 1216 Dallmeyer, R. D., Peucat, J. J. and Ohta, Y.: Tectonothermal evolution of contrasting metamorphic  
1217 complexes in northwest Spitsbergen (Biskayerhalvøya): Evidence from  $^{40}\text{Ar}/^{39}\text{Ar}$  and Rb–  
1218 Sr mineral ages, GSA Bull., 102, 653–663, 1990b.
- 1219 Dewey, J. F. and Strachan, R. A.: Changing Silurian–Devonian relative plate motion in the  
1220 Caledonides: sinistral transpression to sinistral transtension, J. Geol. Soc., London, 160,  
1221 219–229, 2003.
- 1222 Drachev, S. S.: Fold belts and sedimentary basins of the Eurasian Arctic, Arktos, 2:21, 2016.
- 1223 Drachev, S. S., Malyshev, N. A. and Nikishin, A. M.: Tectonic history and petroleum geology of  
1224 the Russian Arctic Shelves: an overview, Petrol. Geol. Conf. series, 7, 591–619, 2010.
- 1225 Dumais, M.-A. and Brönnner, M.: Revisiting Austfonna, Svalbard, with potential field methods – a  
1226 new characterization of the bed topography and its physical properties, The Cryosphere,  
1227 14, 183–197, 2020.
- 1228 Eldholm, O. and Ewing, J.: Marine Geophysical Survey in the Southwestern Barents Sea, J.  
1229 Geophys. Res., 76, 17, 3832–3841, 1971.
- 1230 Engen, Ø., Faleide, J. I. and Dyreng, T. K.: Opening of the Fram Strait gateway: A review of plate  
1231 tectonic constraints, Tectonophysics, 450, 51–69, 2008.
- 1232 Estrada, S., Tessensohn, F. and Sonntag, B.-L.: A Timanian island-arc fragment in North  
1233 Greenland: The Midtkap igneous suite, J. Geodyn., 118, 140–153, 2018.

- 1234 Faehnrich, K., Majka, J., Schneider, D., Mazur, S., Manecki, M., Ziemniak, G., Wala, V. T. and  
1235 Strauss, J. V.: Geochronological constraints on Caledonian strike-slip displacement in  
1236 Svalbard, with implications for the evolution of the Arctic, *Terra Nova*, 2020, 32, 290–299.
- 1237 Fortey, R. A. and Bruton, D. L.: Lower Ordovician trilobites of the Kirtonryggen Formation,  
1238 Spitsbergen, *ossils and Strata*, 59, Wiley Blackwell, 120 pp., 2013.
- 1239 Fountain, D. M., Hurich, C. A. and Smithson, S. B.: Seismic relectivity of mylonite zones in the  
1240 crust, *Geology*, 12, 195–198, 1984.
- 1241 Friend, P. F. and Moody-Stuart, M.: Sedimentation of the Wood Bay Formation (Devonian) of  
1242 Spitsbergen: Regional analysis of a late orogenic basin, *Norsk Polarinst. Skr.*, 157, 80 pp.,  
1243 1972.
- 1244 Friend, P. F., Heintz, N. and Moody-Stuart, M.: New unit terms for the Devonian of Spitsbergen  
1245 and a new stratigraphical scheme for the Wood Bay Formation, *Polarinst. Årbok*, 1965, 59–  
1246 64, 1966.
- 1247 Friend, P. F., Harland, W. B., Rogers, D. A., Snape, I. and Thornley, R. S.: Late Silurian and Early  
1248 Devonian stratigraphy and probable strike-slip tectonics in northwestern Spitsbergen, *Geol.*  
1249 *Mag.*, 134, 4, 459–479, 1997.
- 1250 Gasser, D.: The Caledonides of Greenland, Svalbard and other Arctic areas: status of research and  
1251 open questions, in: *New Perspectives on the Caledonides of Scandinavia and Related Areas*,  
1252 edited by: Corfu, F., Gasser, D. and Chew, D. M., *Geol. Soc., London, Spec. Publi.*, 390,  
1253 93–129, 2014.
- 1254 Gee, D. G. and Moody-Stuart, M.: The base of the Old Red Sandstone in central north Haakon VII  
1255 Land, *Vestspitsbergen, Polarinst. Årbok*, 1964, 57–68, 1966.
- 1256 Gee, D. G. and Pease, V.: The Neoproterozoic Timanide Orogen of eastern Baltica: introduction,  
1257 in: *The Neoproterozoic Timanide Orogen of eastern Baltica*, edited by: Gee, D. G. and  
1258 Pease, V., *Geol. Soc. London, Mem.*, 30, 1–3, 2004.
- 1259 Gee, D. G. and Teben'kov, A. M.: Svalbard: a fragment of the Laurentian margin, in: *The*  
1260 *Neoproterozoic Timanide Orogen of eastern Baltica*, edited by: Gee, D. G. and Pease, V.,  
1261 *Geol. Soc. London, Mem.*, 30, 191–206, 2004.
- 1262 Gee, D. G., Björklund, L. and Stølen, L.-K.: Early Proterozoic basement in Ny Friesland–  
1263 implications for the Caledonian tectonics of Svalbard, *Tectonophys.*, 231, 171–182, 1994.

- 1264 Gee, D. G., Fossen, H., Henriksen, N. and Higgins, A. K.: From the Early Paleozoic Platforms of  
1265 Baltica and Laurentia to the Caledonide Orogen of Scandinavia and Greenland, *Episodes*,  
1266 31, 1, 44–51, 2008.
- 1267 Gernigon, L. and Brönnner, M.: Late Palaeozoic architecture and evolution of the southwestern  
1268 Barents Sea: insights from a new generation of aeromagnetic data, *J. Geol. Soc., London*,  
1269 169, 449–459, 2012.
- 1270 Gernigon, L., Brönnner, M., Roberts, D., Olesen, O., Nasuti, A. and Yamasaki, T.: Crustal and basin  
1271 evolution of the southwestern Barents Sea: From Caledonian orogeny to continental  
1272 breakup, *Tectonics*, 33, 347–373, 2014.
- 1273 Gernigon, L., Brönnner, M., Dumais, M.-A., Gradmann, S., Grønlie, A., Nasuti, A. and Roberts, D.:  
1274 Basement inheritance and salt structures in the SE Barents Sea: Insights from new potential  
1275 field data, *J. Geodyn.*, 119, 82–106, 2018.
- 1276 Griffin, W. L., Nikolic, N., O'Reilly, S. Y. and Pearson, N. J.: Coupling, decoupling and  
1277 metasomatism: Evolution of crust–mantle relationships beneath NW Spitsbergen, *Lithos*,  
1278 149, 115–135, 2012.
- 1279 Gudlaugsson, S. T., Faleide, J. I., Johansen, S. E. and Breivik, A. J.: Late Palaeozoic structural  
1280 development of the South-western Barents Sea. *Mar. Petrol. Geol.*, 15, 73–102, 1998.
- 1281 Haremo, P. and Andresen, A.: Tertiary décollements thrusting and inversion structures along  
1282 Billefjorden and Lomfjorden Fault Zones, East Central Spitsbergen, in: *Structural and  
1283 Tectonic Modelling and its Application to Petroleum Geology*, edited by: Larsen, R. M.,  
1284 Brekke, H., Larsen, B. T. and Talleraas, E., Norwegian Petroleum Society (NPF) Special  
1285 Publications, 1, 481–494, 1992.
- 1286 Harland, W. B.: Contribution of Spitsbergen to understanding of tectonic evolution of North  
1287 Atlantic region, *AAPG Memoirs*, 12, 817–851, 1969.
- 1288 Harland, W. B. and Horsfield, W. T.: West Spitsbergen Orogen, in: *Mesozoic–Cenozoic Orogenic  
1289 Belts, data for Orogenic Studies*, *J. Geol. Soc. London, Spec. Publi.*, 4, 747–755, 1974.
- 1290 Harland, W. B. and Kelly, S. R. A.: Eastern Svalbard Platform, in: *Geology of Svalbard*, edited by:  
1291 Harland, W. B., *Geol. Soc. London, Mem.*, 17, 521 pp., 1997.
- 1292 Harland, W. B. and Wright, N. J. R.: Alternative hypothesis for the pre-Carboniferous evolution of  
1293 Svalbard, *Norsk Polarinst. Skr.*, 167, 89–117, 1979.

- 1294 Harland, W. B., Cutbill, L. J., Friend, P. F., Gobbett, D. J., Holliday, D. W., Maton, P. I., Parker,  
1295 J. R. and Wallis, R. H.: The Billefjorden Fault Zone, Spitsbergen – the long history of a  
1296 major tectonic lineament, *Norsk Polarinst. Skr.*, 161, 1–72, 1974.
- 1297 Harland, W. B., Scott, R. A., Auckland, K. A. and Snape, I.: The Ny Friesland Orogen, Spitsbergen,  
1298 *Geol. Mag.*, 129, 6, 679–708, 1992.
- 1299 Harland, W. B., Hambrey, M. J. and Waddams, P.: Vendian geology of Svalbard, *Norsk Polarinst.*  
1300 *Skri.*, 193, 152 pp., 1993.
- 1301 Hassaan, M., Faleide, J. I., Gabrielsen, R. H. and Tsikalas, F.: Carboniferous graben structures,  
1302 evaporite accumulations and tectonic inversion in the southeastern Norwegian Barents Sea,  
1303 *Mar. Petrol. Geol.*, 112, 104038, 2020a.
- 1304 Hassaan, M., Faleide, J. I., Gabrielsen, R. H. and Tsikalas, F.: Architecture of the evaporite  
1305 accumulation and salt structures dynamics in Tiddlybanken Basin, southeastern Norwegian  
1306 Barents Sea, *Basin Res.*, 33, 91–117, 2020b.
- 1307 Herrevold, T., Gabrielsen, R. H. and Roberts, D.: Structural geology of the southeastern part of the  
1308 Trollfjorden-Komagelva Fault Zone, Varanger Peninsula, Finnmark, North Norway,  
1309 *Norwegian Journal of Geology*, 89, 305-325, 2009.
- 1310 Horsfield, W. T.: Glauconite schists of Caledonian age from Spitsbergen, *Geol. Mag.*, 109, 1,  
1311 29–36, 1972.
- 1312 Hurich, C. A., Smithson, S. B., Fountain, D. M. and Humphreys, M. C.: Seismic evidence of  
1313 mylonite reflectivity and deep structure in the Kettle dome metamorphic core complex,  
1314 Washington, *Geology*, 13, 577–580, 1985.
- 1315 Jakobsson, M., Mayer, L., Coackley, B., Dowdeswell, J. A., Forbes, S., Fridman, B., Hodnesdal,  
1316 H., Noormets, R., Pedersen, R., Rebesco, M., Schenke, H. W., Zarayskaya, Y., Accettella,  
1317 D., Armstrong, A., Anderson, R. M., Bienhoff, P., Camerlenghi, A., Church, I., Edwards,  
1318 M., Gardner, J. V., Hall, J. K., Hell, B., Hestvik, O., Kristoffersen, Y., Marcussen, C.,  
1319 Mohammad, R., Mosher, D., Nghiem, S. V., Pedrosa, M. T., Travaglini, P. G., and  
1320 Weatherall, P.: The International Bathymetric Chart of the Arctic Ocean (IBCAO) Version  
1321 3.0, *Geophys. Res. Lett.*, 39, L12609, <https://doi.org/10.1029/2012GL052219>, 2012.
- 1322 Johansen, S. E., Ostisty, B. K., Birkeland, Ø., Fedorovsky, Y. F., Martirosjan, V. N., Bruun  
1323 Christensen, O., Cheredeev, S. I., Ignatenko, E. A. and Margulis, L. S.: Hydrocarbon  
1324 potential in the Barents Sea region: play distribution and potential, in: *Arctic Geology and*



1325 Petroleum Potential, edited by: Vorren, T. O., Bergsager, E., Dahl-Stamnes, Ø. A., Holter,  
1326 E., Johansen, B., Lie, E. and Lund, T. B., NPF Spec. Publi., 2, 273–320, Elsevier,  
1327 Amsterdam, 1992.

1328 Johansson, Å., Larionov, A. N., Gee, D. G., Ohta, Y., Tebenkov, A. M. and Sandelin, S.:  
1329 Grenvillian and Caledonian tectono-magmatic activity in northeasternmost Svalbard, in:  
1330 The Neoproterozoic Timanide Orogen of Eastern Baltica, edited by: Gee, D. G. and Pease,  
1331 V., Geol. Soc. London Memoirs, 30, 207–232, 2004.

1332 Johansson, Å., Gee, D. G., Larionov, A. N., Ohta, Y. and Tebenkov, A. M.: Grenvillian and  
1333 Caledonian evolution of eastern Svalbard – a tale of two orogenies, *Terra Nova*, 17, 317–  
1334 325, 2005.

1335 Kairanov, B., Escalona, A., Mordascova, A., Sliwinska, K. and Suslova, A.: Early Cretaceous  
1336 tectonostratigraphy evolution of the north central Barents Sea, *J. Geodyn.*, 119, 183–198,  
1337 2018.

1338 Klitzke, P., Franke, D., Ehrhardt, A., Lutz, R., Reinhardt, L., Heyde, I. and Faleide, J. I.: The  
1339 Palaeozoic Evolution of the Olga Basin Region, Northern Barents Sea: A Link to the  
1340 Timanian Orogeny, *Geochem., Geophys., Geosy.*, 20, 614–629, 2019.

1341 Knudsen, C., Gee, D. G., Sherlock, S. C. and Yu, L.: Caledonian metamorphism of metasediments  
1342 from Franz Josef Land, *GFF*, 141, 295–307, 2019.

1343 Koehl, J.-B. P.: Early Cenozoic Eurekan strain partitioning and decoupling in central Spitsbergen,  
1344 Svalbard, *Solid Earth*, 12, 1025–1049, 2020a.

1345 Koehl, J.-B. P.: Impact of Timanian thrusts on the Phanerozoic tectonic history of Svalbard,  
1346 Keynote lecture, EGU General Assembly, May 3<sup>rd</sup>–8<sup>th</sup> 2020, Vienna, Austria, 2020b.

1347 Koehl, J.-B. P. and Muñoz-Barrera, J. M.: From widespread Mississippian to localized  
1348 Pennsylvanian extension in central Spitsbergen, Svalbard, *Solid Earth*, 9, 1535–1558, 2018.

1349 Koehl, J.-B. P., Bergh, S. G., Henningsen, T. and Faleide, J. I.: Middle to Late Devonian–  
1350 Carboniferous collapse basins on the Finnmark Platform and in the southwesternmost  
1351 Nordkapp basin, SW Barents Sea, *Solid Earth*, 9, 341–372, 2018.

1352 Koehl, J.-B. P., Bergh, S. G., Osmundsen, P. T., Redfield, T., Indrevær, K., Lea, H. and Bergø, E.:  
1353 Late Devonian–Carboniferous faulting and controlling structures and fabrics in NW  
1354 Finnmark, *Norw. J. Geol.*, 99, 3, 1–40, 2019.

- 1355 Koehl, J.-B. P., Allaart, L. and Noormets, R.: Devonian–Carboniferous collapse and segmentation  
1356 of the Billefjorden Trough, and Eureka inversion–overprint and strain partitioning and  
1357 decoupling along inherited WNW–ESE-striking faults, in review, 2021.
- 1358 Korago, E. A., Kovaleva, G. N., Lopatin, B. G. and Orgo, V. V.: The Precambrian rocks of Novaya  
1359 Zemlya, in: *The Neoproterozoic Timanide Orogen of Eastern Baltica*, edited by: Gee, D.  
1360 G. and Pease, V., *Geol. Soc. London, Mem.*, 30, 135–143, 2004.
- 1361 Kosminska, K., Majka, J., Mazur, S., Krumbholz, M., Klonowska, I., Manecki, M., Czerny, J. and  
1362 Dwornik, M.: Blueschist facies metamorphism in Nordenskiöld Land of west-central  
1363 Svalbard, *Terra Nova*, 26, 377–386, 2014.
- 1364 Kostyuchenko, A., Sapozhnikov, R., Egorkin, A., Gee, D. G., Berzin, R. and Solodilov, L.: Crustal  
1365 structure and tectonic model of northeastern Baltica, based on deep seismic and potential  
1366 field data, in: *European Lithosphere Dynamics*, edited by: Gee, D. G. and Stephenson, R.  
1367 A., *Geol. Soc. London Mem.*, 32, 521–539, 2006.
- 1368 Labrousse, L., Elvevold, S., Lepvrier, C. and Agard, P.: Structural analysis of high-pressure  
1369 metamorphic rocks of Svalbard: Reconstructing the early stages of the Caledonian orogeny,  
1370 *Tectonics*, 27, 22 pp., 2008.
- 1371 Lamar, D. L. and Douglass, D. N.: Geology of an area astride the Billefjorden Fault Zone, Northern  
1372 Dicksonland, Spitsbergen, Svalbard, *Polarist. Skr.*, 197, 46 pp., 1995.
- 1373 Lamar, D. L., Reed, W. E. and Douglass, D. N.: Billefjorden fault zone, Spitsbergen: Is it part of a  
1374 major Late Devonian transform?, *GSA*, 97, 1083–1088, 1986.
- 1375 Larssen, G. B., Elvebakk, G., Henriksen, L. B., Kristensen, S.-E., Nilsson, I., Samuelsberg, T. J.,  
1376 Svånå, T. A., Stemmerik, L. and Worsley, D.: Upper Palaeozoic lithostratigraphy of the  
1377 Southern part of the Norwegian Barents Sea, *Norges geol. unders. Bull.*, 444, 45 pp., 2005.
- 1378 Lasabuda, A., Laberg, J. S., Knutsen, S.-M. and Safronova, P.: Cenozoic tectonostratigraphy and  
1379 pre-glacial erosion: A mass-balance study of the northwestern Barents Sea margin,  
1380 *Norwegian Arctic, J. Geodyn.*, 119, 149–166, 2018.
- 1381 Lippard, S. J. and Prestvik, T.: Carboniferous dolerite dykes on Magerøy: new age determination  
1382 and tectonic significance, *Norsk Geologisk Tidsskrift*, 77, 159–163, 1997.
- 1383 Livshits, Yu. Ya.: Tectonics of Central Vestspitsbergen, in: *Geology of Spitsbergen*, edited by:  
1384 Sokolov, V. N., National Lending Library of Science and Technology, Boston Spa.,  
1385 Yorkshire, UK, 59–75, 1965a.

- 1386 Livshits, Yu. Ya.: Paleogene deposits of Nordenskiöld Land, Vestspitsbergen, in: *Geology of*  
1387 *Spitsbergen*, edited by: Sokolov, V. N., National Lending Library of Science and  
1388 *Technology*, Boston Spa., Yorkshire, UK, 193–215, 1965b.
- 1389 Lopatin, B. G., Pavlov, L. G., Orgo, V. V. and Shkarubo, S. I.: *Tectonic Structure of Novaya*  
1390 *Zemlya*, *Polarforschung*, 69, 131–135, 2001.
- 1391 Lorenz, H., Männik, P., Gee, D. and Proskurnin, V.: *Geology of the Severnaya Zemlya Archipelago*  
1392 *and the North Kara Terrane in the Russian high Arctic*, *Int. J. Earth Sci.*, 97, 519–547, 2008.
- 1393 Lowell, J. D.: *Spitsbergen tertiary Orogenic Belt and the Spitsbergen Fracture Zone*, *GSA Bull.*,  
1394 83, 3091–3102, 1972.
- 1395 Lyberis, N. and Manby, G.: *Continental collision and lateral escape deformation in the lower and*  
1396 *upper crust: An example from Caledonide Svalbard*, *Tectonics*, 18, 1, 40–63, 1999.
- 1397 Majka, J. and Kosminska, K.: *Magmatic and metamorphic events recorded within the Southwestern*  
1398 *Basement Province of Svalbard*, *Arktos*, 3:5, 2017.
- 1399 Majka, J., Mazur, S., Manecki, M., Czerny, J. and Holm, D. K.: *Late Neoproterozoic amphibolite-*  
1400 *facies metamorphism of a pre-Caledonian basement block in southwest Wedel Jarlsberg*  
1401 *Land, Spitsbergen: new evidence from U–Th–Pb dating of monazite*, *Geol. Mag.*, 145, 6,  
1402 822–830, 2008.
- 1403 Majka, J., Larionov, A. N., Gee, D. G., Czerny, J. and Prsek, J.: *Neoproterozoic pegmatite from*  
1404 *Skoddefjellet, Wedel Jarlsberg Land, Spitsbergen: Additional evidence for c. 640 Ma*  
1405 *tectonothermal event in the Caledonides of Svalbard*, *Polish Polar Res.*, 33, 1–17, 2012.
- 1406 Majka, J., De’eri-Shlevin, Y., Gee, D. G., Czerny, J., Frei, D. and Ladenberger, A.: *Torellian (c.*  
1407 *640 Ma) metamorphic overprint of Tonian (c. 950 Ma) basement in the Caledonides of*  
1408 *southwestern Svalbard*, *Geol. Mag.*, 151, 4, 732–748, 2014.
- 1409 Manby, G. M. and Lyberis, N.: *Tectonic evolution of the Devonian Basin of northern Spitsbergen*,  
1410 *Norsk Geol. Tidsskr.*, 72, 7–19, 1992.
- 1411 Manby, G. M., Lyberis, N., Chorowicz, J. and Thiedig, F.: *Post-Caledonian tectonics along the*  
1412 *Billefjorden fault zone, Svalbard, and implications for the Arctic region*, *Geol. Soc. Am.*  
1413 *Bul.*, 105, 201–216, 1994.
- 1414 Manecki, M., Holm, D. K., Czerny, J. and Lux, D.: *Thermochronological evidence for late*  
1415 *Proterozoic (Vendian) cooling in southwest Wedel Jarlsberg Land, Spitsbergen*, *Geological*  
1416 *Magazine*, 135, 63–9, 1998.

- 1417 Mareello, L., Ebbing, J. and Gernigon, L.: Magnetic basement study in the Barents Sea from  
1418 inversion and forward modelling, *Tectonophys.*, 493, 153–171, 2010.
- 1419 Mareello, L., Ebbing, J. and Gernigon, L.: Basement inhomogeneities and crustal setting in the  
1420 Barents Sea from a combined 3D gravity and magnetic model, *Geophys. J. Int.*, 193, 2,  
1421 557–584, 2013.
- 1422 Mazur, S., Czerny, J., Majka, J., Manecki, M., Holm, D., Smyrak, A. and Wypych, A.: A strike-  
1423 slip terrane boundary in Wedel Jarlsberg Land, Svalbard, and its bearing on correlations of  
1424 SW Spitsbergen with the Pearya terrane and Timanide belt, *J. Geol. Soc. London*, 166, 529–  
1425 544, 2009.
- 1426 McCann, A. J.: Deformation of the Old Red Sandstone of NW Spitsbergen; links to the Ellesmerian  
1427 and Caledonian orogenies, in: *New Perspectives on the Old Red Sandstone*, edited by:  
1428 Friends, P. F. and Williams, B. P. J., *Geol. Soc. London*, 180, 567–584, 2000.
- 1429 Merdith, A. S., Williams, S. E., Collins, A. S., Tetley, M. G., Mulder, J. A., Blades, M. L., Young,  
1430 A., Armistead, S. E., Cannon, J., Zahirovic, S. and Müller, R. D.: Extending full-plate  
1431 tectonic models into deep time: Linking the Neoproterozoic and the Phanerozoic, *Earth-  
1432 Sci. Rev.*, 214, 103477, 2021.
- 1433 Müller, R., Klausen, T. G., Faleide, J. I., Olaussen, S., Eide, C. H. and Suslova, A.: Linking regional  
1434 unconformities in the Barents Sea to compression-induced forebulge uplift at the Triassic-  
1435 Jurassic transition, *Tectonophys.*, 765, 35–51, 2019.
- 1436 Murascov, L. G. and Mokin, Ju. I.: Stratigraphic subdivision of the Devonian deposits of  
1437 Spitsbergen, *Polarinst. Skr.*, 167, 249–261, 1979.
- 1438 Nasuti, A., Roberts, D. and Gernigon, L.: Multiphase mafic dykes in the Caledonides of northern  
1439 Finnmark revealed by a new high-resolution aeromagnetic dataset, *Norwegian Journal of  
1440 Geology*, 95, 251–263, 2015.
- 1441 Norton, M. G., McClay, K. R. and Way, N. A.: Tectonic evolution of Devonian basins in northern  
1442 Scotland and southern Norway, *Norsk Geol. Tidsskr.*, 67, 323–338, 1987.
- 1443 Oakey, G. N. and Chalmers, J. A.: A new model for the Paleogene motion of Greenland relative to  
1444 North America: Plate reconstructions of the Davis Strait and Nares Strait regions between  
1445 Canada and Greenland, *J. of Geophys. Res.*, 117, B10401, 2012.
- 1446 Ogata, K., Mulrooney, M. J., Braathen, A., Maher, H., Osmundsen, P. T., Anell, I., Smyrak-Sikora,  
1447 A. A. and Balsamo, F.: Architecture, deformation style and petrophysical properties of

1448 growth fault systems: the Late Triassic deltaic succession of southern Edgeøya (East  
1449 Svalbard), *Basin Res.*, 30, 5, 1042–1073, 2018.

1450 Ohta, Y., Dallmeyer, R. D. and Peucat, J. J.: Caledonian terranes in Svalbard, *GSA Spec. Paper*,  
1451 230, 1–15, 1989.

1452 Ohta, Y., Krasil'scikov, A. A., Lepvrier, C. and Teben'kov, A. M.: Northern continuation of  
1453 Caledonian high-pressure metamorphic rocks in central-western Spitsbergen, *Polar Res.*,  
1454 14, 3, 303–315, 1995.

1455 Olovyanishnikov, V. G., Roberts, D. and Siedlecka, A.: Tectonics and Sedimentation of the  
1456 Meso- to Neoproterozoic Timan-Varanger Belt along the Northeastern Margin of Baltica,  
1457 *Polarforschung*, 68, 267–274, 2000.

1458 Osmundsen, P-T., Braathen, A., Rød, R. S. and Hynne, I. B.: Styles of normal faulting and fault-  
1459 controlled sedimentation in the Triassic deposits of Eastern Svalbard, *Norwegian Petroleum*  
1460 *directorates Bulletin*, 10, 61–79, 2014.

1461 Petersen, T. G., Thomsen, T. B., Olaussen, S. and Stemmerik, L.: Provenance shifts in an evolving  
1462 Eurekan foreland basin: the Tertiary Central Basin, Spitsbergen, *J. Geol. Soc., London*, 173,  
1463 634–648, 2016.

1464 Peucat, J.-J., Ohta, Y., Gee, D. G. and Bernard-Griffiths, J.: U-Pb, Sr and Nd evidence for  
1465 Grenvillian and latest Proterozoic tectonothermal activity in the Spitsbergen Caledonides,  
1466 *Arctic Ocean, Lithos*, 22, 275–285, 1989.

1467 Phillips, T., Jackson, C. A-L., Bell, R. E., Duffy, O. B. and Fossen, H.: Reactivation of  
1468 intrabasement structures during rifting: A case study from offshore southern Norway,  
1469 *Journal of Structural Geology*, 91, 54–73, 2016.

1470 Piepjohn, K.: The Svalbardian–Ellesmerian deformation of the Old Red Sandstone and the pre-  
1471 Devonian basement in NW Spitsbergen (Svalbard), in: *New Perspectives on the Old Red*  
1472 *Sandstone*, edited by: Friend, P. F. and Williams, B. P. J., *Geol. Soc. London Spec. Publi.*,  
1473 180, 585–601, 2000.

1474 Piepjohn, K.: von Gosen, W., Läufer, A., McClelland, W. C. and Estrada, S.: Ellesmerian and  
1475 Eurekan fault tectonics at the northern margin of Ellesmere Island (Canadian High Arctic),  
1476 *Z. Dt. Ges. Geowiss.*, 164, 1, 81–105, 2013.

1477 Piepjohn, K., Dallmann, W. K. and Elvevold, S.: The Lomfjorden Fault Zone in eastern Spitsbergen  
1478 (Svalbard), in: *Circum-Arctic Structural Events: Tectonic Evolution of the Arctic Margins*

1479 and Trans-Arctic Links with Adjacent Orogens, edited by: Piepjohn, K., Strauss, J. V.,  
1480 Reinhardt, L. and McClelland, W. C., GSA Spec. Paper, 541, 95–130, 2019.

1481 Ramsay, J. G.: Interference Patterns Produced by the Superposition of Folds of Similar Type, J.  
1482 Geol., 70, 4, 466–481, 1962.

1483 Rice, A. H. N.: Restoration of the External Caledonides, Finnmark, North Norway, in: New  
1484 Perspectives on the Caledonides of Scandinavia and Related Areas, Corfu, F., Gasser, D.  
1485 and Chew, D. M. (eds), Geological Society, London, Special Publications, 390, 271-299,  
1486 2014.

1487 Roberts, D.: Tectonic Deformation in the Barents Sea Region of Varanger Peninsula, Finnmark,  
1488 Norges geol. unders., 282, 1–39, 1972.

1489 Roberts, D. and Olovyanishshnikov, V.: Structural and tectonic development of the Timanide  
1490 orogeny, in: The Neoproterozoic Timanide Orogen of Eastern Baltica, edited by: Gee, D.  
1491 G. and Pease, V., Geol. Soc. London, Mem., 30, 47–57, 2004.

1492 Roberts, D. and Siedlecka, A.: Timanian orogenic deformation along the northeastern margin of  
1493 Baltica, Northwest Russia and Northeast Norway, and Avalonian-Cadomian connections,  
1494 Tectonophysics, 352, 1r69-184, 2002.

1495 Roberts, D. and Williams, G. D.: Berggrunnskart Kjøllefjord 2236 IV, M 1:50.000, foreløpig  
1496 utgave, Norges geol. unders., 2013.

1497 Roberts, D., Mitchell, J. G. and Andersen, T. B.: A post-Caledonian dyke from Magerøy North  
1498 Norway: age and geochemistry, Norwegian Journal of Geology, 71, 289-294, 1991.

1499 Rosa, D., Majka, J., Thrane, K. and Guarnieri, P.: Evidence for Timanian-age basement rocks in  
1500 North Greenland as documented through U–Pb zircon dating of igneous xenoliths from the  
1501 Midtkap volcanic centers, Precambrian Res., 275, 394–405, 2016.

1502 Schiffer, C., Doré, A. G., Foulger, G. R., Franke, D., Geoffroy, L., Gernigon, L., Holdsworth, B.,  
1503 Kuszniir, N., Lundin, E., McCaffrey, K., Peace, A. L., Petersen, K. D., Phillips, T. B.,  
1504 Stephenson, R., Stoker, M. S. and Welford, J. K.: Structural inheritance in the North  
1505 Atlantic, Earth-Science Reviews, 206, 102975, 2020.

1506 Senger, K., Roy, S., Braathen, A., Buckley, S., Bælum, K., Gernigon, L., Mjelde, R., Noormets,  
1507 R., Ogata, K., Olausson, S., Planke, S., Ruud, B. O. and Tveranger, J.: Geometries of  
1508 doleritic intrusions in central Spitsbergen, Svalbard: an integrated study of an onshore-

1509 offshore magmatic province with applications to CO<sub>2</sub> sequestration, *Norw. J. Geol.*, 93,  
1510 143–166, 2013.

1511 Siedlecka, A.: Late Precambrian Stratigraphy and Structure of the North-Eastern Margin of the  
1512 Fennoscandian Shield (East Finnmark – Timan Region), *Nor. geol. unders.*, 316, 313-348,  
1513 1975.

1514 Siedlecka, A. and Roberts, D.: Report from a visit to the Komi Branch of the Russian Academy of  
1515 Sciences in Syktyvkar, Russia, and from fieldwork in the central Timans, August 1995,  
1516 *Norges geol. unders. report*, 95.149, 32 pp., 1995.

1517 Siedlecka, A. and Siedlecki, S.: Some new aspects of the geology of Varanger peninsula (Northern  
1518 Norway), *Nor. geol. unders.*, 247, 288-306, 1967.

1519 Siedlecka, A. and Siedlecki, S.: Late Precambrian sedimentary rocks of the Tanafjord–  
1520 Varangerfjord region of Varanger Peninsula, Northern Norway, in: *The Caledonian  
1521 Geology of Northern Norway*, edited by: Roberts, D. and Gustavson, M., *Norges geol.  
1522 unders.*, 269, 246–294, 1971.

1523 Smyrak-Sikora, A., Osmundsen, P. T., Braathen, A., Ogata, K., Anell, I., Mulrooney, M. J. and  
1524 Zuchuat, V: Architecture of growth basins in a tidally influenced, prodelta to delta-front  
1525 setting: The Triassic succession of Kvalpynten, East Svalbard, *Basin Research*, 32, 5, 959–  
1526 988, 2020.

1527 Stouge, S., Christiansen, J. L. and Holmer, L. E.: Lower Palaeozoic stratigraphy of  
1528 Murchisonfjorden and Sparreneset, Nordaustlandet, Svalbard, *Geografiska Annaler: Series  
1529 A, Physical Geography*, 93, 209–226, 2011.

1530 Sturt, B. A., Pringle, I. R. and Ramsay, D. M.: The Finnmarkian phase of the Caledonian Orogeny,  
1531 *J. Geol., Soc., London*, 135, 597–610, 1978.

1532 Thiede, J., Pfirman, S., Schenke, H.-W. and Reil, W.: Bathymetry of Molloy Deep: Fram Strait  
1533 Between Svalbard and Greenland, *Mar. Geophys. Res.*, 12, 197–214, 1990.

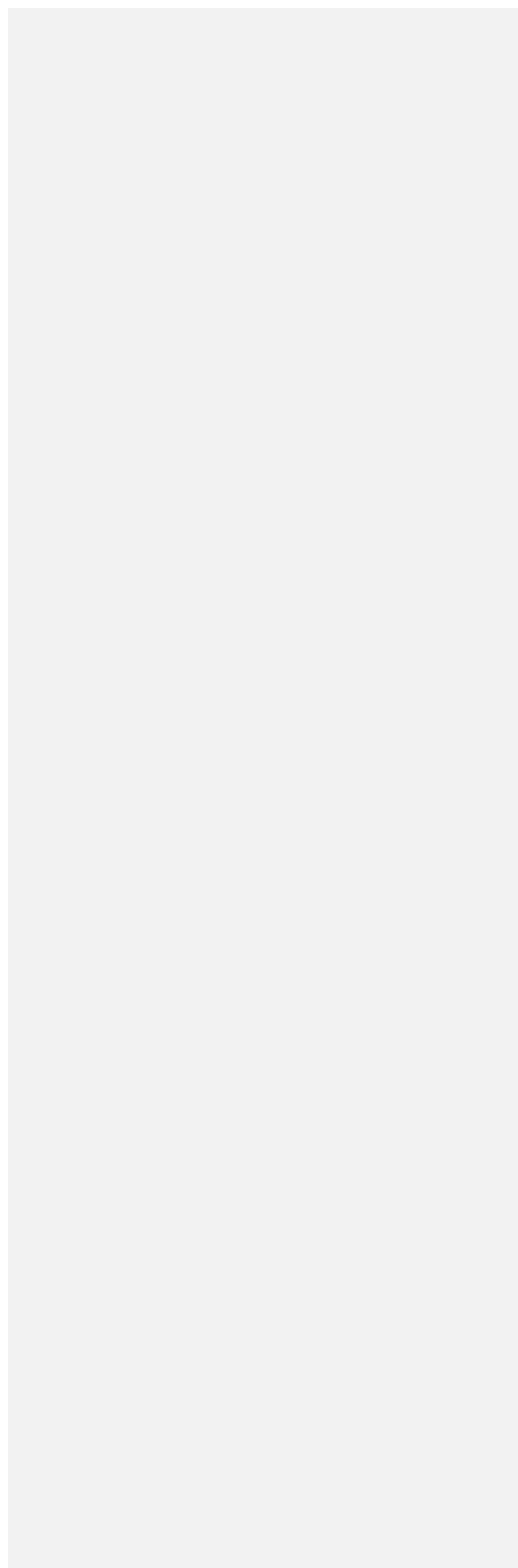
1534 Tonstad, S. A.: The Late Paleozoic development of the Ottar basin from seismic 3D interpretation,  
1535 *Master's Thesis*, University of Tromsø, Tromsø, Norway, 135 pp., 2018.

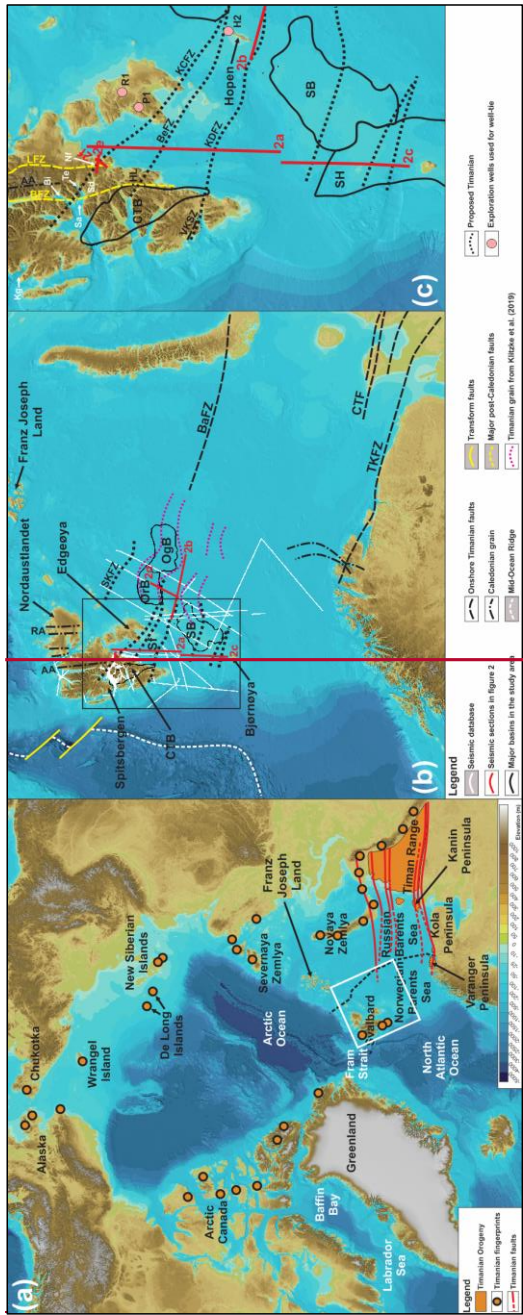
1536 Torsvik, T. H. and Trench, A.: The Ordovician history of the Iapetus Ocean in Britain: new  
1537 palaeomagnetic constraints, *J. Geol. Soc., London*, 148, 423–425, 1991.

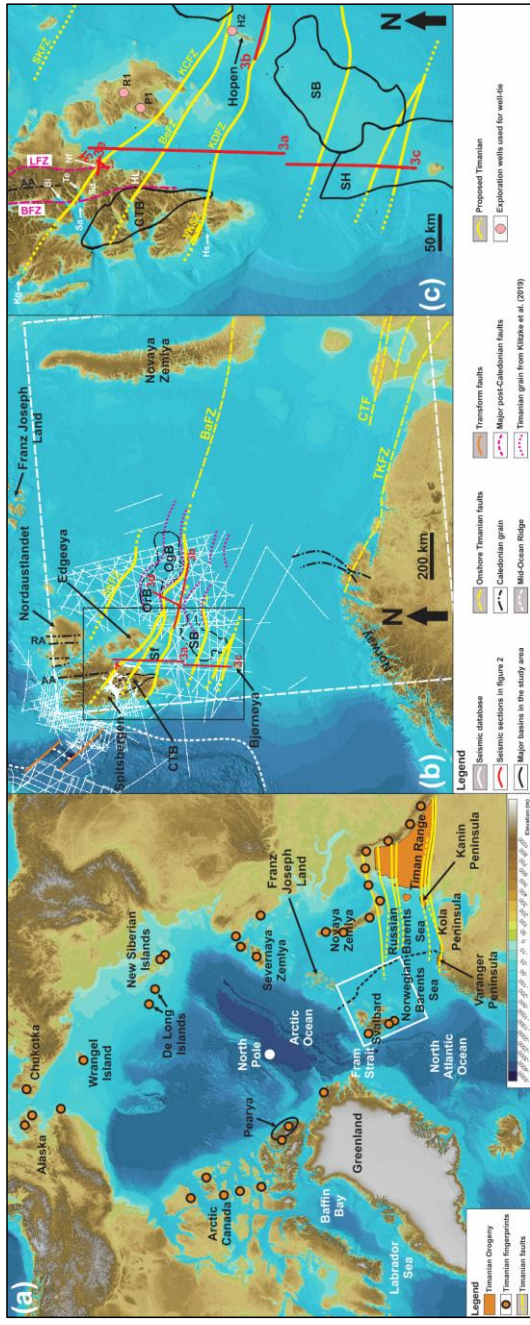
1538 Torsvik, T. H., Burke, K., Steinberger, B., Webb, S. J. and Ashwal, L. D.: Diamond sampled by  
1539 plumes from the core–mantle boundary, *Nature Lett.*, 466, 352–355, 2010.

- 1540 Townsend, C.: Thrust transport directions and thrust sheet restoration in the Caledonides of  
1541 Finnmark, North Norway, *J. Structural Geol.*, 9, 3, 345–352, 1987.
- 1542 Vernikovskiy, V. A., Metelkin, D. V., Vernikovskaya, A. E., Matushkin, N. Yu., Lobkovskiy, L. I.  
1543 and Shipilov, E. V.: Early evolution stage of the arctic margins (Neoproterozoic-Paleozoic)  
1544 and plate reconstructions, ICAM VI Proceedings, May 2011, Fairbanks, Alaska, USA, 265–  
1545 285, 2011.
- 1546 Von Gosen, W. and Piepjohn, K.: Polyphase Deformation in the Eastern Hornsund Area, *Geol. Jb.*,  
1547 B91, 291–312, 2001.
- 1548 Witt-Nilsson, P., Gee, D. G. and Hellman, F. J.: Tectonostratigraphy of the Caledonian Atomfjella  
1549 Antiform of northern Ny Friesland, Svalbard, *Norsk Geol. Tidsskr.*, 78, 67–80, 1998.
- 1550 Worsley, D., Agdestein, T., Gjelberg, J. G., Kirkemo, K., Mørk, A., Nilsson, I., Olausson, S., Steel,  
1551 R. J. and Stemmerik, L.: The geological evolution of Bjørnøya, Arctic Norway:  
1552 implications for the Barents Shelf, *Norsk Geol. Tidsskr.*, 81, 195–234, 2001.
- 1553 Ziegler, P. A.: Evolution of the Arctic–North Atlantic and the Western Tethys, *AAPG Mem.* 43,  
1554 1988.
- 1555



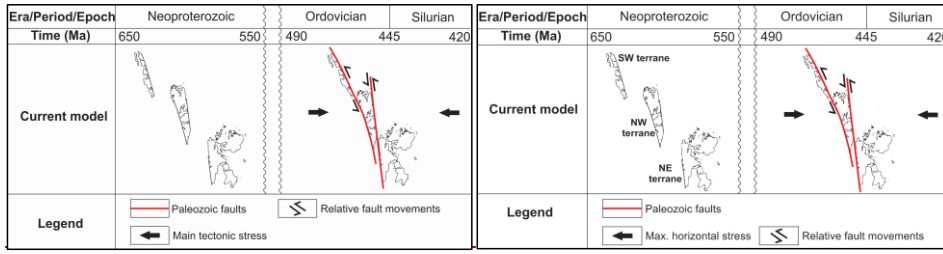




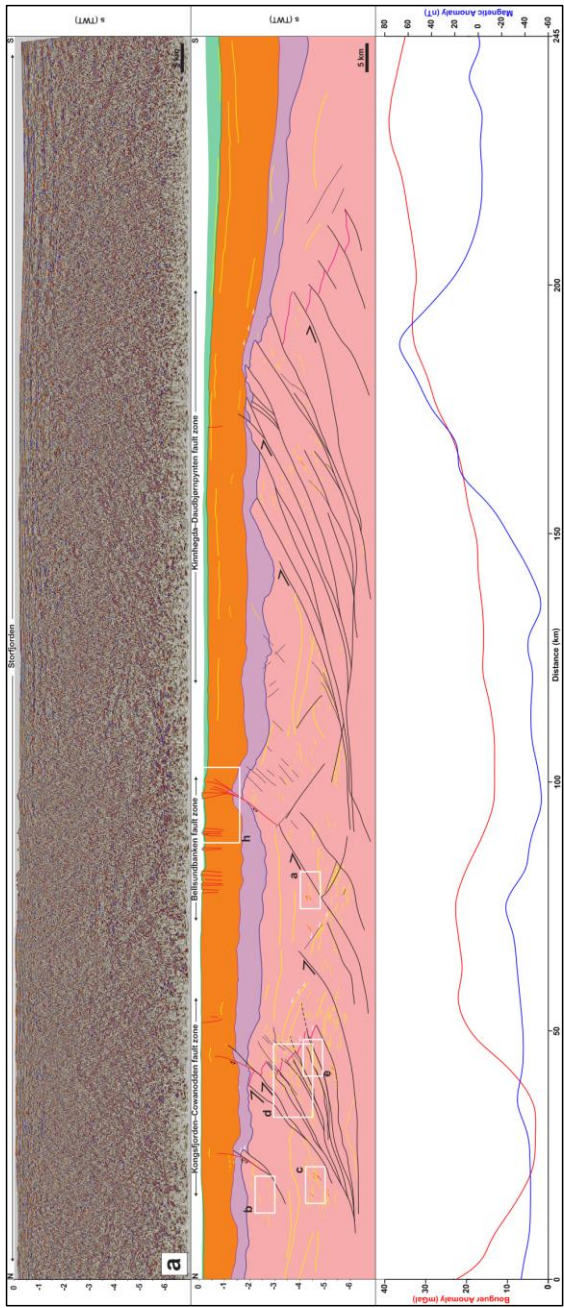


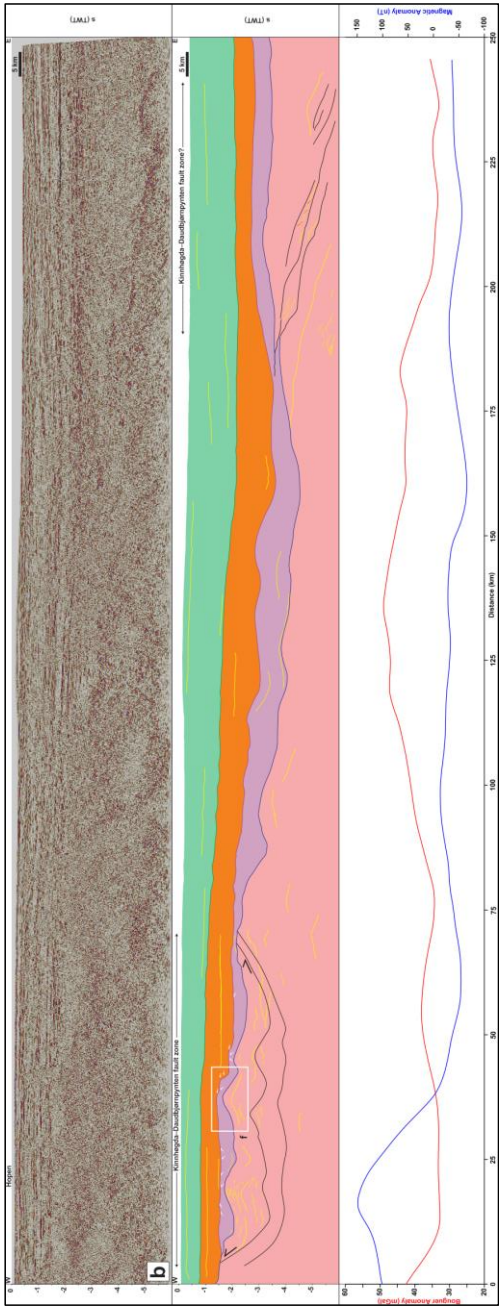
1559 Figure 1: (a) Overview map showing the Timanian belt in Russia and Norway, and occurrences of Timanian fingerprints  
1560 throughout the Arctic; (b) Regional map of Svalbard and the Barents Sea the main geological elements and the seismic  
1561 database used in the present study. The location of (b) is shown as a white frame in (a); (c) Zoom in the northern Norwegian  
1562 Barents Sea and Svalbard showing the main faults and basins in the study area, and the proposed Timanian structures. The  
1563 location of (c) is shown as a black frame in (b). The location of the Raddedalen-1 well is from Smyrak-Sikora et al. (2020).  
1564 Topography and bathymetry are from Jakobsson et al. (2012). Abbreviations: AA: Atomfjella Antiform; BaFZ: Baidaratsky  
1565 fault zone; BeFZ: Bellsundbanken fault zone; BFZ: Billefjorden Fault Zone; Bi: Billefjorden; CTB: Central Tertiary Basin;  
1566 HL: Heer Land; **Hs: Hornsund**; H2: Hopen-2; KCFZ: Kongsfjorden–Cowanodden fault zone; KDFZ: Kinnhøgda–  
1567 Daudbjørnpynten fault zone; Kg: Kongsfjorden; LFZ: Lomfjorden Fault Zone; Nf: Nordmannsfonna; OgB: Olga Basin;  
1568 OrB: Ora Basin; P1: Plurdalen-1; RA: Rijpdalen Anticline; R1: Raddedalen-1; Sa: Sassenfjorden; SB: Sørkapp Basin; Sf:  
1569 Storfjorden; SH: Stappen High; SKFZ: Steiløya–Krylen fault zone; Te: Tempelfjorden; TKFZ: Trollfjorden–Komagelva  
1570 Fault Zone; VKSZ: Vimsodden–Kosibapasset Shear Zone.

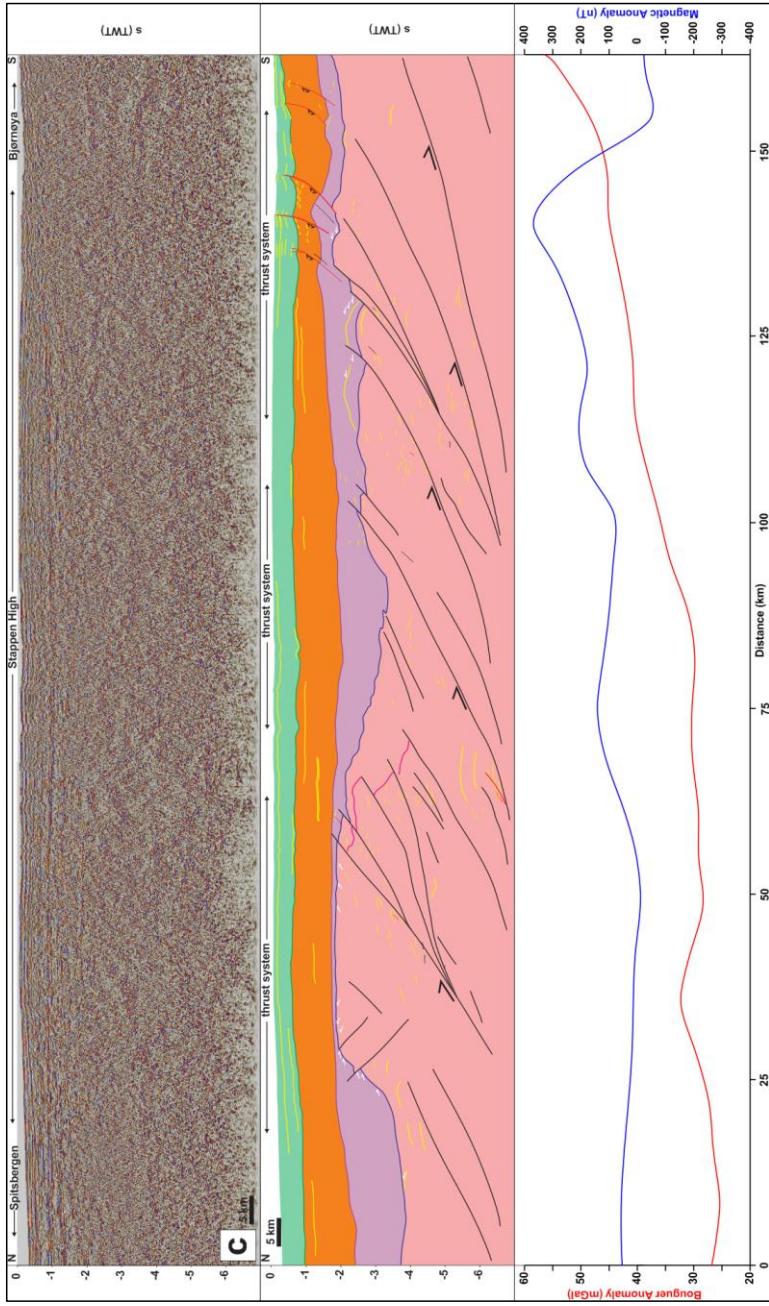
1571



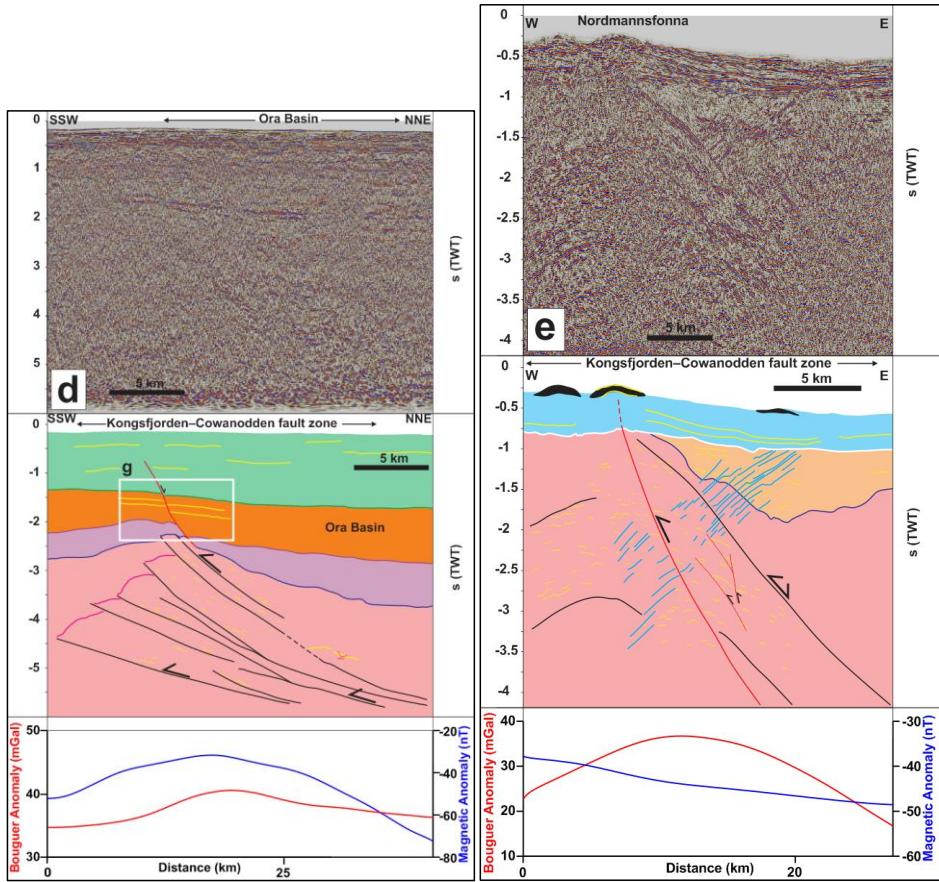
1572 **Figure 2: Paleogeographic reconstruction of the Svalbard Archipelago in the latest Neoproterozoic during the Timanian**  
1573 **Orogeny and in the early–mid Paleozoic during the Caledonian Orogeny according to previous models (e.g., Harland, 1969;**  
1574 **Labrousse et al., 2008).**

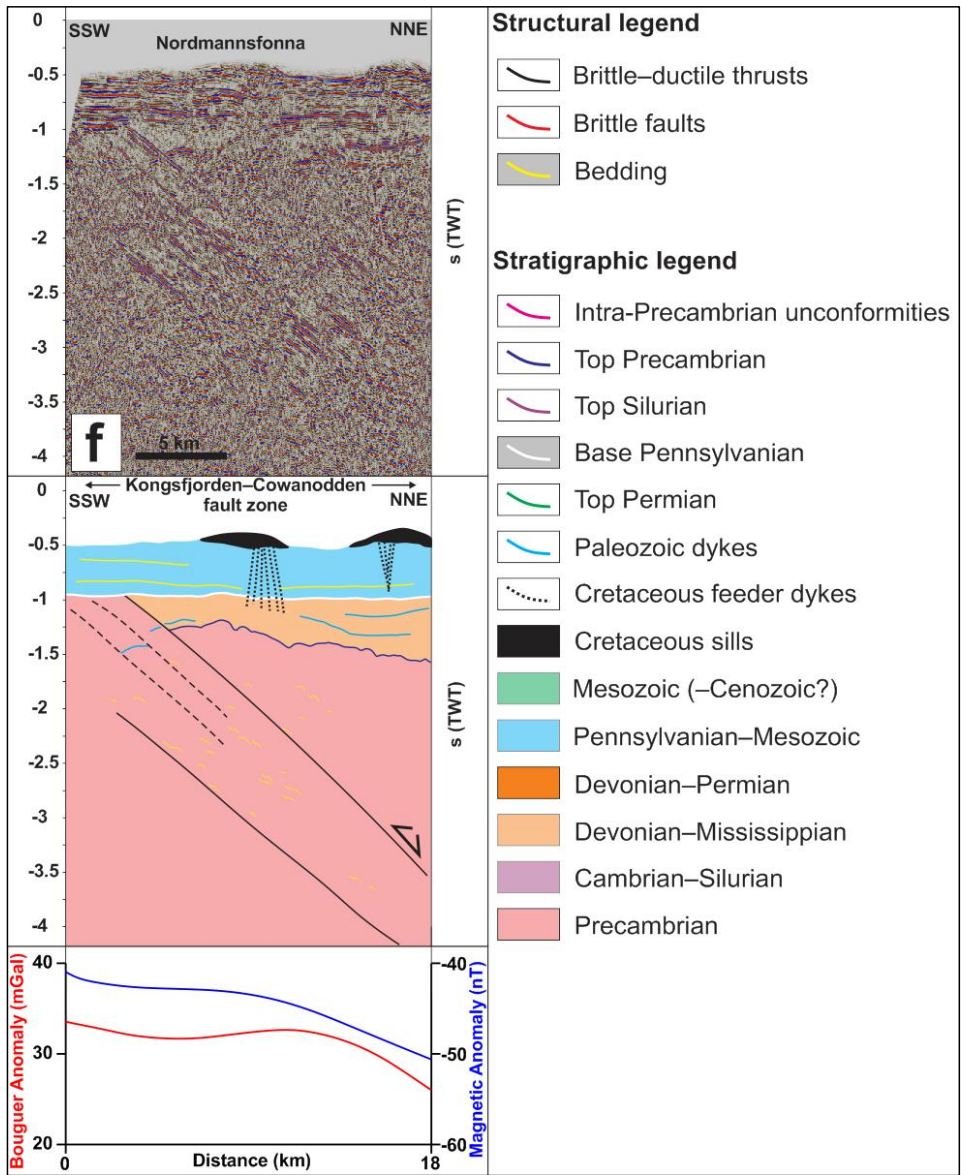








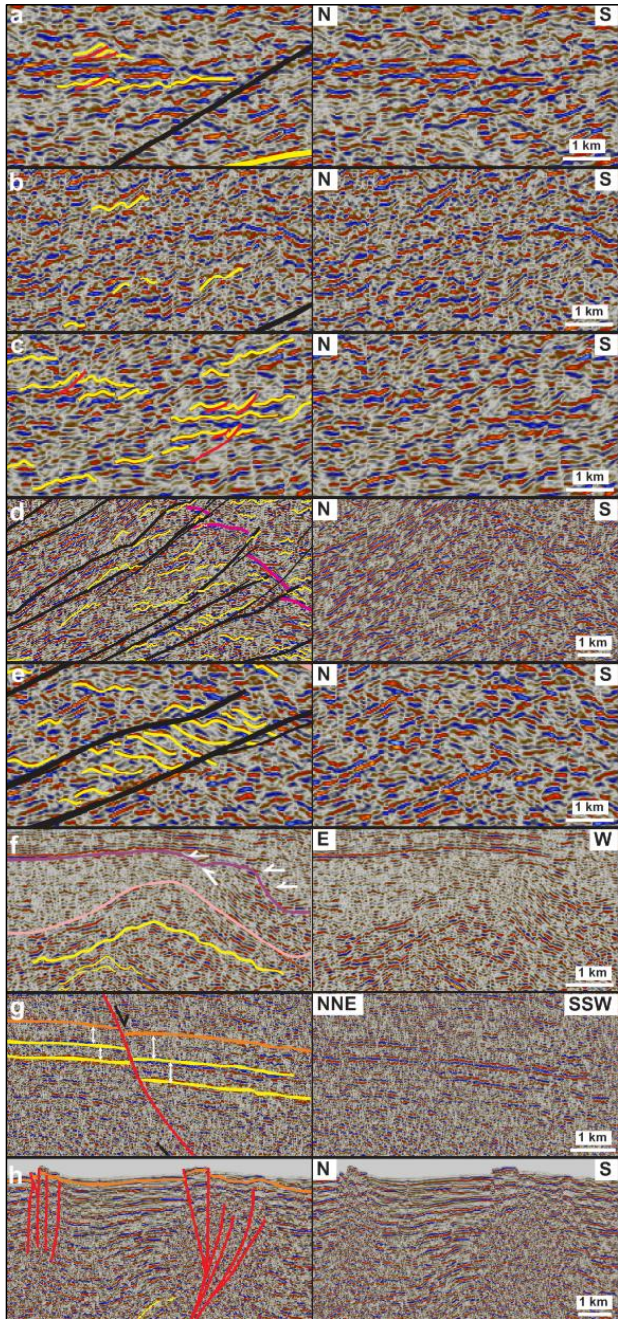




1579  
 1580 Figure 3: Interpreted seismic profiles and associated potential field data (a) in Storfjorden, (b) south of Hopen, (c) on the  
 1581 Stappen High in the northwestern Norwegian Barents Sea between Spitsbergen and Bjørnøya, (d) on the southern flank of  
 1582 the Ora Basin in the northeastern Norwegian Barents Sea, and (e and f) in Nordmannsonna in eastern Spitsbergen. The  
 1583 seismic profiles show top-SSW Timanian thrusts that were reactivated and overprinted during subsequent tectonic events  
 1584 such as Caledonian contraction, Devonian-Carboniferous late-post Caledonian collapse and rifting, Eurekan contraction,  
 1585 and present-day contraction. Profiles (e) and (f) also show Paleozoic and Cretaceous intrusions. The white frames show the

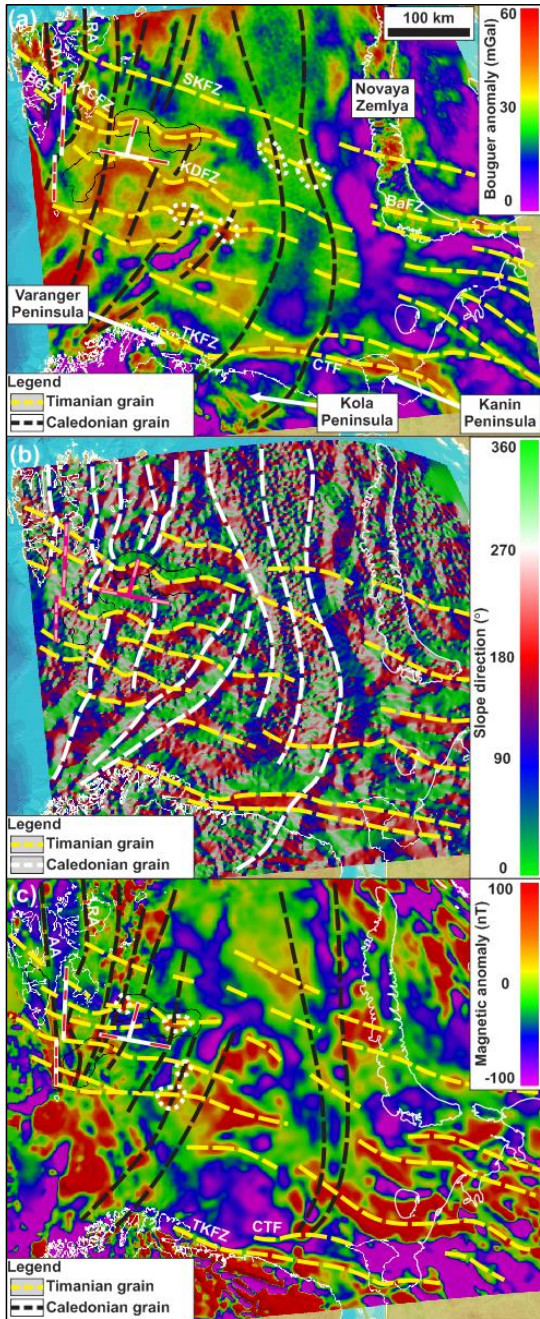
1586 location of zoomed-in portions of the profiles displayed in [Figure 4](#). Potential field data below the seismic profiles  
1587 include Bouguer anomaly (red lines) and magnetic anomaly (blue lines). The potential field data show consistently high  
1588 gravimetric anomalies and partial correlation with high magnetism towards the footwall of each major thrust systems (i.e.,  
1589 towards thickened portions of the crust).

1590



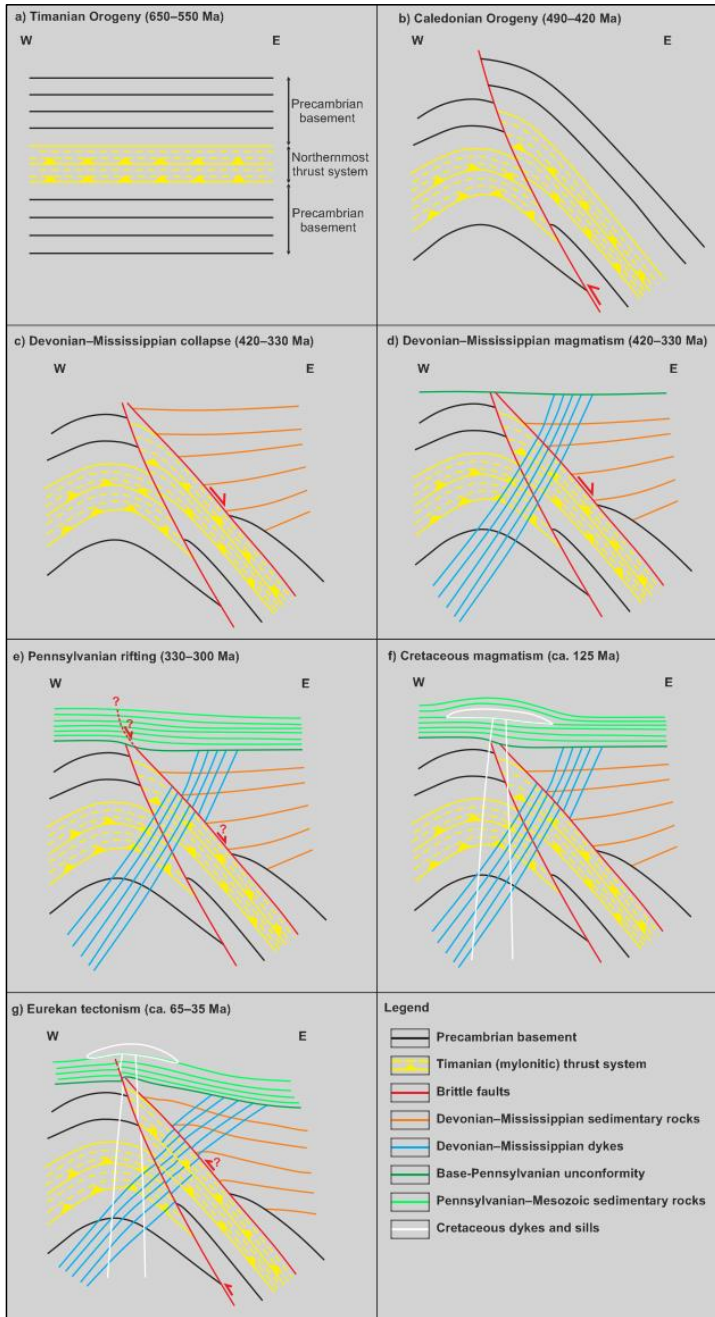
1592 Figure 4: Zooms in seismic profiles shown in [Figure 3](#) showing (a) upright fold structures, (b) SSW-verging folds  
1593 and (c) top-SSW minor thrusts in Precambrian–lower Paleozoic (meta-) sedimentary basement rocks, (d) SSW-verging folds  
1594 and NNE-dipping mylonitic shear zones within a major thrust that offsets major basement unconformities (fuchsia lines)  
1595 top-SSW, (e) duplex structures within a major top-SSW thrust, (f) a N–S- to NNE–SSW-trending, 5–15 kilometers wide,  
1596 symmetrical, upright macro-fold and associated, kilometer- to hundreds of meter-scale, parasitic macro- to meso-folds, (g)  
1597 syn-tectonic thickening in Devonian–Carboniferous (–Permian?) sedimentary strata offset down-NNE by a normal fault  
1598 that merges with a thick mylonitic shear zone at depth, and (h) recent–ongoing reverse offsets of the seafloor reflection by  
1599 multiple, inverted, NNE-dipping normal faults in Storfjorden. See [Figure 3](#) for location of each zoom and for legend.

1600



1602 Figure 5: Gravimetric (a and b) and magnetic (c) anomaly maps over the Barents Sea and adjacent onshore areas in Russia  
1603 (see location as a dashed white frame in Figure 1b), Norway and Svalbard showing E–W- to NW–SE-trending anomalies  
1604 (dashed yellow lines) that correlate with the proposed NNE-dipping Timanian thrust systems in Svalbard and the northern  
1605 Norwegian Barents Sea. Note the high obliquity of E–W- to NW–SE-trending Timanian grain with NE–SW- to N–S-trending  
1606 Caledonian grain (dashed black/white lines). Note that dashed lines in (a) and (c) denote high gravimetric and magnetic  
1607 anomalies. Also notice the oval-shaped high gravimetric and magnetic anomalies (dotted white lines) at the intersection of  
1608 WNW–ESE- and N–S- to NNE–SSW-trending anomalies in (a) and (c) resulting from the interaction of the two (Timanian  
1609 and Caledonian) thrust and fold trends. The location of seismic profiles presented in Figure 3a–d are shown as thick  
1610 white lines in (a) and (c) and as fuchsia lines in (b). Within these thick white and fuchsia lines, the location and extent of  
1611 thrust systems evidenced on seismic data (Figure 3) is shown in white in (a) and (c) and in pink in (b). For the E–  
1612 W-trending seismic profile shown in Figure 3b, this implies that the red and pink lines represent N–S-trending  
1613 synclines. Abbreviations: AA: Atomfjella Antiform; BaFZ: Baidaratsky fault zone; BeFZ: Bellsundbanken fault zone; CTF:  
1614 Central Timan Fault; KCFZ: Kongsfjorden–Cowanodden fault zone; KDFZ: Kinnhøgda–Daudbjørnpynten fault zone;  
1615 RA: Rijpdalen Anticline; SKFZ: Steiløya–Krylen fault zone; TKFZ: Trollfjorden–Komagelva Fault Zone.

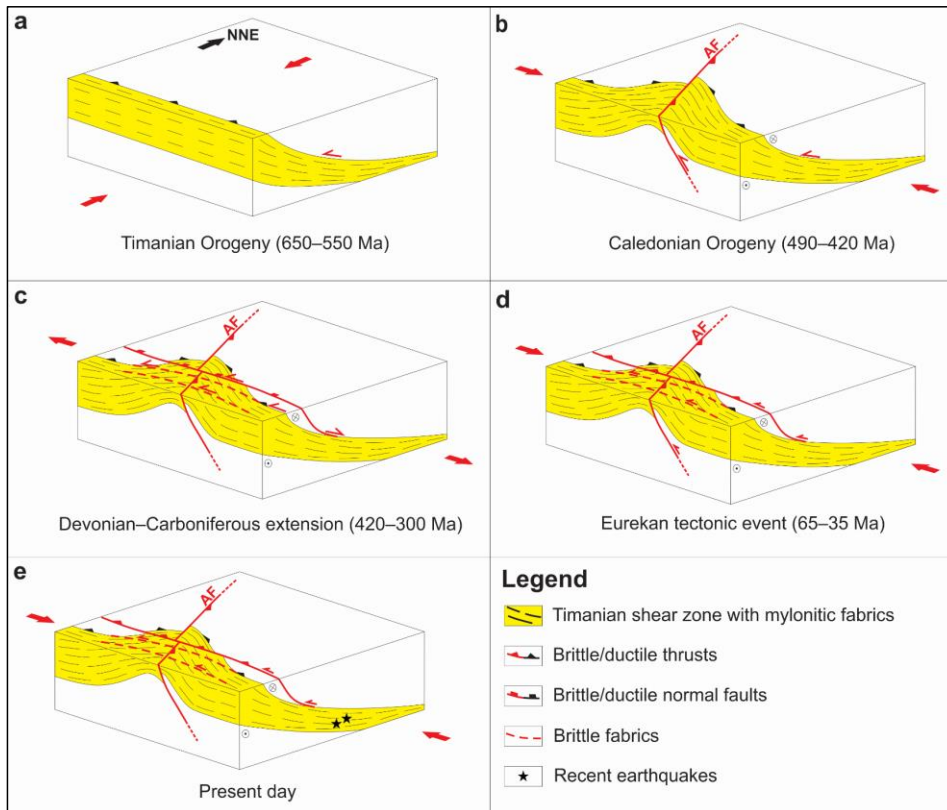
1616





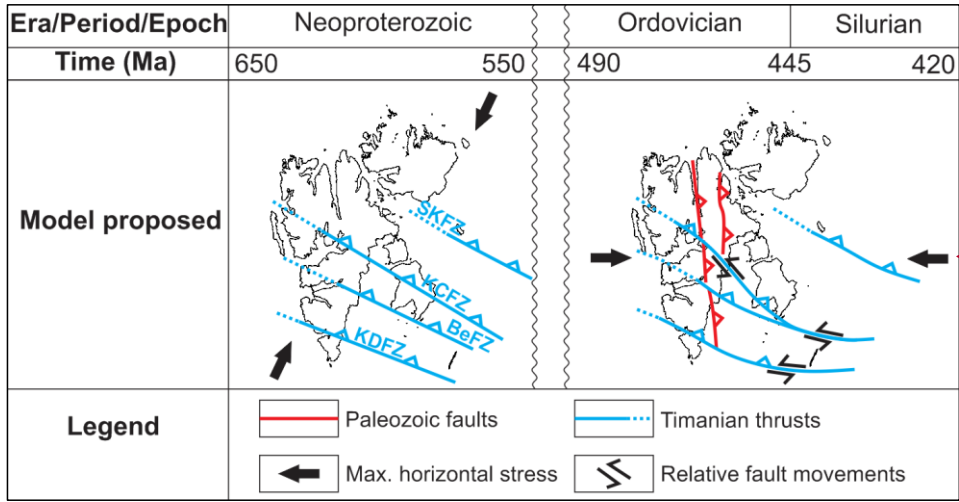
1618 Figure 6: Sketches showing a possible reconstruction of the tectonic history of the E–W seismic profile in Nordmannsfonna  
1619 shown in [Figure 3](#) ~~Figure 3e~~. (a) Formation of a NNE-dipping, mylonitic thrust system (Kongsfjorden–Cowanodden fault  
1620 zone) within Precambrian basement rocks during the Timanian Orogeny in the latest Neoproterozoic. The NNE-dipping  
1621 Kongsfjorden–Cowanodden fault zone appears near horizontal on the E–W transect; (b) Top-west thrusting along the east-  
1622 dipping Agardhbukta Fault and folding of the Kongsfjorden–Cowanodden fault zone into a broad, moderately NNE-  
1623 plunging anticline during the Caledonian Orogeny; (c) Inversion of the Kongsfjorden–Cowanodden fault zone along the  
1624 eastern flank of the Caledonian anticline and deposition of thickened, gently west-dipping, syn-tectonic, Devonian (–  
1625 Mississippian?) sedimentary strata during post-Caledonian collapse-related extension; (d) Intrusion of Precambrian  
1626 basement and Devonian (–Mississippian?) sedimentary rocks by steeply west-dipping dykes in the Devonian–Mississippian;  
1627 (e) Regional erosion in the mid-Carboniferous (latest Mississippian) and deposition of Pennsylvanian sedimentary strata,  
1628 possibly along a high-angle brittle splay of the inverted portion of the Kongsfjorden–Cowanodden fault zone during rift-  
1629 related extension; (f) Deposition of Mesozoic sedimentary strata and intrusion of Cretaceous dolerite dykes and sills; (g)  
1630 Erosion of Pennsylvanian–Mesozoic strata and reactivation of the Kongsfjorden–Cowanodden fault zone and Agardhbukta  
1631 Fault with minor reverse movements in the early Cenozoic during the Eurekan tectonic event as shown by mild folding and  
1632 offset of overlying post-Caledonian sedimentary strata, dykes and Base-Pennsylvanian unconformity. Also note the back-  
1633 tilting (i.e., clockwise rotation) of Devonian–Mississippian dykes in the hanging wall of the Agardhbukta Fault and of the  
1634 Kongsfjorden–Cowanodden fault zone.

1635



1636  
 1637 **Figure 7: Tectonic evolution of Timanian thrust systems in eastern Spitsbergen, Storfjorden and the northwestern**  
 1638 **Norwegian Barents Sea including (a) top-SSW thrusting during the Timanian Orogeny, (b) reactivation as oblique-slip**  
 1639 **sinistral-reverse thrusts and offset by top-west brittle thrust overprints (e.g., Agardhbukta Fault – AF) under E-W**  
 1640 **contraction during the Caledonian Orogeny, (c) reactivation as low-angle, brittle–ductile, normal–sinistral extensional**  
 1641 **detachments and overprinting by high-angle normal–sinistral brittle faults during Devonian–Carboniferous, late–post-**  
 1642 **Caledonian extensional collapse and rifting, (d) reactivation as brittle–ductile sinistral–reverse thrusts, overprinting by**  
 1643 **high-angle sinistral–reverse brittle thrusts, and mild offset by reactivated top-west thrusts (e.g., Agardhbukta Fault – AF)**  
 1644 **during E–W Eurekan contraction, and (e) renewed, recent–ongoing, sinistral–reverse reactivation and overprinting possibly**  
 1645 **due to ongoing magma extrusion and transform faulting (ridge-push?) in the Fram Strait.**

1646



**Formatted:** Keep with next

**Figure 8: Paleogeographic reconstruction of the Svalbard Archipelago in the latest Neoproterozoic during the Timanian Orogeny and in the early–mid Paleozoic during the Caledonian Orogeny according to the present study.**

**Formatted:** Font: (Default) Times New Roman, Bold, Not Italic

**Formatted:** Caption